159

PRICE FIVE SHILLINGS.

The Institution of Electrical Engineers

ORIGINALLY

The Society of Telegraph Engineers

FOUNDED 1871

INCORPORATED BY ROYAL CHARTER 1921

SAVOY PLACE, VICTORIA EMBANKMENT, LONDON, W.C.2.

Telegrams : "VOLTAMPERE, PHONE, LONDON." Telephone : TEMPLE BAR 7676.

PROCEEDINGS OF THE WIRELESS SECTION

OF THE INSTITUTION.

EDITED BY P. F. ROWELL, SECRETARY.

Vol. 13 **MARCH, 1938.** **No. 37**

(Issued two or three times yearly.)

CONTENTS.

(The Institution is not, as a body, responsible for the opinions expressed by individual authors or speakers.)

PAGE

Chairman's Address .... T. WADSWORTH, M.Sc. 1

The Dependence of the Inter-Electrode Capacitances of Valves upon the Operating Conditions. T. IORWERTH JONES, M.Sc. 11

The Apparent Inter-Electrode Capacitance of a Planar Diode .... E. B. MOULLIN, M.A. 23

An Improved Medium-Wave Adcock Direction-Finder. R. H. BARFIELD, M.Sc., and R. A. FEREDAY, Ph.D. 33

A Short-Wave Adcock Direction-Finder ...... R. H. BARFIELD, M.Sc., and W. ROSS, M.A. 39

The Reflection Coefficient of the Earth's Surface for Radio Waves .. J. S. MCPETRIE, Ph.D., B.Sc. 48

Thermal Fluctuations in Complex Networks .... F. C. WILLIAMS, M.Sc., D.Phil. 53

Theory and Performance of the Iconoscope. V. K. ZWORYKIN, Ph.D., G. A. MORTON, Ph.D., and L. E. FLORY 63

Meetings 72

E. and F. N. SPON, LIMITED, 57 HAYMARKET, LONDON, S.W.1

CHEMICAL PUBLISHING COMPANY OF N.Y. INC., 148 LAFAYETTE STREET, NEW YORK.

The Institution of Electrical Engineers.

FOUNDED 1871

INCORPORATED BY ROYAL CHARTER 1921

PATRON: HIS MAJESTY KING GEORGE VI.

COUNCIL, 1937-1938.

President.

SIR GEORGE LEE, O.B.E., M.C.

Past-Presidents.

COLONEL R. E. CROMPTON, C.B., F.R.S.
SIR JAMES SWINBURNE, BART., F.R.S.
W. M. MORDEY.
SIR JOHN SNELL, G.B.E.
CHARLES P. SPARKS, C.B.E.
ROGER T. SMITH.
LL. B. ATKINSON.
J. S. HIGHFIELD.
F. GILL, O.B.E.
A. RUSSELL, M.A., D.Sc., LL.D., F.R.S.
W. B. WOODHOUSE.
W. H. ECCLES, D.Sc., F.R.S.
SIR ARCHIBALD PAGE.
LIEUT.-COL. K. EDGCUMBE, T.D.
COLONEL SIR THOMAS F. PURVES, O.B.E.
CLIFFORD C. PATERSON, O.B.E., D.Sc.
J. M. DONALDSON, M.C.
PROF. E.W. MARCHANT, D.Sc.
P. V. HUNTER, C.B.E.
PROF. W. M. THORNTON, O.B.E., D.Sc., D.Eng.
J. M. KENNEDY, O.B.E.
H. T. YOUNG.

Vice-Presidents.

SIR NOEL ASHBRIDGE, B.Sc. (Eng.).
J. R. BEARD, M.Sc.
A. P. M. FLEMING, C.B.E., D.Eng., M.Sc.
JOHNSTONE WRIGHT.

Honorary Treasurer.

W. MCCLELLAND, C.B., O.B.E.

Ordinary Members of Council.

T. E. ALLIBONE, D.Sc., Ph.D.
COL. A. S. ANGWIN, D.S.O., M.C.
E. S. BYNG.
T. CARTER.
C. E. FAIRBURN, M.A.
F. FORREST.
PROF. C. L. FORTESCUE, O.B.E., M.A.
P. GOOD.
E. M. LEE, B.Sc.
E. LEETE.

Ordinary Members of Council—(*Continued*).

S. W. MELSOM.
F. E. J. OCKENDEN.
P. L. RIVIÈRE.
P. J. ROBINSON, M.Eng.
C. RODGERS, O.B.E., B.Sc., B.Eng.
C. D. TAITE.
C. R. WESTLAKE.
G. A. WHIPPLE, M.A.

Chairmen and Past-Chairmen of Local Centres.

Argentine Centre:
H. C. SIDDELEY.
*R. WRIGHT.

China Centre:
S. FLEMONS.
*C. R. WEBB.

Irish Centre:
LT.-COL. K. E. EDGEWORTH, D.S.O., M.C.
*W. STOREY.

Mersey and North Wales (Liverpool) Centre:
G. K. PATON.
*F. E. SPENCER.

North-Eastern Centre:
W. D. HORSLEY.
*D. M. BUIST.

North Midland Centre:
J. G. CRAVEN.
*S. R. SIVIOUR.

North-Western Centre:
J. W. THOMAS, LL.B., B.Sc.Tech.
*G. L. PORTER.

Scottish Centre:
MAJOR H. BELL, O.B.E., T.D.
*H. C. BABB.

South Midland Centre:
H. HOOPER.
*E. A. REYNOLDS, M.A.

Western Centre:
H. G. WEAVER.
*J. W. SPARK.

* Past-Chairman.

Chairmen of Sections.

H. COBDEN TURNER (*Meter and Instrument*).
J. L. EVE (*Transmission*).
T. WADSWORTH, M.Sc. (*Wireless*).

Secretary.

P. F. ROWELL.

Assistant Secretaries.

F. W. HEWITT, M.Sc.; A. E. RAYNER.

WIRELESS SECTION COMMITTEE, 1937-1938.

Chairman: T. WADSWORTH, M.Sc.
Vice-Chairman: W. J. PICKEN.
Immediate Past-Chairman: E. MALLETT, D.Sc.(Eng.).

J. R. BEARD, M.Sc. (nominated by the Council).
H. BISHOP, B.Sc.(Eng.).
W. J. BROWN, B.Sc.
S. BRYDON, D.Sc.
R. P. G. DENMAN, M.A.
W. T. DITCHAM.
COL. R. ELSDALE, O.B.E., M.C. (nominated by the War Office).
A. J. GILL, B.Sc.(Eng.) (nominated by the Post Office).
CAPT. P. F. GLOVER, R.N. (nominated by the Admiralty).
T. E. GOLDUP.
N. F. S. HECHT (nominated by the Air Ministry).
H. L. KIRKE.
SIR GEORGE LEE, O.B.E., M.C. (*President, I.E.E.*).
E. B. MOULLIN, M.A.
A. H. MUMFORD, B.Sc.(Eng.).
S. B. SMITH.
R. L. SMITH-ROSE, Ph.D., D.Sc.
W. URE, B.Sc.

And the Chairman of the I.E.E. Papers Committee.

The Institution is not, as a body, responsible for the opinions expressed by individual authors or speakers.

PROCEEDINGS OF
THE WIRELESS SECTION OF
The Institution of Electrical Engineers
VOL. 13.

WIRELESS SECTION: CHAIRMAN'S ADDRESS*

By T. WADSWORTH, M.Sc., Member.

"A REVIEW OF IMPROVEMENTS IN CINEMA SOUND REPRODUCTION SINCE 1928"

(*Address delivered* 3*rd November*, 1937.)

INTRODUCTION

I wish to express my appreciation of the honour that you have conferred upon me in electing me Chairman of this Section. As the Chairman's Address is not open for discussion, I shall endeavour to avoid controversial subjects and shall confine my remarks to a review of the advances in cinema sound reproduction which have been achieved since 1928.

Improvement in the quality of sound reproduction in the cinemas of this country since the introduction of talking pictures in 1928 has been rapid and is still proceeding. The introduction of any new recording technique is followed immediately by the announcement of an improved sound-reproducing system capable of demonstrating the latest product of the recording studio. The continued study of the acoustic properties of cinemas, both in the design of the building and in the treatment of troublesome walls and other surfaces with acoustic material, has resulted in a steady and almost imperceptible improvement in each succeeding cinema, which over a series of years has been as marked as the changes in the equipment itself. Attention to details in the installation, and in particular to the correct location and design of the loud-speaker units, has contributed to a final result which bears little resemblance to early examples of sound-film reproduction.

It is the purpose of this Address to trace in the broadest manner the course of these developments and to indicate the trend of further research.

GENERAL CONSIDERATION OF EARLY EQUIPMENTS—1928–30

The average human ear can appreciate sounds having frequencies ranging from 16 to 20 000 cycles per sec., but its discrimination of power differences varies widely over this range. At a frequency of 1 000 cycles per sec. a power range of 130 decibels can be appreciated between the threshold of audibility and maximum audibility.

The early equipments of 1928–30 had a frequency range of 100 to 4 000 cycles per sec. and a power range of 30 db.; the reproduction was also marred by frequency and amplitude distortion introduced by the equipment and by the acoustic properties of the halls in which the equipment was installed. This power range can of course be situated at any region of the ear sensitivity curve between threshold and maximum limits of audibility, and its position depends upon the average maximum intensity used in a particular cinema (Fig. 1). The difficulty of maintaining a recording power range of 30 db. on the film led to serious deformation of the character of the recorded sound. Distortion introduced by the film-propelling mechanism took the form of gearwheel and sprocket tooth ripple, which modulated the sound record and produced harsh and "throaty" reproduction.

The need for acoustic treatment of the halls was recognized from the first, but little was known of the absorption properties of the material available or of the measurement of reverberation and its optimum value for a given auditorium. It became the practice to treat the walls with sufficient material to bring the reverberation time of a 500-cycle note to somewhere between 1¼ and 1½ sec., depending upon the size of the hall. The reverberation periods of notes of higher or lower frequency were ignored, and the usual result was that reverberation was too high at low frequencies and too low at high frequencies. This gave accentuated bass response and a hard "dead" response of the higher frequencies.

OUTLINE OF DEVELOPMENTS SINCE 1928–30

In tracing the developments that have taken place since these first sets were installed, the survey is divided into four sections:—

(*a*) The sound record on the film.
(*b*) The sound head (or film-propelling mechanism and scanning system).
(*c*) Amplifiers and loud-speakers.
(*d*) Cinema acoustics.

---

* Reprinted from *Journal I.E.E.*, 1938, vol. 82, p. 10.

(a) The Sound Record on the Film

The film forms the first link in the reproducing system. A photographic image can portray both shape and density, and so two distinct forms of record are available, known as " variable area " and " variable density " recording respectively (Fig. 2). An ideal in either case is that the sound-modulated light beam imaged on the film shall be infinitely narrow in a direction perpendicular to the film travel. In practice the speed of the film is fixed at 18 in. per sec. and the upper-frequency limit of recording is fixed by the minimum possible width of the recording slit and the photographic properties of the film. In addition, the stray light of the recording optical system must be zero.

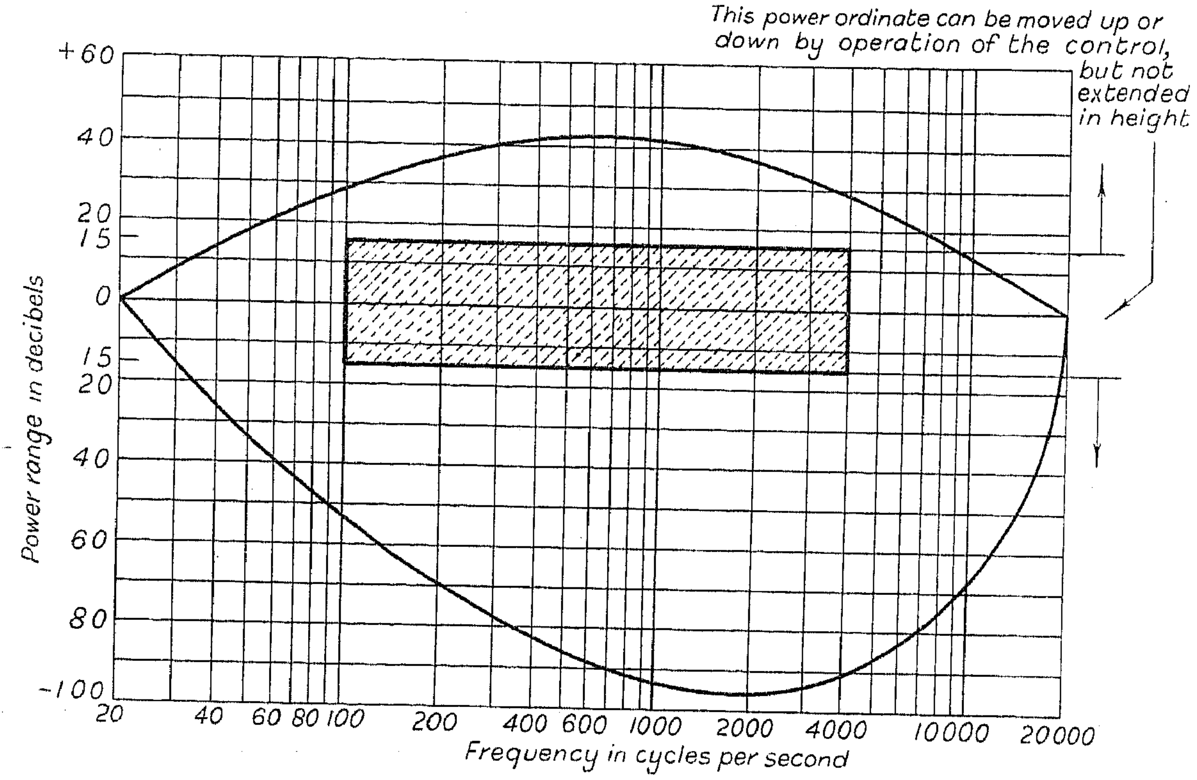

Fig. 1.—Average reproducer overall characteristic (1928–30).

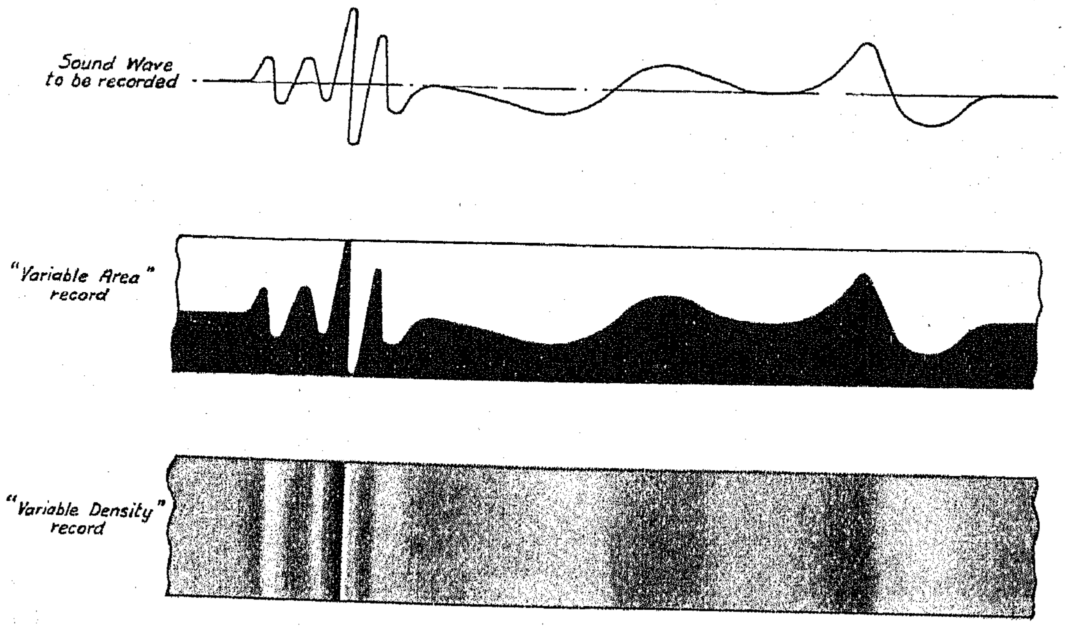

Fig. 2.—Diagrams to illustrate that a sound record can be portrayed as a variation of either shape or density of photographic material.

The photographic limitation to the frequency range is due to lack of resolving power of the emulsion. This can roughly be defined as the emulsion's ability to record fine detail. Light falling on the silver-halide particles of the emulsion during the recording or printing operation is scattered and exposes other neighbouring particles. Thus instead of a sharp, well-defined change of contour from black to white the boundary of the sound wave has a density gradient (Fig. 3). This light scatter is not serious at low frequencies where the wavelength is large, but becomes serious at high frequencies and produces a loss of output and the introduction of spurious harmonics in the case of variable-area recording (Fig. 4).

In addition to the limitation of finite slit-width and the photographic light scatter, early recordings were limited still further by the mechanical details of the recording light modulator, and at the lower end of the frequency scale by the coupling circuits in the recorder amplifier. The final result was a frequency range on the film of 100–150 to 4 000–5 000 cycles per sec.

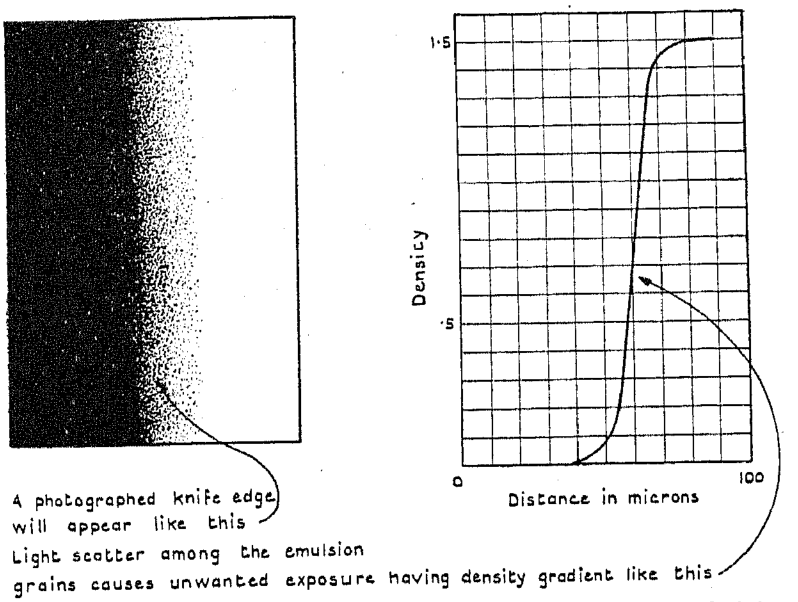
1·5
Density
·5
0
100
Distance in microns
A photographed knife edge will appear like this
Light scatter among the emulsion grains causes unwanted exposure having density gradient like this

Fig. 3.—Diagrams illustrating limitation of record definition by emulsion resolving-power.

The volume range of the film is expressed as the ratio of the amplitude of the maximum signal that can be recorded on the track to the amplitude of the background noise from the film itself. To be inaudible, the background level should be 30 db. below the maximum signal, but this cannot be achieved at present. The maximum amplitude of the track is 0·071 in., and the equivalent amplitude of the background noise of an elementary variable-area track is approximately 0·0025 in., giving a signal/background ratio of 25 to 30 db.

One of the earliest improvements introduced into sound recording was the principle of ground-noise elimination. The background noise from a film is due to accidental variations in film transmission over extremely small areas and to shot effect in the photocell. If the track transmission is made proportional to the recorded amplitude the background noise is reduced to the lowest possible value, and the volume range increased accordingly (Fig. 5). To achieve this end the clear part of the sound track is reduced to a minimum. Ground-noise elimination has been achieved in various ways for the different types of track, and has resulted in an increase in volume range of 10 to 15 db.

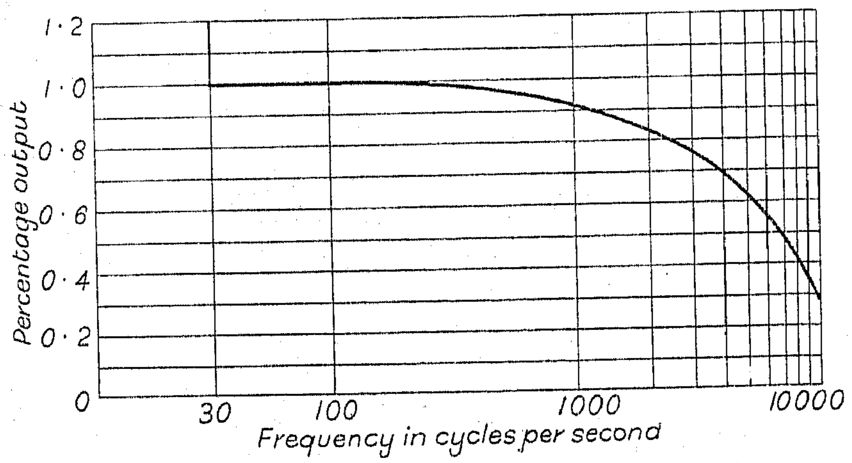

Fig. 4.—Graph showing attenuation with frequency caused by "scatter exposure." The curve indicates the theoretical minimum attenuation due to photographic defects in a 35-mm. negative record.

Continued efforts were made to extend the frequency range to 10 000 cycles per sec. Improved recording light modulators were built with their mechanical resonance beyond 10 000 cycles per sec., and film recorders were improved to overcome sprocket ripple. Constant-frequency recording showed good sound records up to 10 000 cycles per sec., which could be demonstrated over improved reproducers, but the result in the cinema was discouraging. The reproduction of sibilants was harsh, and what was known as "S distortion" became common. As a result the frequency range of the reproducers was still curtailed to about 6 000 cycles per sec. The cause of the trouble was traced to the lack of emulsion resolving-power previously mentioned. Fogging in the valleys of the high-frequency records produced not only attenuation of the output but also rectification.

The extension of the recording range at the lower end made audible at 30 cycles per sec. the change in mean track transmission used for ground-noise elimination. These difficulties were met by control of the processing and the redesign of the ground-noise elimination system, but the results still left much to be desired and development centred round methods of recording that would avoid the difficulties. Some improvements can be claimed for such forms of variable-area tracks as the single and multi-bilateral, because here the amplitude of an individual component track is lowered at a given frequency and so the effective valley angle is increased. In other words, all effects due to lack of emulsion resolving-power are somewhat lessened.

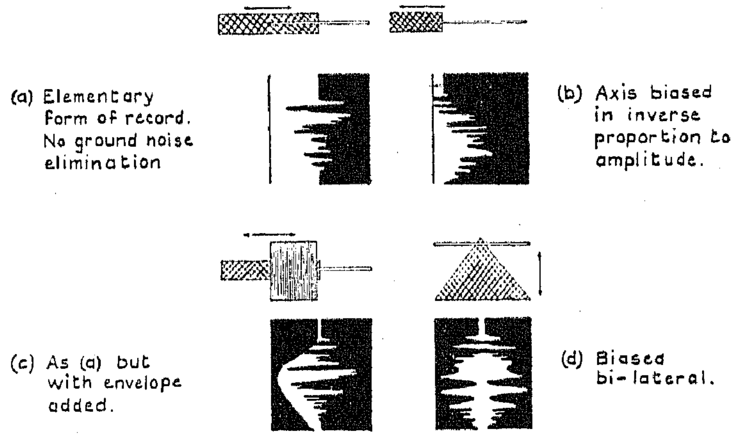
(a) Elementary form of record. No ground noise elimination
(b) Axis biased in inverse proportion to amplitude.
(c) As (a) but with envelope added.
(d) Biased bi-lateral.

Fig. 5.—Ground-noise elimination on variable-area positive record.

For ground-noise elimination, all unnecessary clear track is removed. The rate of change of axis or envelope must be less than that of the minimum reproducible frequency.

The greatest advance of recording technique which has occurred recently, and which is, I believe, still not in use commercially, is termed push-pull recording. In principle the positive and negative half-cycles are divorced, and recorded on either side of a clear space along the track centre. In addition, both positive and negative half-cycles are halved in amplitude and each half amplitude recorded symmetrically on either side of axes displaced one-quarter and three-quarters of the track width respectively.

Many optical arrangements may be used for reproduction, but in principle the light modulated by the two halves of the track must be directed to two separate photo-electric cells or to two separate cathodes in one cell. The cathodes are connected each to one half-winding of the push-pull transformer.

This kind of track has two important advantages. In the first place, ground-noise elimination is provided automatically because on the positive film the mean transmission is always proportional to the amplitude. The second advantage is concerned with the reduction of harmonic distortion due to lack of resolving power and due to stray light following the recording edge. In the case of any other system of variable-area recording the density gradient at the record edge extends on the same side of the axis for both positive and negative half-cycles. As previously mentioned, this gives rise to a shifting of the axis, which introduces a harmonic content variable with frequency and an attendant superimposed distortion if the track amplitude varies at audio frequency. In the case of push-pull track the image-spread occurs in opposite directions, and there is no axis-shift. This does not of course remove harmonic distortion completely, but only one cause of it.

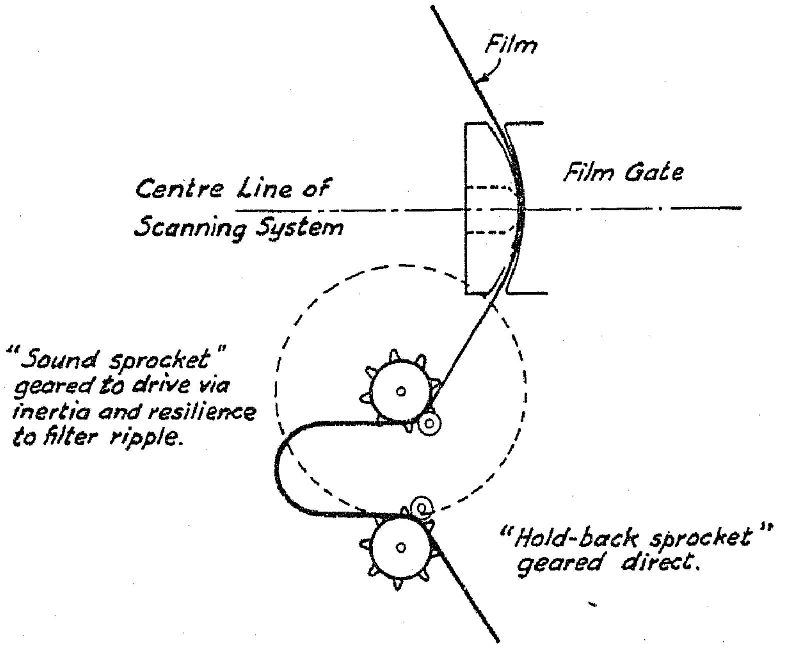
Film
Film Gate
Centre Line of Scanning System
"Sound sprocket" geared to drive via inertia and resilience to filter ripple.
"Hold-back sprocket" geared direct.

Fig. 6.—Diagrammatic arrangement of simple sound head.

(b) The Sound Head

Under this heading can be included all equipment which has as a primary function the task of converting the photographic record into equivalent electrical energy.

Equipment for propelling the film at constant speed in the correct path.

The major difficulty in the way of obtaining sufficiently constant velocity of film travel is the fact that film shrinks irregularly throughout its useful life. In the picture projector the speed of propulsion must be related to the perforation pitch to obtain registration. It is necessary to propel the film by means of its perforations in the sound head, also because the actual length of film per unit perforation pitch is a variable quantity. The tooth pitch of the propelling sprockets is fixed, whereas the perforation pitch of the film is continually varying and therefore constant velocity of propulsion at the sprocket is impossible.

In addition to sprocket-tooth ripple, irregular film propulsion is caused by sprocket and shaft eccentricity and by disturbances due to gears and driving chains. All these causes of irregular propulsion result in frequency modulation of the reproduced sound. The maximum acceptable value of frequency modulation is related to the power range of the reproducer equipment because the aural effect must be kept below the minimum signal. Increases of power range have all been achieved by lowering the total background noise so that a smaller minimum signal can be reproduced. (This statement excludes volume expansion, which will be referred to later.) The extension of the power range in the direction of the minimum signal has called for a corresponding decrease in the value of frequency modulation due to sprocket ripple, etc.

In the early days of the talking film the available power range of 35 db. called for certain limits of eccentricity and partial filtering of gear and chain disturbances. This was usually achieved by a mechanical filter system in the drive to the sound sprocket, and the isolation of " take up " disturbance by following the sound sprocket by a free film loop prior to a " hold back " sprocket: this mechanical filter usually consisted of inertia attached to the sprocket shaft receiving rotational power through a resilient member (Fig. 6), the whole being damped to a value of approximately half critical damping by means of fluid friction.

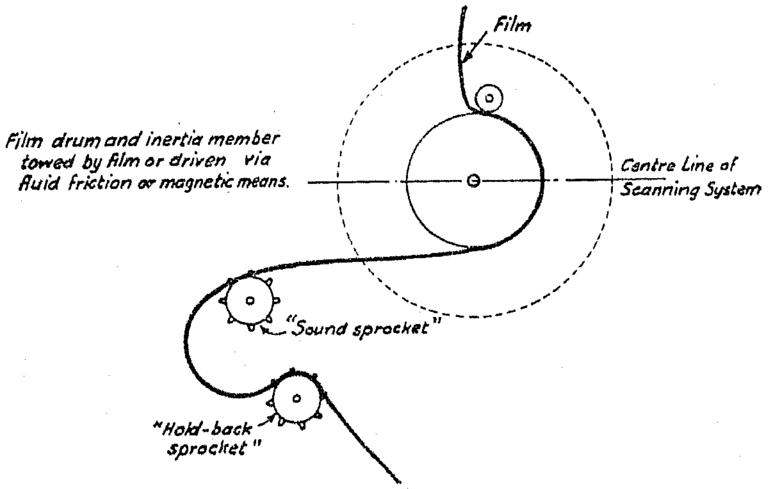
Film
Film drum and inertia member towed by film or driven via fluid friction or magnetic means.
Centre Line of Scanning System
"Sound sprocket"
"Hold-back sprocket"

Fig. 7.—Diagrammatic arrangement of " drum " sound head.

The more recent increase of power range to 50 or 55 db. has called for more complete filtering in the existing position and the addition of a mechanical filter to limit the amplitude of sprocket-tooth ripple and sprocket eccentricity. This must obviously be located between the " sound sprocket " and the scanning point, and a convenient mechanical arrangement consists in what is usually referred to as a " drum head " (Fig. 7). The track is scanned as the film moves in contact with the periphery of a rotating drum. This drum has associated with it an inertia member which operates in conjunction with film loop resilience between the drum and the towing sprocket. Free oscillation of such a combination has been damped in various ways, notably by eddy-current coupling with an additional inertia member, or by separating the original inertia member into two components of widely differing inertia with fluid frictional coupling. The major portion of the inertia is free running, and the minor portion solidly coupled to the film drum.

The " sound " sprocket which provides the driving force for this assembly may still be driven via its own mechanical filter system to lower the value of transmitted gear and chain ripple. Alternatively, the drum filter system may be sufficiently large to take care of all mechanical frequency modulation. This latter is difficult to achieve if the film is called upon to transmit all driving power to the drum system. The eddy-current filter system, however, provides an ideal means for supplying rotational power to the drum, leaving the film to supply only sufficient power to hold the drum at the mean film velocity.

The drum head in its various forms has another advantage over a fixed scanning gate in that it prevents the " pile up " of emulsion with " green " film. This occurrence normally changes the plane of the track at the scanning point, with consequent loss of optical focus and attenuation of the frequency characteristic.

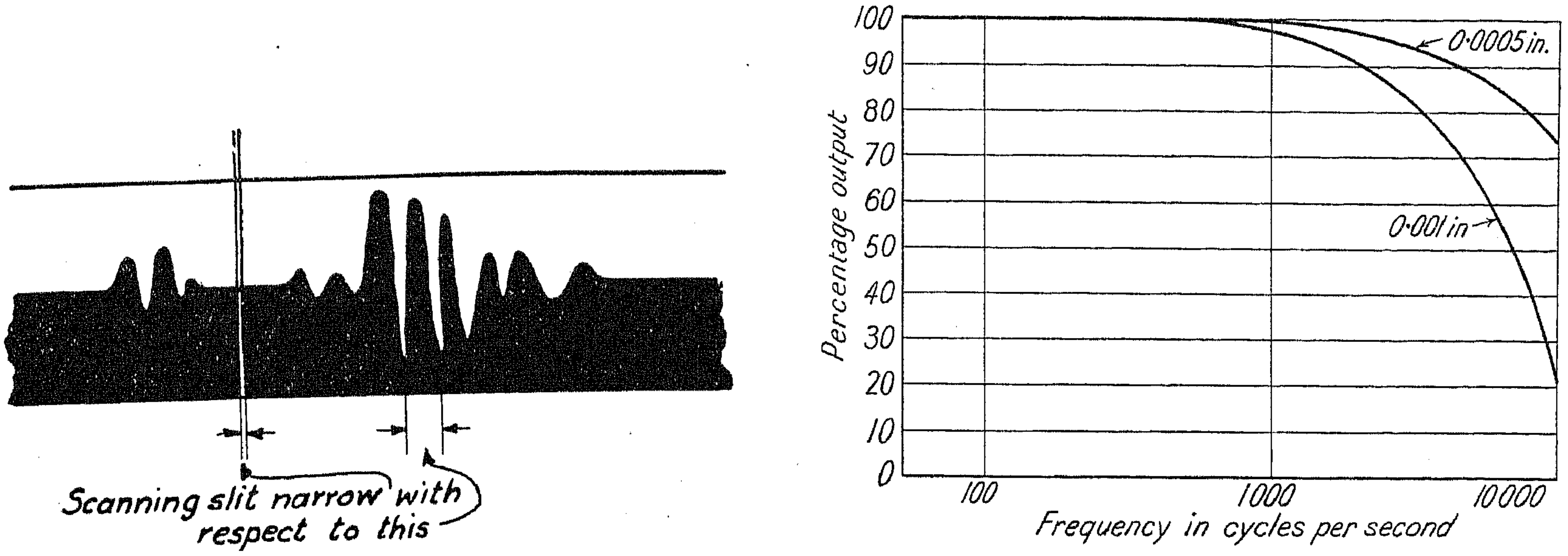

Fig. 8.—Diagrams illustrating that the recorder and reproducer scanning slits must be narrow by comparison with the recorded wavelength of highest frequency.

NOTE.—The right-hand diagram shows the attenuation with frequency for 0·0005-in. and 0·001-in. slits.

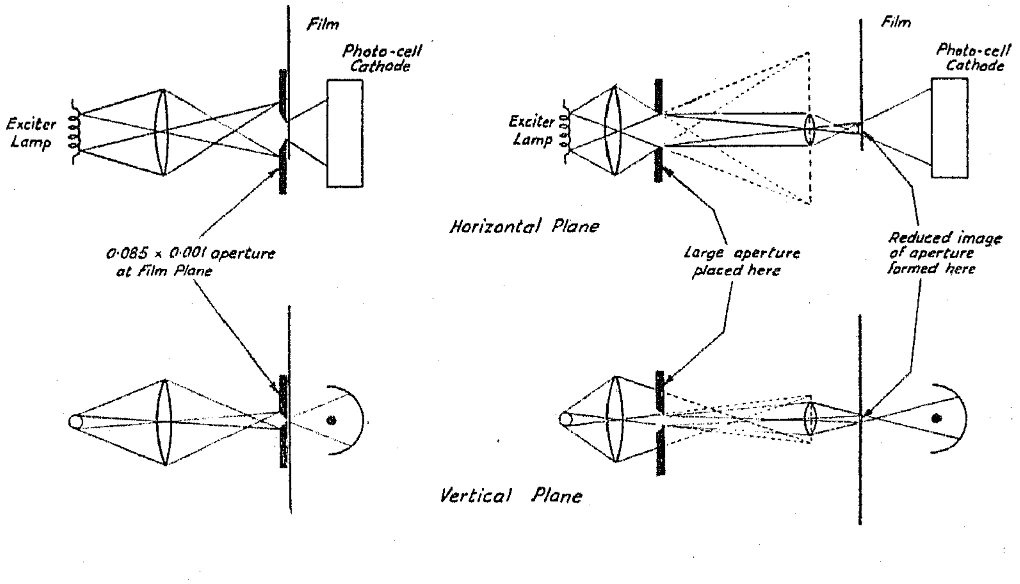
Film
Photo-cell Cathode
Exciter Lamp
0·085 × 0·001 aperture at Film Plane
Film
Photo-cell Cathode
Exciter Lamp
Horizontal Plane
Large aperture placed here
Reduced image of aperture formed here
Vertical Plane

Elementary Arrangement. *Normal "Imaged Slit" Arrangement.*

Fig. 9.—Two methods for scanning " track."

The optical scanning system and photocell.

It is probable that more development work remains to be done on this part of the equipment than on that discussed in the previous section.

The sound track is scanned by a slit of rectangular area bounded by the full sound-track width but very narrow in a direction longitudinal to the film travel. The actual dimension in this narrow direction is determined by the velocity of film travel and the permissible attenuation over the frequency range to be reproduced (Fig. 8). It is apparent that the scanning slit must be narrow compared with the wavelength of the highest frequency recorded on the track, because when the slit width becomes equal to the recorded width of the cycle the modulated output at that frequency will be zero.

For 35-mm. film in commercial practice the track wavelength at 10 000 cycles per sec. is 0·0018 in. The effective width of the film scanned at any instant is usually 0·0004 or 0·0005 in.

The simplest way of providing the required scanning is to place a rectangular aperture of the required size in contact with the emulsion side of the moving film together with a source of illumination on one side and a photo-electric cell on the other. This elementary method was used in the early days, but was soon discarded owing to the mechanical difficulties of making a slit of the required narrow dimension and keeping it free from dust and dirt during operation.

A logical development of the foregoing was to provide a slit of, say, 5 to 10 times the required size and use an image of this slit formed on the film by the use of a corrected objective lens (Fig. 9). Illumination is provided by means of a single-coil horizontal-filament lamp. The filament image is formed in the objective by means of a condenser and the mechanical slit placed at the waist of the beam. This general arrangement has become almost standard practice.

It is possible to reverse the conventional layout and use what is termed the projection scanning system. The sound track is illuminated in the same way as the mechanical slit in the previous case, and an enlarged image of the illuminated track formed on the slit is placed with its objective at the rear of the film. This arrangement has particular optical advantages in a system designed for the production of " push-pull " track.

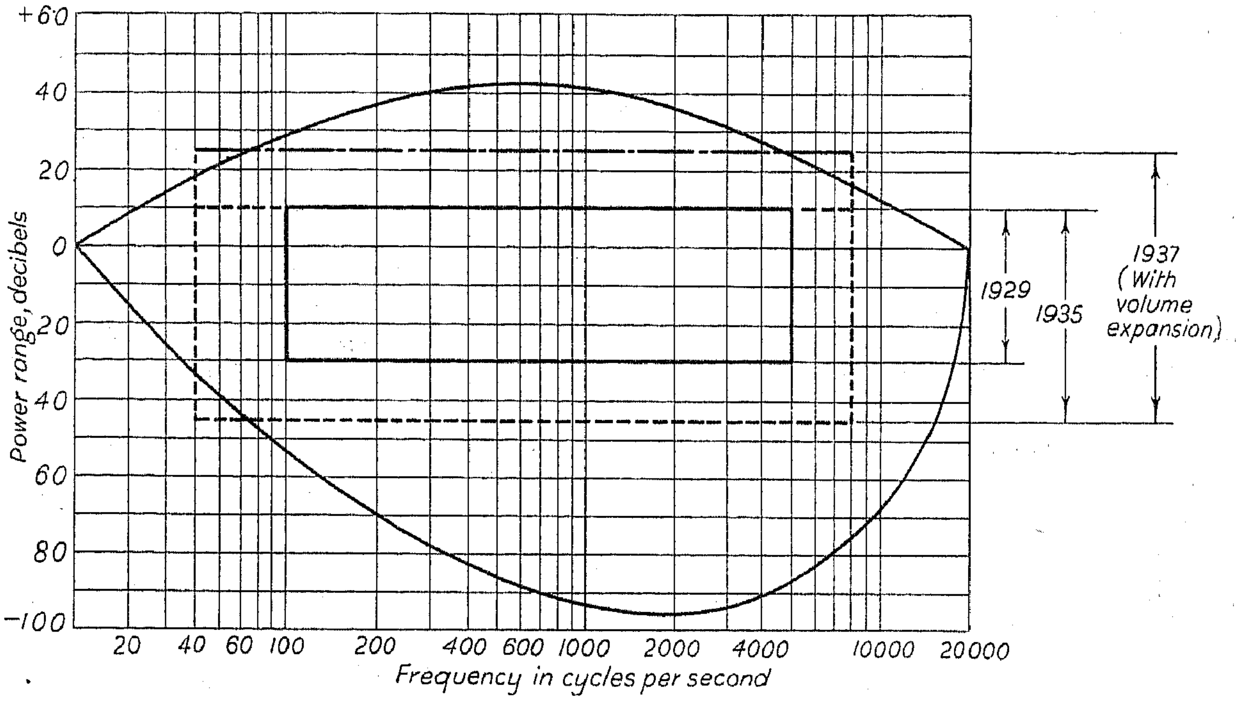

Fig. 10.—Improvements in amplifier power range, 1929–37.

In passing, it should be mentioned that some work has been done on systems employing a single stretched horizontal wire filament lamp imaged directly with the required reduction on to the track. Optically this is ideal, but it is very difficult to make a filament of the required size which will remain exactly straight and have a constant temperature at all points along its length.

Other improvements which have taken place can be summarized as follows:—

The accuracy of form of the image slit has been improved by paying particular attention to the requirements of optical correction in the objective. The caesium photocell commonly used has a spectral sensitivity composed chiefly of two peaks, one in the red and the other in the violet end of the spectrum. As the energy emission of the exciter lamp is all in the yellow to infra-red end, it has been found advisable to provide chromatic correction of the objective for a band in the red. A second factor which must be considered in this connection is the depth of focus of the objective related to the possible movement of the moving film from the plane of nominal focus.

The distribution of illumination along the length of the slit image is of great importance in the reproduction of variable-area track. A falling-off at the slit ends due to optical characteristics and a variation along the length due to filament structure must be taken care of, and these factors have only recently received the attention which they deserve.

Unequal sensitivity over the cathode surface of the photocell has sometimes been overlooked, and modern apparatus takes special care to ensure that the modulated light falling on the cell cathode covers a constant area and varies only in intensity.

Finally, it can be stated that improvements have been made in the means for focusing and aligning accurately the slit image upon the track, particularly the normality of the slit length to the direction of film motion. With increases of reproduced frequency-range, it has become more and more important to work to very small tolerances in this connection.

(c) Amplifiers and Loud-Speakers

It is almost essential that the improvements which have been made in amplifier design should be considered in relation to the loud-speakers which they are to feed.

In early equipments the amplifier frequency-response was limited to the range between 100 and 5 000 cycles per sec. and had its peak at 4 000 cycles, partially to compensate for attenuation in recording and loud-speaker characteristics. The power range of the amplifier was considerably restricted by residual noise in the valves and thermal agitation in the coupling circuits. Its value was usually little more than that available from the film (approximately 30 db.). As the amplifier range was at least as great as the film range, it was considered to be satisfactory, although modern practice obtains a volume range of 70–75 db. (Fig. 10).

Amplifier distortion was measured as the percentage of 2nd harmonic introduced in the output circuit when a sinusoidal voltage was applied to the last-stage grid. A value of 5 % 2nd harmonic at full load was considered to be satisfactory and all higher harmonics were neglected, as they were assumed to be of lower amplitude and less audible.

The trend of amplifier design has been towards a wider frequency range, a reduction in background noise with its corresponding increase in available power range, and a reduction in harmonic content. A frequency range flat between 50 and 8 000 cycles per sec. is found to be satisfactory at the present stage of the art, although there is no difficulty of course in considerably extending this range in either direction (Fig. 11). It is found, however, that an upward extension increases the background out of all proportion to the gain in quality, whilst a downward extension would interfere too much with the problem of providing the ground-noise elimination on the track. These two points have been considered in the first section of this Address.

It is now agreed that harmonics higher than the 2nd, whilst of smaller amplitude, are liable to be more readily audible as distortion; 1 % of 7th, 9th, 11th, or 13th harmonic can be detected as readily as 5 % of 2nd harmonic. In modern amplifiers, therefore, the overall harmonic distortion is limited to a value of less than 1 % of the fundamental over the whole power and frequency range.

Power outputs used vary largely with the size of cinema and the type of loud-speaker employed. Outputs of from 5 to 75 watts are common. In early equipments there was a tendency to use very large power outputs in an attempt to compensate for lack of intelligibility and low loud-speaker efficiency due to limited frequency range. Following this there was a general tendency towards lower powers, but to-day outputs are again on the up grade to allow for the incorporation of volume expansion.

One of the most interesting of recent developments is the extension of the power range by a volume-expansion circuit. The circuit is so arranged that small input signals are amplified less than large input signals (Fig. 12). The result is an automatic extension of the volume range of some 10 to 15 db. To make the maximum use of automatic volume expansion, it is necessary to use automatic volume constriction during the recording process to some predetermined characteristic, and then to introduce the equivalent expansion in the reproducer. Restriction of the volume range is always necessary during recording and is achieved at present by manual control, but, even with the incorrect matching of the manual control and automatic expansion, considerable improvement is achieved in the sound reproduction by the volume-expander circuit. The improvement is less marked on speech than on music, but some advantage is gained here by the reduction of background noise during all low-amplitude sections.

Early loud-speaker assemblies consisted of groups of cone-type moving-coil speakers mounted on flat baffles, arranged down each side of the screen, or two or four horn-type speakers driven by moving-coil units and assembled behind the screen and in the orchestra pit. The frequency response was limited to the range 150–4 000 cycles per sec. approximately, generally with a considerable peak in the response in the 2 500- to 4 000-cycle band. Non-linear distortions were appreciable.

Directional baffles and exponential horns fitted to moving-coil speaker units increased the efficiency and the directional control of the sound in consequence; commercial speakers were generally of two types—the large-cone short-horn and the small-diaphragm long-horn types. A similar order of performance was produced from either type.

The limited frequency-range offered opportunities of improvements, and the first approach to the problem

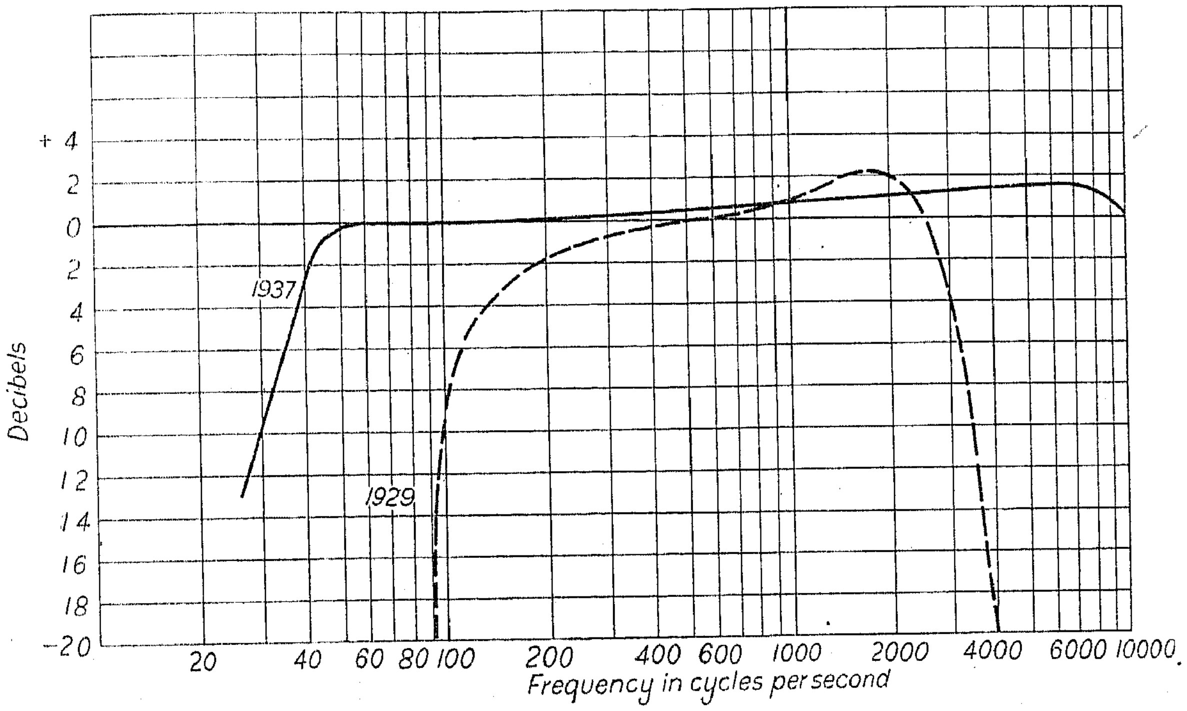

Fig. 11.—Improvement in amplifier frequency characteristic, 1929–37.

consisted of adding extra speakers to cover the bands above 4 000 cycles and below 150 cycles per sec., or in some cases modifying the existing speaker to improve the low-frequency response and adding extra speakers to cover the range above 4 000 cycles per sec. In the 3-way speaker system the extension of the low-frequency end of the range was obtained by a group of two, three, or four large-diameter cones mounted on a large flat baffle; while in all cases the extension of the high-frequency end was obtained by small high-frequency speakers, generally mounted in the mouth of medium-frequency speakers.

Filter networks were added in the amplifier output circuit in order to divide the frequency range between speakers.

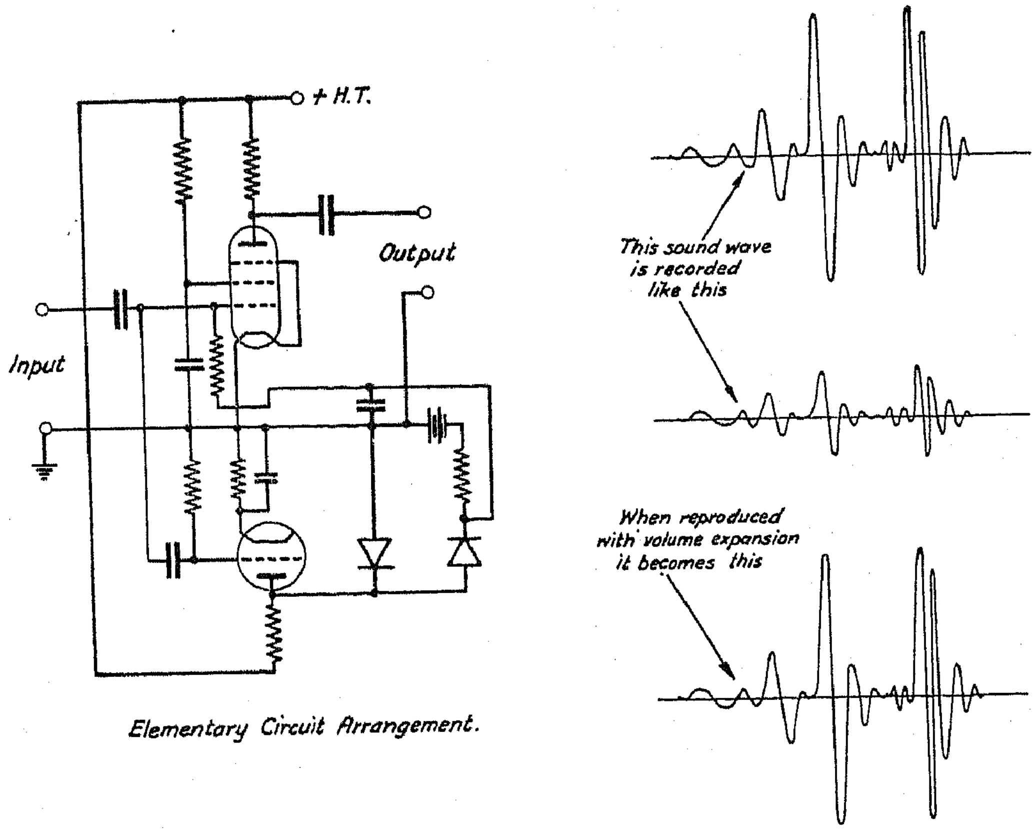
+ H.T.
Output
Input
This sound wave is recorded like this
When reproduced with volume expansion it becomes this

Elementary Circuit Arrangement.

Fig. 12.—Volume expansion in reproducer: effective increase in power range 10–15 db.

The extension of the upper end of the frequency range to 10 000 cycles per sec. proved a little premature, mainly owing to the emphasis it placed upon distortion occurring in certain parts of the system, but in part owing to the method of extending the range.

Further research made it possible to cover the whole range of 50–8 000 cycles per sec. with a maximum of two speaker groups, one group generally consisting of several large cones in a folded horn covering the range from 50 cycles to 300–500 cycles; and the second group consisting of one, or, more rarely, two horns, driven by two units covering the range from 300–500 cycles to 8 000–8 500 cycles.

Careful design of the low-frequency and high-frequency speaker units produced a characteristic which deviated from the mean by a much smaller amount, and reduced the non-linear distortion prevalent in earlier systems (Fig. 13).

Non-uniformity of distribution at high frequency was overcome by subdivision of the high-frequency horn into a large number (3–18) of smaller horns, all mounted together and driven from a single header operated by two units wired in parallel to minimize risk of failure.

Transient distortion is minimized by the improvement in frequency range, by achieving linearity within the range, by the improved damping of the moving system due to parallel operation of speaker units, and by the use of amplifiers presenting a low output impedance to the speakers together with gap diversities in the region of 20 kilolines per cm^2. This is the present state of the art. Perfection has not been reached.

Future development along the same lines will consist in further improvements in efficiency, linearity of response, and reduction of non-linear distortion. It is a little more difficult to forecast the development along different lines, but it seems probable that single-unit mechanism covering the complete range will eventually return.

(d) Cinema Acoustics

It is impossible to conclude this survey of sound-film equipment without considering cinema acoustics. In fact, it is probably true to say that the next step towards perfect sound rests with the acoustics of the auditorium rather than with the apparatus.

The acoustic properties of the auditorium have always been the greatest variable and the one most difficult to cope with in sound reproduction. The shape, size, properties, and materials used all play a most important part in the final result, and even to-day it is difficult to predict with certainty the effect of any scheme unless it is an exact copy of some previous construction.

W. C. Sabine laid the groundwork for auditorium acoustics and established the relation between optimum reverberation time and volume of the hall for good aural results. If the reverberation time is too long, successive sound impulses are interfered with by the reflected sound

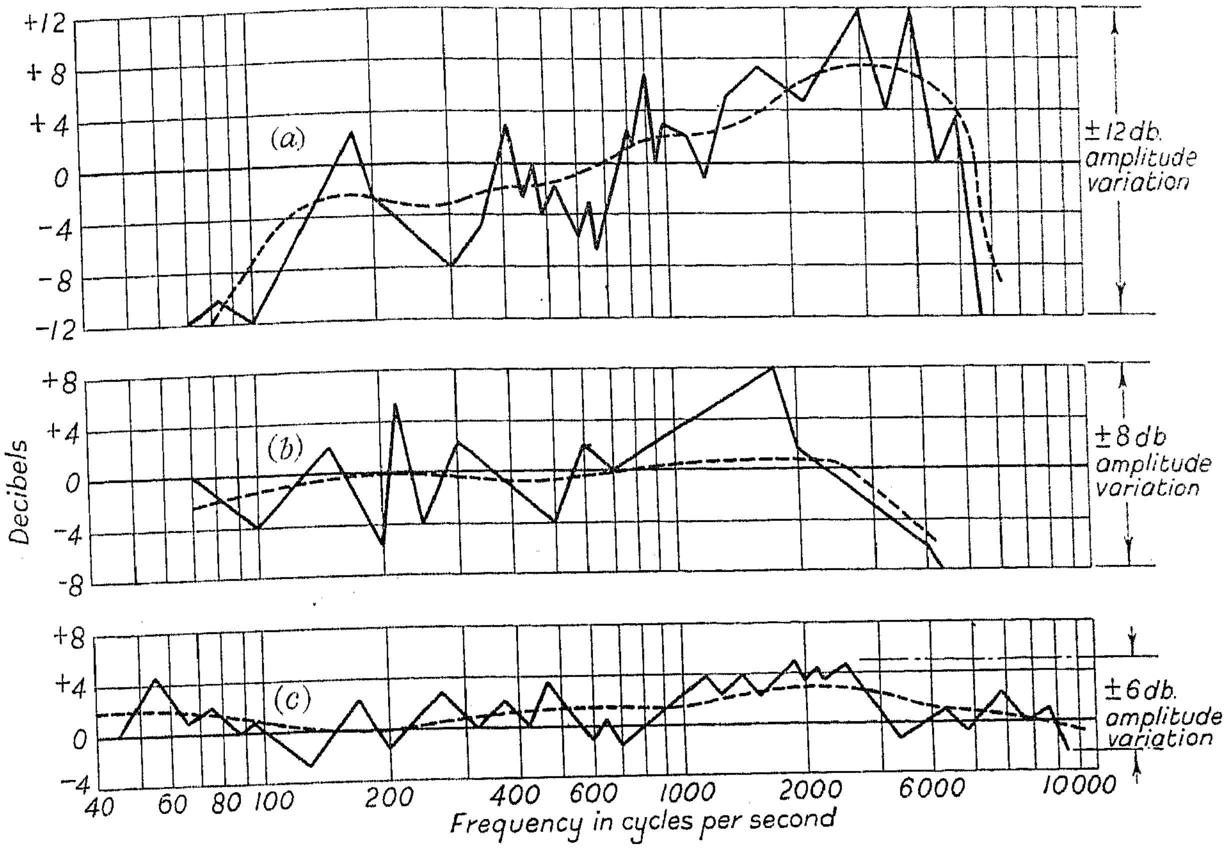

Fig. 13.—Frequency characteristics of loud-speaker assemblies, 1929–37.

(*a*) Loud-speaker on flat baffle, ± 5 db. spread from mean.
(*b*) Loud-speaker in directional baffle, ± 6 db. spread from mean.
(*c*) 1937 combination, ± 2 db. spread from mean.

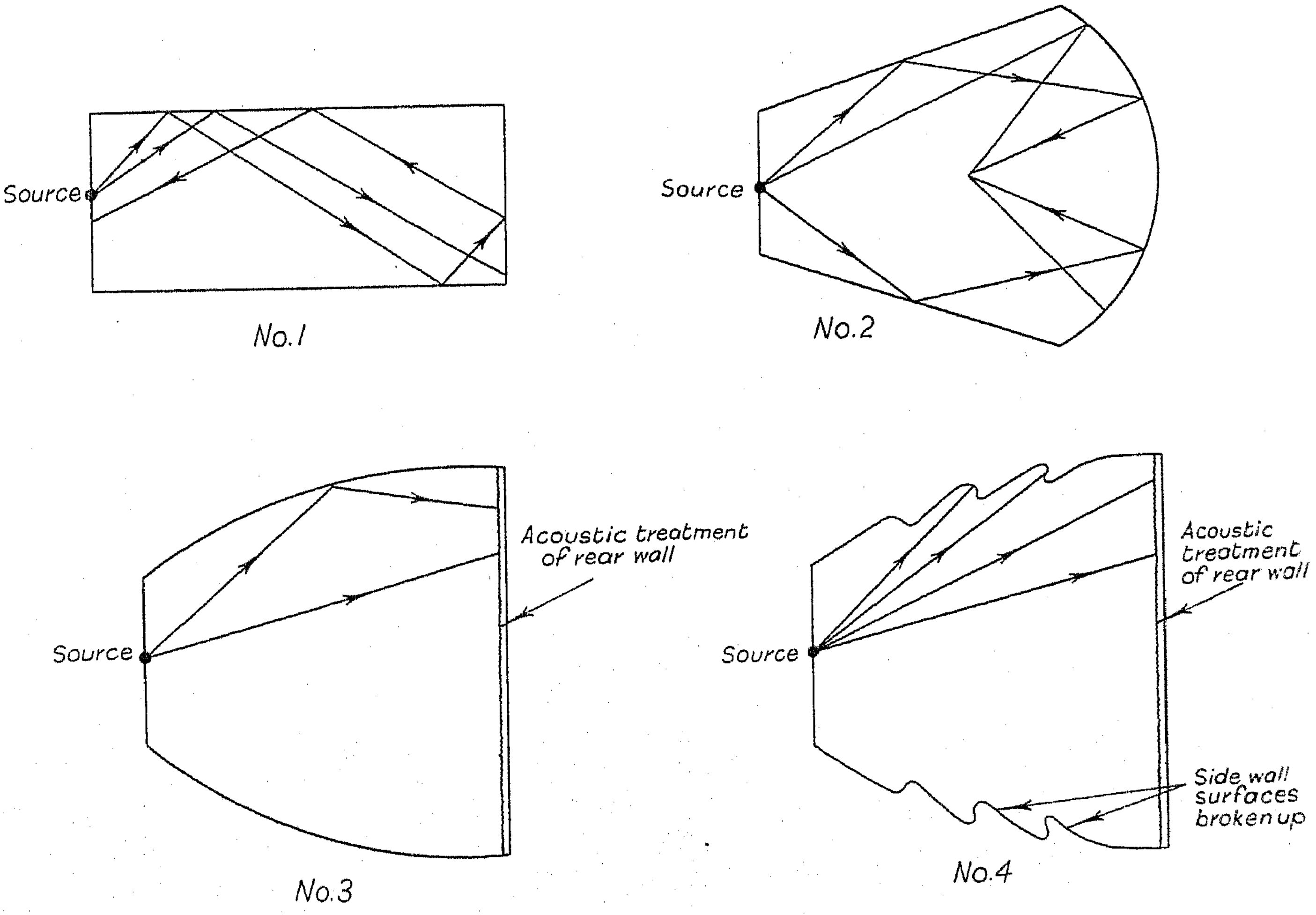
Source
No.1
Source
No.2
Source
Acoustic treatment of rear wall
No.3
Source
Acoustic treatment of rear wall
Side wall surfaces broken up
No.4

Fig. 14.—General trend of auditorium plans.

No. 1. Rectangular plan gave continuous cross-reflection.
No. 2. Curved rear wall tends to focus sound at one point.
No. 3. Some reflection from side walls.
No. 4. Scattered reflection towards source.

waves of previous impulses, and the intelligibility of speech is lost, while too short a reverberation time causes a hard "dead" quality in the reproduction. The accuracy of Sabine's curve was surprising, obtained as it was by experimental methods from a study of numerous halls, and more recent data calculated on the basis of physiological characteristics of the ear show a close agreement with the original data.

The reverberation time is controlled by the quantity and absorbing characteristic of all sound-absorbing material in the auditorium, including the audience, chair upholstery, carpets, curtains, etc., and in all the early work the distribution of the sound absorbent was not considered important as long as the requisite quantity was present. In cinema auditoriums, however, the position of the sound-absorbing material is important, because the source is situated at one end of the hall and sound is directed down the hall on to the audience. First reflections from the walls and ceiling are very important, and in many cases over-treatment of the hall has resulted from the addition of too much sound-absorbing material on these danger points.

The importance of the correct reverberation time in the hall was realized from the first introduction of the sound film, but it was the practice to measure the reverberation at a fixed frequency, usually 500 cycles per sec., without reference to the fact that the reverberation-time/frequency characteristic was not linear. It was some years before suitable equipment was available for measuring the reverberation time at all frequencies. With improved methods of measurement and the greater demand, more suitable materials became available, and the question of accurate placing of the material was considered.

Modern halls are carefully proportioned to give the maximum seating capacity per cubic foot of auditorium, and it is common experience to find that the carpets, seats, and audience supply the majority of the sound absorbent required (Fig. 14). Additional sound-absorbing material to reduce serious first reflections (usually necessary on the back wall directly opposite the loud-speakers) must be sparingly used, and chosen to complement the characteristics of other absorbents. Wherever the auditorium or the decorations can be so designed as to assist in the reduction of the first reflections, this should be done, rather than rely upon acoustic treatment to obtain the required result.

THE TENDENCY OF FUTURE DEVELOPMENTS

It is evident that amplifiers and loud-speakers are in a more advanced state of development than the other links in the chain. Cinema acoustics is becoming better understood, but it is not yet possible to predict exactly with confidence the overall characteristics to be expected from a known equipment when installed in a new and untried auditorium.

The sound record itself is undoubtedly the place where improvement is most necessary. In particular, the standard of recorded quality on release prints should be brought nearer to the faithfulness which can now be obtained under carefully-controlled laboratory conditions. Whether this required improvement will be brought about by the general adoption of push-pull methods is a moot point. It seems possible that a similar improvement might be obtained by advances in the photographic materials and technique, coupled with an intensive development in the associated electro-optical components. In this connection the scanning system in the reproducer is not free from suspicion. A possible compromise may be provided by the general adoption of push-pull recording in the studios, assisted by the aforementioned developments aiding the re-recording of the sound to conventional tracks for general release.

The one link in the chain of faithful sound reproduction which is entirely missing is concerned with binaural listening. A normal person hearing original sound is able to locate the position of the source in space by virtue of the fact that the ears receive the sound in two components which differ slightly in phase, frequency characteristic, and amplitude. When sound is recorded and reproduced on a single channel this effect is lost and the listener is only able to judge the position of the reproducing loud-speaker and not the position of the original source with respect to the camera lens via which he views the scene.

A single-channel system can only be true for an observer who was born and has always lived with the use of one ear. It is only true in this case if reproduction is heard with a headphone.

For a normal listener the binaural effect can be obtained with a 2-channel system if headphones are worn, and for faithful results the two microphones must be placed at the ends of ear passages in a model of the observer's head.

When we attempt to reproduce sounds in the cinema the conditions are still further modified. In the first place, each member of the audience looking at the picture expects the sound to be reproduced at the screen as though the screen were at the sound source. Secondly, the acoustic properties of the hall add their own coloration to the sound in its passage between loud-speaker and listener.

One possible method which has given promising experimental results is to use three completely separated channels. The three microphones are placed round the source, and the loud-speakers are placed in similar relative positions. Movements of the source within the range of the microphones are thus accompanied by similar movements of the source image at the screen. Certain obvious difficulties such as the need for multiple sound records on the film, the varying acoustic conditions of the studio and the auditorium, and the limitations of a 2-dimensional screen, prevent the rapid growth of this development. It is, however, conceivable that we shall one day have binaural sound reproduction to complement stereoscopic and true-colour pictures.

In conclusion, I wish to express my thanks to the directors of the British Thomson-Houston Co., Ltd., for permission to publish many of the details embodied in this Address; to Mr. H. Warren, for the loan of the equipment used in the demonstration; and to my colleagues, Mr. G. S. Lucas, Mr. S. R. Eade, and Mr. J. Moir, for information which they kindly supplied.

THE DEPENDENCE OF THE INTER-ELECTRODE CAPACITANCES OF VALVES UPON THE OPERATING CONDITIONS[*]

By T. IORWERTH JONES, M.Sc.

[From the National Physical Laboratory.]

(Paper first received 9th April and in final form 18th June, 1937.)

SUMMARY

The results of the measurement at a frequency of 1 million cycles per sec. of the effective inter-electrode capacitances under working conditions of a variety of valves are tabulated, together with an estimate of the net capacitance residing between the active elements themselves.

The grid-filament capacitance shows an increment which increases with anode current up to the point at which grid current flows. The increment diminishes at a given value of anode current as the anode voltage is increased. Experiment shows that this increment in capacitance is not a simple function of anode current, neither of anode-filament nor of mutual conductance. It is augmented the higher the filament temperature and is probably a function of the initial velocity of the electrons.

The effective grid-anode capacitance suffers a reduction as the anode current increases, but the reduction is much smaller proportionately than the increase in grid-filament capacitance.

Every type of valve examined displays the effect—even the small acorn triodes and pentodes, in which the increment represents a 50% augmentation of the "cold" value of C_{fg}.

(1) INTRODUCTION

In view of the evidence furnished by the work of Hartshorn,[†] Benham,[‡] Moullin,[§] and Baker,[||] on variations in the effective value of the inter-electrode capacitances of thermionic valves, efforts have been made to effect experimentally a separation of these capacitances under working conditions and to study the changes in their effective values due to modifications of the operating conditions. It was considered that the radio-frequency bridge[¶] secured more stable conditions than were attainable using resonance methods and that its suitability for testing three-terminal apparatus should enable a separation of the individual capacitances to be made. The latter advantage was realized as far as the grid-anode capacitance (C_{ag}) and the grid-filament capacitance (C_{fg}) were concerned.

Since the observations of Baker and Moullin had confirmed the existence of the effect in the case of the dynatron condition, the initial stages of the present investigation were directed to a study of the case of the valve with a negative potential applied to the grid. The primary object was to decide whether some instability of the frequency of valve oscillators might be due in part to the dependence of the effective inter-electrode capacitances on the working conditions and whether the effect was a characteristic of valves in general. If all valves suffered from this defect then it was clear that it would affect a master oscillator in virtue of the variability of the input impedance of the succeeding power amplifier as well as by the changes in effective value of its own inter-electrode capacitances.

A close dependence of the effective grid-filament capacitance on the steady operating voltages—anode (V_a), grid (V_g), and filament (V_f)—would imply a dependence of the natural frequency of the system, of which the valve formed a part, upon the operating voltages, especially at very high frequencies, when the inter-electrode capacitance forms a large proportion of the total tuning capacitance. If the relation found connecting the mean anode current (I_a) and the increment in effective grid-filament capacitance proved to be non-linear, there might be a dependence of the mean frequency of a transmitter upon the depth of modulation employed.

Measurements were made on a miscellaneous collection of valves which did not require too extreme a range of anode voltage, since the size of the battery was limited by the necessity for enclosing all the components of the valve circuit in a screening box. A number of these valves were broken open in order to derive an approximate estimate of the capacitance residing between the active elements themselves and of the proportion in which they changed under working conditions. The remainder of the work covered by this paper attempts to correlate the changes observed with the simultaneous changes in grid-anode conductance and mutual conductance taking place in the valve, and with changes in filament temperature.

It is considered that insufficient prominence has been given to the effect in the past, and that such an assessment of its order in present-day types of valves as is undertaken in this paper is highly desirable.

(2) METHODS OF MEASUREMENT

The radio-frequency bridge is suitable for the measurement of inter-electrode capacitances under working conditions, either collectively or individually, with very little modification.

Apart from the circuits employed the procedure in each case was the same. The appropriate valve electrodes were connected to the bridge terminals, and condensers of $0 \cdot 1\ \mu F$ were maintained across each battery. An initial balance was obtained with the filament cold ($V_f = 0$) for the condition of zero anode current and large negative bias of the grid. The battery circuits were then completed, and the grid bias reduced until anode current flowed. After the milliammeter had been read a low-

---

[*] Reprinted from *Journal I.E.E.*, 1937, vol. 81, p. 658.

[†] See Reference (1).

[‡] *Ibid.*, (2).

[§] *Ibid.*, (3).

[||] *Ibid.*, (4).

[¶] *Ibid.*, (5).

resistance shunt was inserted across its terminals before re-balancing the bridge. Bridge balances were adjusted for a number of anode currents, and the increments or reductions in inter-electrode capacitances were deduced without the necessity for disconnecting any electrode from the bridge. This procedure enabled a consistency in the results of $0{\cdot}01\ \mu\mu\text{F}$ to be attained in the quantities $\Delta(C_{fg} + C_{ag})$ and ΔC_{ag}.

(a) $\Delta(C_{fg} + C_{ag})$

The simplest combination to measure is the input capacitance $(C_{fg} + C_{ag})$, for the condition of no anode load. The schematic circuit diagram of Fig. 1 shows the input circuit connected across the capacitance arm of the network in parallel with an open-scale cylindrical condenser capable of observations to $0{\cdot}005\ \mu\mu\text{F}$. The bridge was balanced by the adjustment of this condenser and of a phase-angle device (not shown) in the resistance arm. The alterations required in the setting of the open-scale condenser at a number of grid-bias tappings (or different values of anode current) were noted. Provided negligible phase-angle changes were involved, the differences corresponded exactly to $\Delta(C_{fg} + C_{ag})$. In the absence of grid current this condition was normally satisfied. The complete valve equipment was effectively screened by inclusion within a large copper box which was connected to the top point of the bridge and to the screens of the condensers in the capacitance arms.

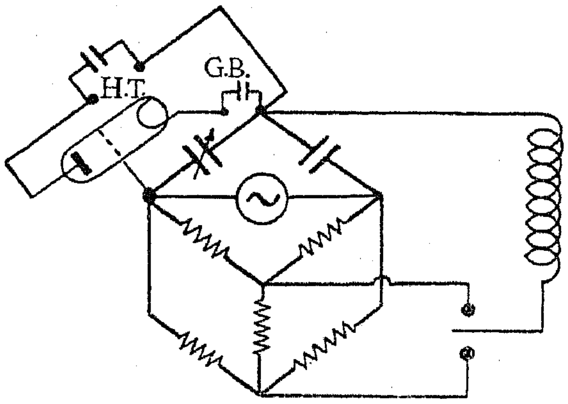

Fig. 1.—Measurement of $\Delta(C_{fg} + C_{ag})$.

It is clear that the anode and the filament are at the same a.c. potential and that the input capacitance is actually $(C_{fg} + C_{ag})$.

(b) ΔC_{ag}

The separation of the effect contributed by the grid-anode capacitance necessitated one or two minor adjustments to the bridge network, as shown in Fig. 2. The box was connected directly to the earthed screen of the bridge. For the measurements, grid and anode had to be connected to the two ends of the capacitance arms. The grid was joined to the detector point and the filament to the screen, i.e. the detector point directly earthed. This arrangement kept filament and grid at the same alternating potential. A circuit consisting of a 2-volt cell and a variable resistance was included to balance the difference in steady potential across the small resistance r due to the anode current flowing through the resistance-arms to the filament. The variable resistance was adjusted each time until the anode current observed in the valve circuit was the same to whichever bridge circuit the detector was applied.

It will be realized that the anode-filament resistance, R_{af}, is thrown across one resistance arm of the Wagner earthing device. This necessitated the connection of a screened resistance box across the other arm in order to balance the bridge.

(c) ΔC_{af}

The case of the anode-filament capacitance, C_{af}, measured either singly or in combination with the anode-grid capacitance as $(C_{af} + C_{ag})$, presents considerable difficulty owing to the necessity in bridge methods of replacing the effective shunting resistance, R_{af}, by an exactly equivalent resistance in the process of substitution. A variable resistance is precluded on the score of variable and indeterminate phase-angle, which would introduce considerable uncertainty into the capacitance measurement. The only alternative available is to use fixed resistances possessing identical shunt capacitances in parallel with the valve and to adjust one or other of the operating voltages V_a or V_g, on lighting up the valve filament and substituting an infinite resistance of the same design for the original one, until the anode-filament resistance satisfies the same balancing conditions of the bridge. This procedure involves repeated interference with the operating conditions of the valve, which takes time after each readjustment to settle down. Another difficulty was the necessity to keep the input voltage low in order to avoid errors due to wave-form distortion in the arm to which the valve was consigned.

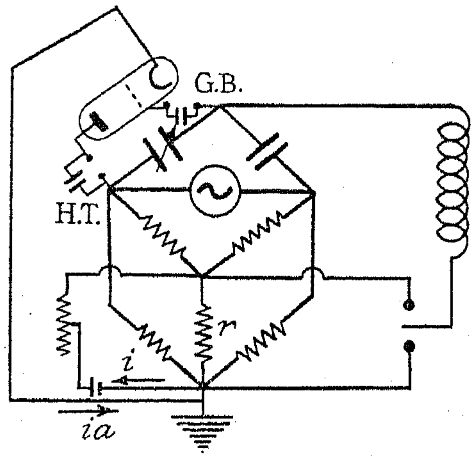

Fig. 2.—Measurement of ΔC_{ag}.

In view of these difficulties in obtaining reliable measurements of the anode-filament capacitance it was decided to seek another method which did not require the substitution of a resistance for the valve when either the filament or the anode circuit was broken. This measurement is of considerable importance, especially in the simpler case of the diode, and is to be pursued further.

In the present paper the account will be confined to the capacitances $(C_{fg} + C_{ag})$ and C_{ag}, from which the behaviour of C_{fg} may be deduced. The separation is desirable from a practical standpoint since the total input capacitance of a valve depends upon these two items separately. Thus if Z = external anode impedance, and R_a = a.c. resistance of valve,

$$\textit{Input capacitance} \simeq C_{fg} + C_{ag} + \frac{\mu Z}{R_a} C_{ag}$$

(3) MEASUREMENTS ON TYPICAL VALVES

The first measurements were made on two power valves, of the small-output and the moderate-output class respectively. These were the PM202 of low filament consumption (0·2 amp.) and the DO/24 of high filament consumption (2 amps.), the anode current for the anode voltages used being restricted to about 20 milliamps. The majority of the observations were obtained at 1 000 kilocycles per sec. by the methods described above.

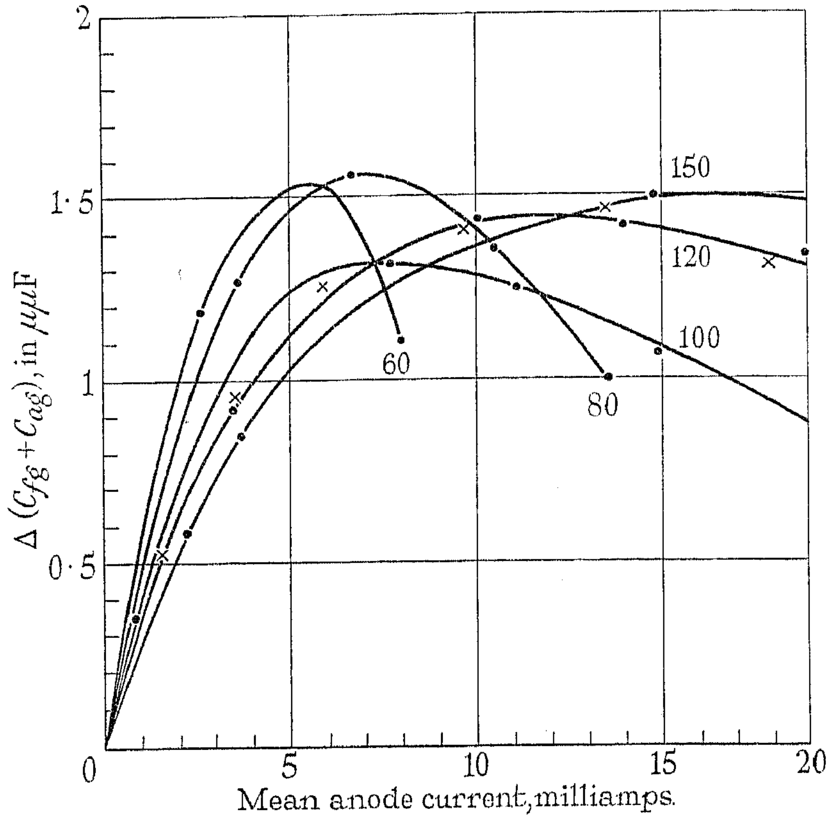

Fig. 3.—Values of $\Delta(C_{fg} + C_{ag})$ plotted against mean anode current (varying grid bias), for PM202 valve.

● Measurements at 1 000 kc.
× Measurements at 100 kc. with $V_a = 120$ volts.

$I_f = 0{\cdot}190$ amp.; $V_a = 60, 80, 100, 120, 150$ volts. Inter-electrode capacitances (cold values): $C_{fg} = 6{\cdot}1\ \mu\mu$F, $C_{ag} = 5{\cdot}2\ \mu\mu$F.

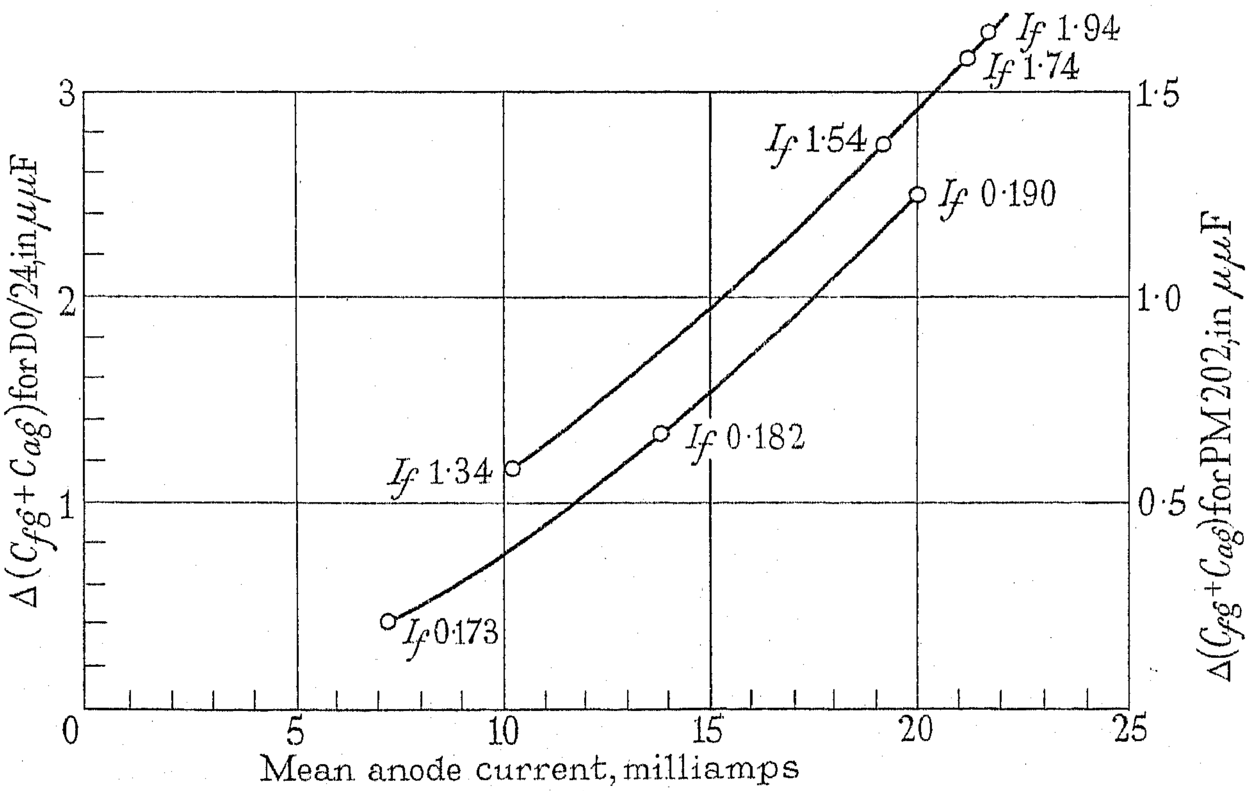

Fig. 4.—$\Delta(C_{fg} + C_{ag})$ plotted against mean anode current at 1 000 kc. (varying filament current), for DO/24 and PM202 valves. $V_a = 150$ volts, $V_g = -10$ volts.

(a) PM202 Valve

The measurements made on the PM202 valve were limited to those of the increments observed in the input capacitance, with no load in the anode circuit, over a range of anode- and grid-voltages. For a number of values of anode voltage, the grid bias was varied to give mean anode currents ranging from zero to 20 milliamps. The diversity of the curves obtained may be seen in Fig. 3. As the anode current increased, readjustments of the filament rheostat became necessary in order to maintain the filament current constant. It was therefore presumed that constancy of filament temperature was not maintained, and that constant filament current did not secure a condition which was capable of exact definition in terms of the primary variables entering into the theory of thermionics. The large dependence of the effective values upon filament current, as shown in Fig. 4, for the PM202 valve, suggested the desirability of resort to a valve of higher filament consumption which could be operated over precisely the same range of voltages.

(b) DO/24 Valve

(i) $\Delta(C_{fg} + C_{ag})$.

Measurements of the input capacitance were repeated for this valve, with the results shown in Fig. 5. As far as can be judged at present, the divergences cannot be regarded as due to errors of measurement. Over the range of anode voltages which have been investigated the curves approach one another far closer than those obtained with the PM202 valve. To a first approximation the increments in $(C_{fg} + C_{ag})$ may be taken to vary with anode current almost independently of anode

Table 1

Valve	V_a	I_a	$\Delta(C_{fg}+C_{ag})$	C_{fg}	C_{ag}	C_{af}
	volts	milliamps.	μμF	μμF	μμF	μμF
VR12B	120	0·0	$(0{\cdot}0_0)$			
(cylindrical thor-tungsten)		0·6	0·21	3·3 (*gross*)	2·7 (*gross*)	2·5 (*gross*)
		1·0	$0{\cdot}2_6$			
		1·4	$0{\cdot}2_8$	0·3 (*net*)	1·1 (*net*)	0·3 (*net*)
		2·0	$0{\cdot}2_8$			
		2·8	$0{\cdot}2_7$			
VR12F	120	0·0	(0·01)			
(flat, oxide-coated)		$0{\cdot}5_5$	0·35	3·4 (*gross*)	6·4 (*gross*)	2·4 (*gross*)
		1·0	0·45			
		1·6	0·50			
		2·4	0·54	0·5 (*net*)	4·6 (*net*)	0·4 (*net*)
		3·2	0·57			
		4·2	0·57			
VT1A	150	0·0	—			
(cylindrical, tungsten)		$0{\cdot}3_5$	0·32	3·4 (*gross*)	2·4 (*gross*)	3·0 (*gross*)
		1·2	0·55			
		2·7	0·74	0·3 (*net*)	1·0 (*net*)	0·3 (*net*)
		3·6	0·80			
R	100	0·0	(0·01)			
(cylindrical)		0·3	0·31	3·4 (*gross*)	2·0 (*gross*)	2·8 (*gross*)
		$0{\cdot}5_5$	0·44			
		0·9	0·48	1·4 (*net*)	0·6 (*net*)	1·3 (*net*)
DER	100	0·0	(0·00)			
(cylindrical)		0·3	0·26			
		0·6	0·39			
		1·05	0·49			
DEA	150	0·0	—			
(flat)		1·4	0·65			
		3·6	0·86			
		6·7	0·93			
		10·4	0·92			
		12·2	0·92			
		14·1	0·91			
LS5b	150	0·0	(0·13)			
(flat)		0·4	0·52	4·4 (*gross*)	3·6 (*gross*)	3·2 (*gross*)
		1·0	0·97			
LS5	150	0·0	—			
(flat)		0·9	0·41	4·3 (*gross*)	3·2 (*gross*)	2·6 (*gross*)
		2·5	0·70			
		4·7	0·88			
		7·8	1·00	1·6 (*net*)	1·6 (*net*)	0·4 (*net*)
		11·3	1·07			
		15·0	1·05			

Table 1—*Continued*

Valve	V_a	I_a	$\Delta(C_{fg} + C_{ag})$	C_{fg}	C_{ag}	C_{af}
	volts	milliamps.	μμF	μμF	μμF	μμF
LS6a		*Filament volts* 4·8				
	150	0·0	(0·21)			
		12·2	0·85	5·0 (*gross*)	6·8 (*gross*)	4·0 (*gross*)
		19·6	1·09			
		25·4	1·23			
		36·5	1·40	2·0 (*net*)	5·1 (*net*)	0·5 (*net*)
		48·5	1·53			
		66	1·57			
		Filament volts 6·0				
	150	13	0·92			
		30	1·45			
		53	1·86			
		70	2·09			
PX25 .. .. .. (flat)	150	0·0	(0·18)			
		0·3	0·41	11·4 (*gross*)	15·0 (*gross*)	5·8 (*gross*)
		1·25	1·16			
		3·9	2·55			
		9·3	$4{\cdot}4_1$			
		17·3	$6{\cdot}1_5$			
		28·2	$7{\cdot}2_5$			
Special VSW150 .. .. (flat, indirectly-heated; grid and anode leads at top)		0·0	(0·05)	1·4	2·0	2·5
		0·25	0·15			
		0·55	0·28			
		1·2	0·46			
		$2{\cdot}5_5$	0·71			
		4·5	0·97			
		7·3	1·18			

Gross denotes normal inter-electrode capacitances of valve in holder.
Net denotes direct capacitances between electrode elements themselves.

voltage. It is conceivable that the divergences may partly be due to progressive approach towards smaller negative grid bias at the lower anode voltages, which necessarily implies a greater amount of grid-filament conductance.

The effect is much less dependent upon the filament current, as will be seen in Fig. 4, for the DO/24 valve.

In all cases the increments have been plotted against mean anode current. The voltage applied to the input circuit being approximately 2 volts (r.m.s.), it is clear that this current may not precisely indicate a definite thermionic condition. With an infinitely small amplitude the mean would not differ appreciably from the normal anode current. It is conceivable, therefore, that some or the divergences may be attributable to this factor.

The dependence of the effect upon frequency was tested by repeating one set of observations at a frequency of 100 kc. The reproduction obtained of the curve relating to an anode voltage of 120 volts, in Fig. 3, was considered to support the assumption that the effect was the same at 100 as at 1 000 kc.

(ii) ΔC_{ag}.

The measurements previously described were obtained with the valves connected to the bridge network as shown in Fig. 1. The circuit of Fig. 2 was then set up for the measurement of ΔC_{ag}.

Time only permitted of a limited investigation of this quantity. The results have been plotted at the bottom of Fig. 6 against the open scale shown in the bottom right-hand corner. In the same Figure, $\Delta(C_{fg} + C_{ag})$ for the same voltage conditions has been plotted, and, using the known values of ΔC_{ag}, deduced values of ΔC_{fg} have been represented on the upper curve.

It will be perceived that the variations in C_{ag} are opposite in sign from those in C_{fg} and of about one-tenth the magnitude. In terms of the cold values of C_{fg} and C_{ag}, the incremental percentage in the latter is only onesixteenth of that in C_{fg}, since $C_{fg} = 9\cdot0\ \mu\mu\text{F}$ and $C_{ag} = 15\cdot1\ \mu\mu\text{F}$.

In the PM202 valve the "hot" capacitances ($i_a = 0$) did not differ from the "cold" values. In the DO/24 valve, on the other hand, C_{fg} did show a slight temperature effect, but C_{ag} showed no change.

(c) Miscellaneous Triodes

A number of valves were collected incorporating the cylindrical and the flat types of electrodes. Some of these were receiving valves and some were small transmitting valves. In one case the grid and the anode leads were brought out at the top.

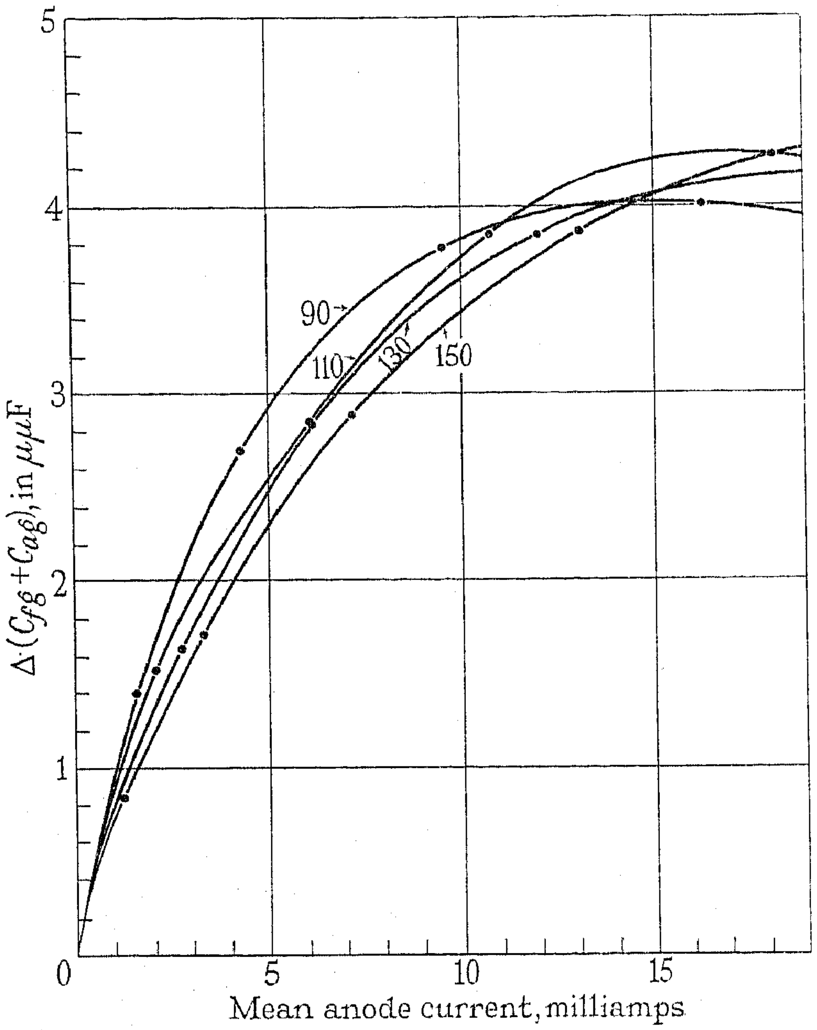

Fig. 5.—Δ(C_{fg} + C_{ag}) plotted against mean anode current at 1 000 kc. (varying grid bias), for DO/24 valve. $I_f = 1\cdot95$ amps., V_a = 90, 110, 130, 150 volts.

Following the methods previously described, the input capacitance was measured for various values of anode current, the filament and the anode battery voltages being maintained constant throughout. Since the effect is of the same order at all anode voltages, measurements, in general, were limited to a small value of anode voltage. In most cases the effect on the input capacitance of lighting the filament was observed. This increment in capacitance is given in brackets for I_a=0 in Table 1. The increment with increase in anode current is expressed as the difference from the capacitance observed with the filament hot. The increase in capacitance is considerably larger in the power valves with a high emission, and in these cases it does not approach a limiting value in the region under examination, whereas in the smaller types there are indications of a maximum value for the small amplitude of input voltage which was employed. This condition cannot be taken, of necessity, to represent the case of a valve in an oscillating circuit, where the amplitude is large. It is conceivable that in such a case a limiting value in the increment may be reached in the operating region, in which case the effect now being explored would only be of secondary consequence as regards frequency variation.

The results embodied in Table 1 indicate that all valves having a filament inside the anode show the effect. The flat electrodes represent a worse case when the initial capacitance is larger.

The inter-electrode capacitances, C_{fg}, C_{ag}, and C_{af}, were measured for most of the valves. One set of values, designated the "gross" values, represents the valve in its ordinary condition in a valve-holder. Such valves as could be broken were tested before and after removing the filament and the grid elements respectively. From the two sets of values an estimate was obtained of the "net" capacitance existing between the active elements. These estimates are scarcely correct to 0·1 μμF.

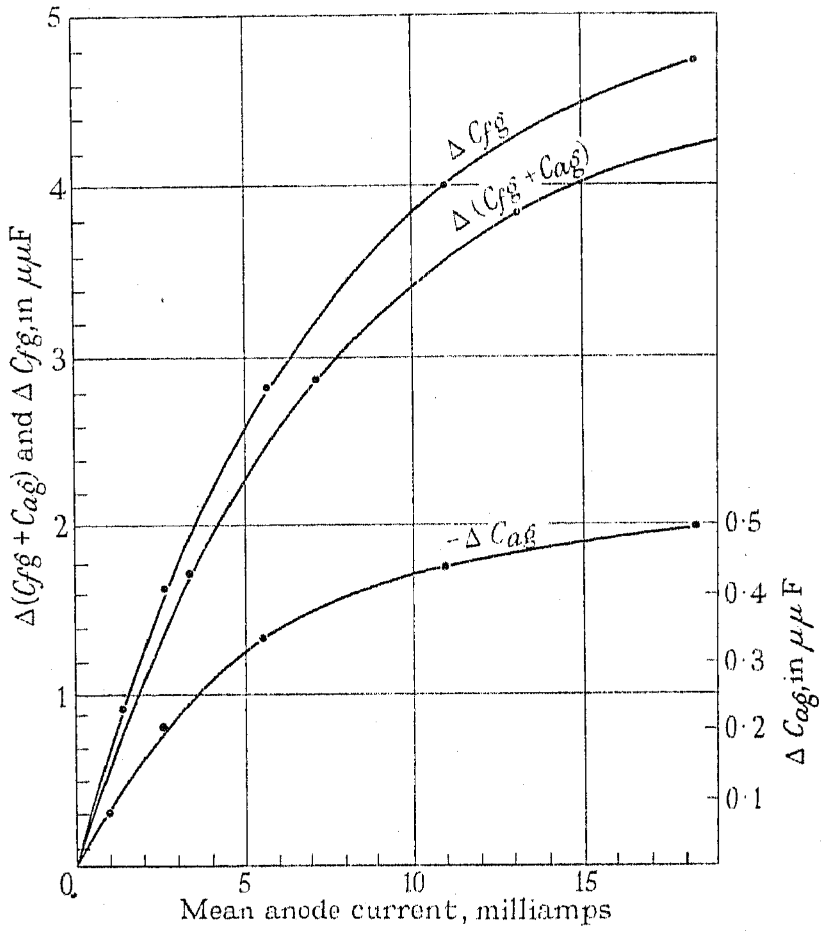

Fig. 6.—Δ(C_{fg} + C_{ag}), ΔC_{ag}, and ΔC_{fg} plotted against mean anode current (varying grid bias), for DO/24 valve.
V_a = 150 volts, I_f = 1·95 amps. Inter-electrode capacitances (cold valves): C_{fg} = 9·0 μμF, C_{ag} = 15·1 μμF.

It will be seen that the increments in several cases are almost equal to the net value of the grid-filament capacitance.

(d) Special Short-Wave Valves (Acorn Type)

Measurements on R.C.A. valves, Types Nos. 954 (pentode) and 955 (triode), were made in accordance with the method previously described. These measurements included an estimate of the contribution of the leads to the gross inter-electrode capacitances of the triode type, made by utilizing a defective valve and breaking it open. The results led to an estimate of the net capacitances between the elements of three triodes examined, and the average values (in $\mu\mu$F) deduced for the individual capacitances were as follows: $C_{fg} = 0\cdot 9$, $C_{af} = 0\cdot 4_5$, $C_{ag} = 1\cdot 2$. The lead capacitances associated with each were as follows: $C'_{fg} = 0\cdot 1_2$, $C'_{af} = 0\cdot 2_0$, $C'_{ag} = 0\cdot 3_2$. The measurements of incremental input capacitance $\Delta(C_{fg} + C_{ag})$ gave the results plotted in Figs. 7 and 8.

(4) FACTORS CONTROLLING THE EFFECT

It has not been possible to deduce any comprehensive results about the nature of the effect from measurements hitherto made, but such conclusions as have been drawn may be briefly stated and illustrated.

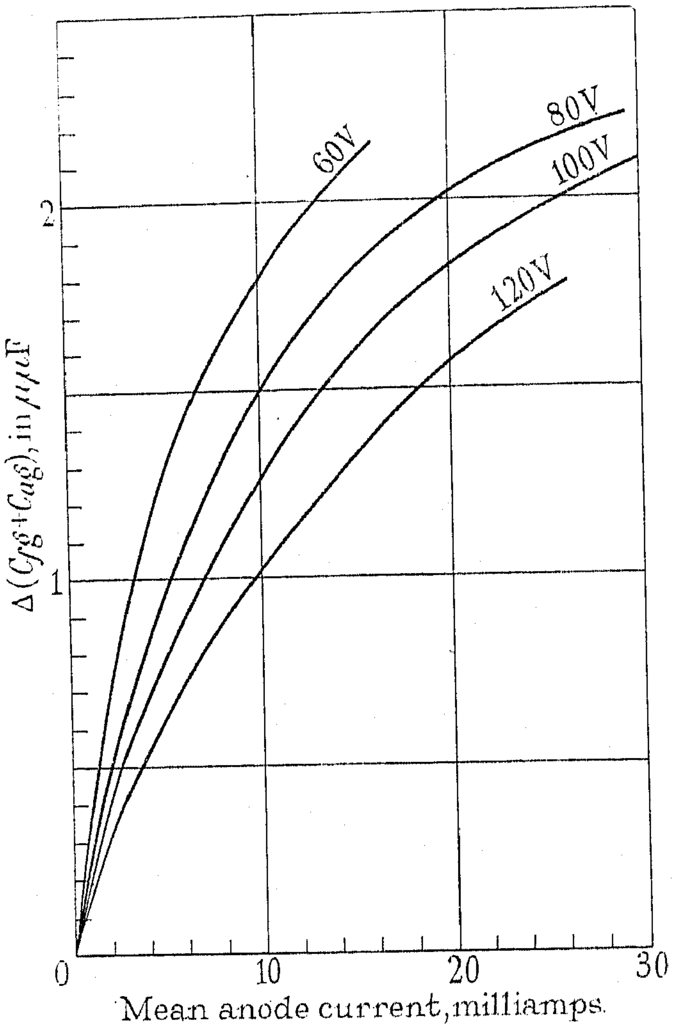

Fig. 7.—$\Delta(C_{fg} + C_{ag})$ plotted against mean anode current at 1 000 kc. (varying grid bias), for 4XP valve with barium-oxide coating. $V_f = 4$ volts, $V_a = 60$, 80, 100, 120 volts.

(a) Influence of Frequency

Reference to Fig. 3 will show that the curve obtained for the PM202 valve at 1 000 kc. was reproduced by measurements at 100 kc. It is not to be expected that any effect due to the time of transit of the electrons should be detectable at these frequencies.

(b) Influence of Filament Temperature

An effort was made to determine the effect in the case of a series of valves differing only in filament coating, in order that an estimate might be made of the contribution of the initial velocity of the electrons to the magnitude of the effect. With the coatings selected, the filament temperatures would have ranged from 1 093° K. (barium oxide) to 2 400° K. (pure tungsten). Unfortunately the valves were not sufficiently alike in construction to eliminate all other variables. It was therefore decided to compare the results given by the same valve run at two different temperatures, its thoriated tungsten filament being run in the normal way at 1 700° K. and then heated up to 2 400° K. (approximately), i.e. to such a temperature as reproduced the initial i_a/v_g characteristic observed at the lower temperature.

The effect reached a limiting value at an anode current of 15 to 20 milliamps. in each case, with two different LS5A valves. These limiting values and their ratio are given in Table 2.

The effect of initial velocity between the temperatures 1 700° K. and 2 400° K. therefore enhances the increment in input capacitance in the ratio of $1\cdot 2_8 : 1$. The enhancement is greater the larger the anode current, so that the effect of initial velocity is greater the larger the emission stream. The effect of initial velocity is probably

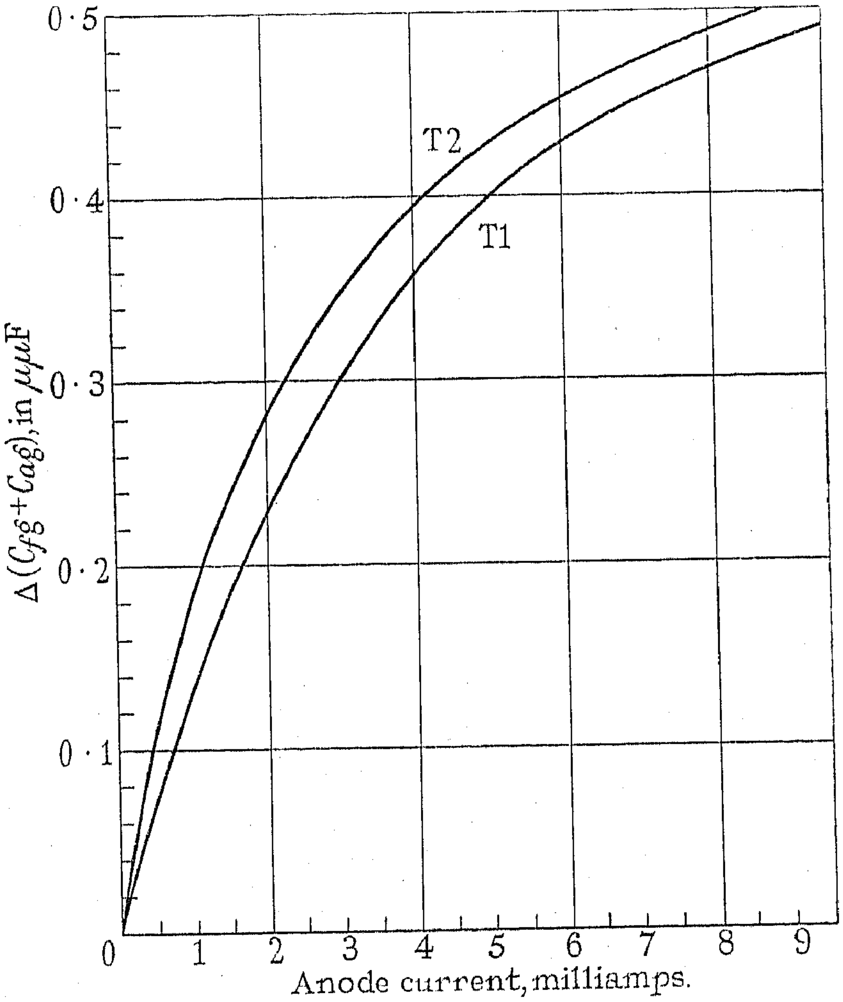

Fig. 8.—$\Delta(C_{fg} + C_{ag})$ plotted against anode current (varying grid bias), for two "acorn" triodes.
Valve type RCA No. 955, $V_f = 6$ volts, $V_a = 160$ volts.

Table 2

Valve	$\Delta C_{fg}) + C_{ag})$ limit, in $\mu\mu$F		Ratio
	Thoriated tungsten	Pure tungsten	
LS5A(1)	$0\cdot 6_5$	$0\cdot 8_4$	$1\cdot 2_9$
LS5A(2)	$0\cdot 7_0$	$0\cdot 8_9$	$1\cdot 2_7$

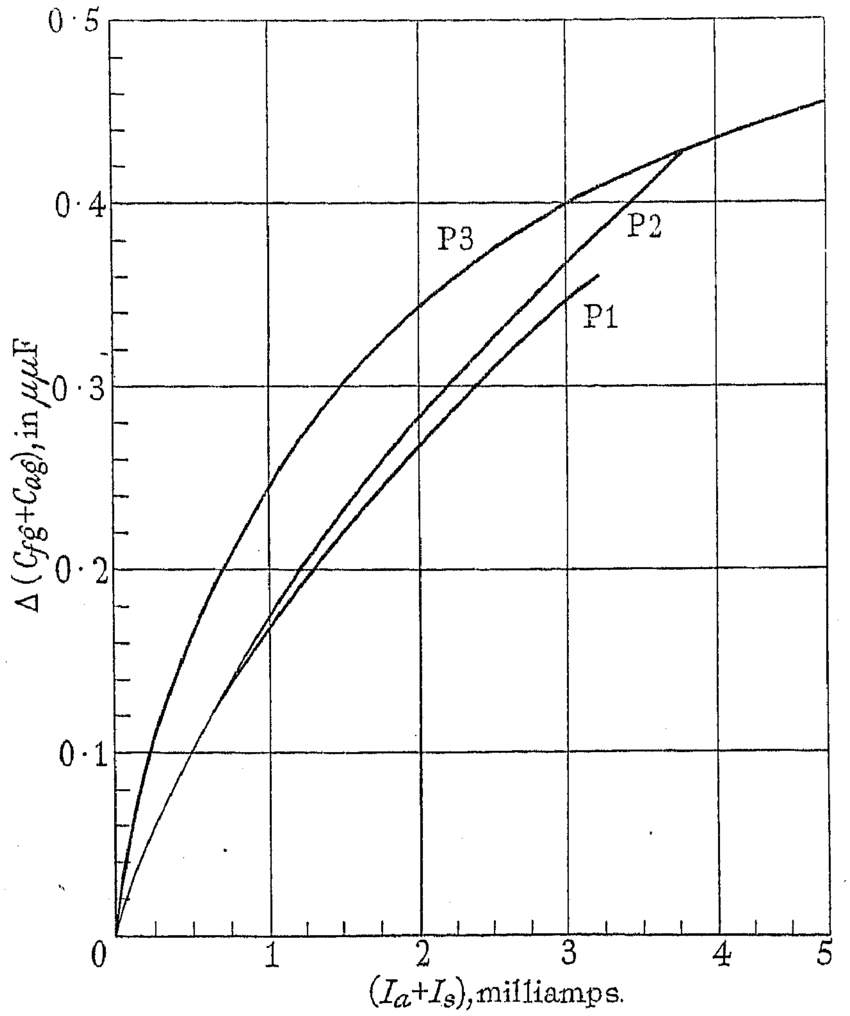

Fig. 9.—$\Delta(C_{fg} + C_{ag})$ plotted against emission current (varying grid bias), for three acorn pentodes.

Valve type RCA No. 954, $V_f = 6$ volts, $V_a = 220$ volts, $V_s = 100$ volts.

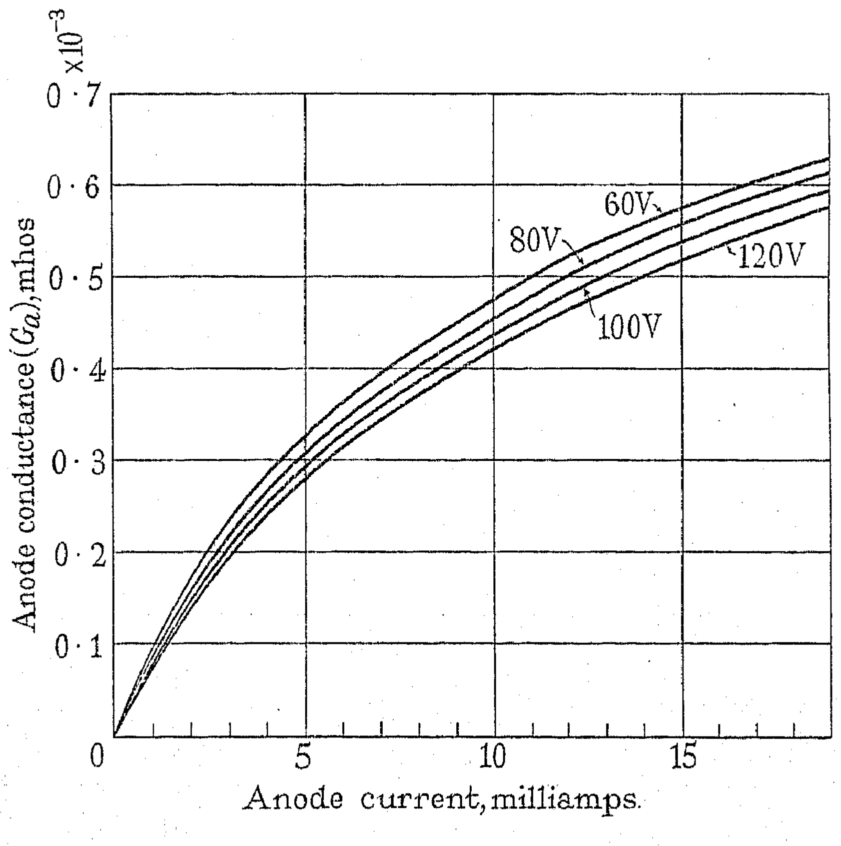

Fig. 10.—Anode conductance plotted against anode current, for 4XP valve with barium-oxide coating. $V_f = 4$ volts, $V_a = 60, 80, 100, 120$ volts.

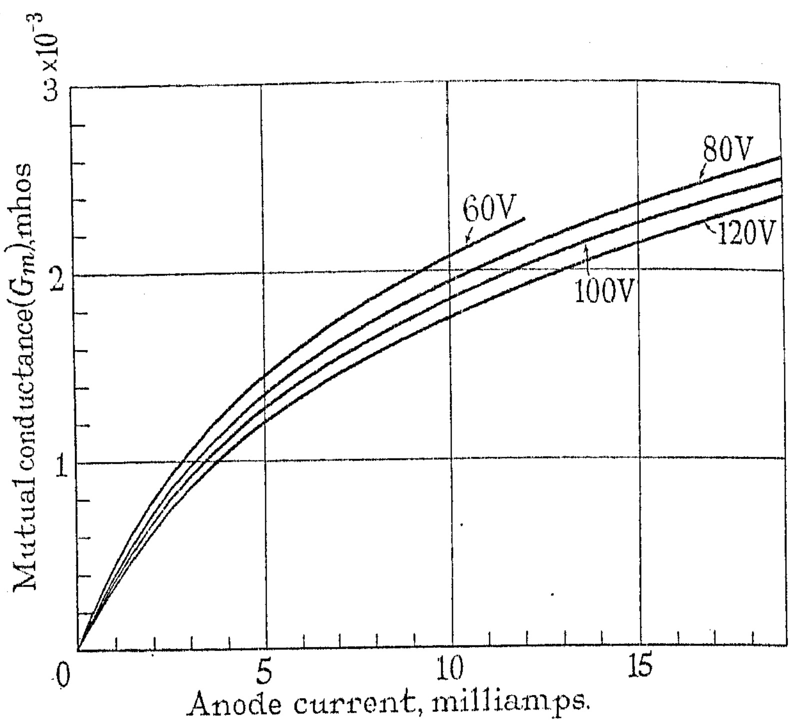

Fig. 11.—Mutual conductance plotted against anode current, for 4XP valve with barium-oxide coating. $V_f = 4$ volts, $V_a = 60, 80, 100, 120$ volts.

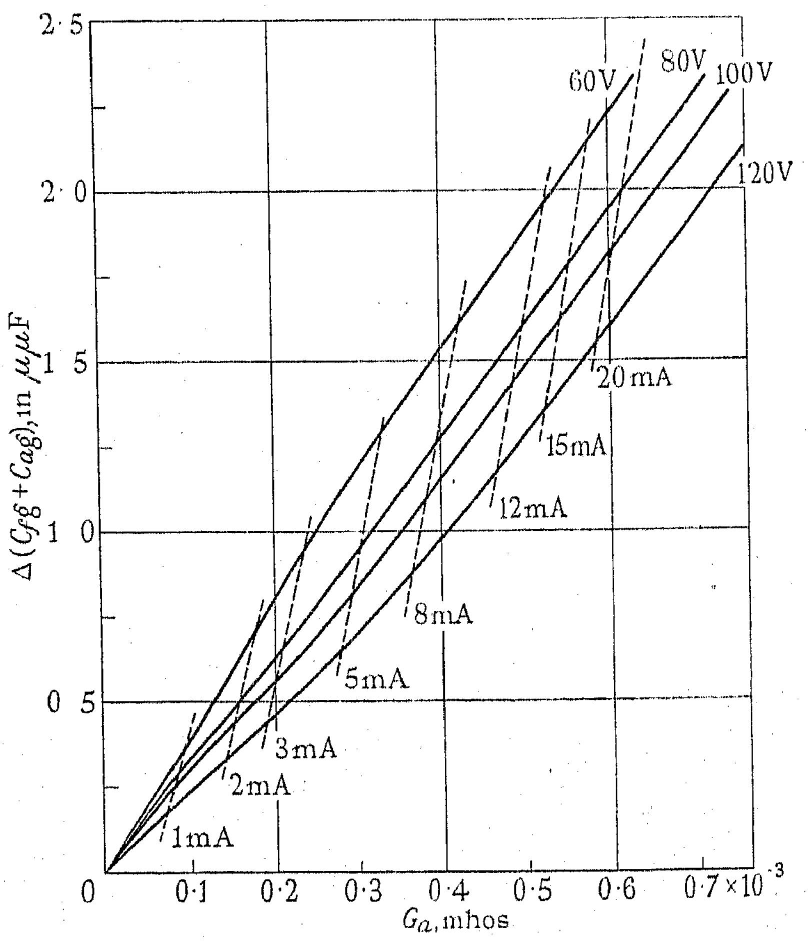

Fig. 12.—$\Delta(C_{fg} + C_{ag})$ plotted against anode conductance for 4XP valve with barium-oxide coating. $V_f = 4$ volts, $V_a = 60, 80, 100, 120$ volts.

considerable for pure tungsten filament valves, but it is impossible to determine how much it is diminished by the adoption of oxide filaments run at lower temperatures. This question must be answered by further experiments.

(c) Influence of Anode Voltage

In the case of the DO/24 valve (Fig. 5) it was assumed that to a first order the effect was almost independent of anode voltage, but measurements subsequently made on a 4XP valve with a barium-oxide filament and an LS5A valve did not bear this out. Reference to Fig. 9 indicates a considerable divergence at the lower voltages for the 4XP valve, and at anode voltages approaching those normally employed in the case of the LS5A valve for an anode current of 20 milliamps., as shown in Table 3.

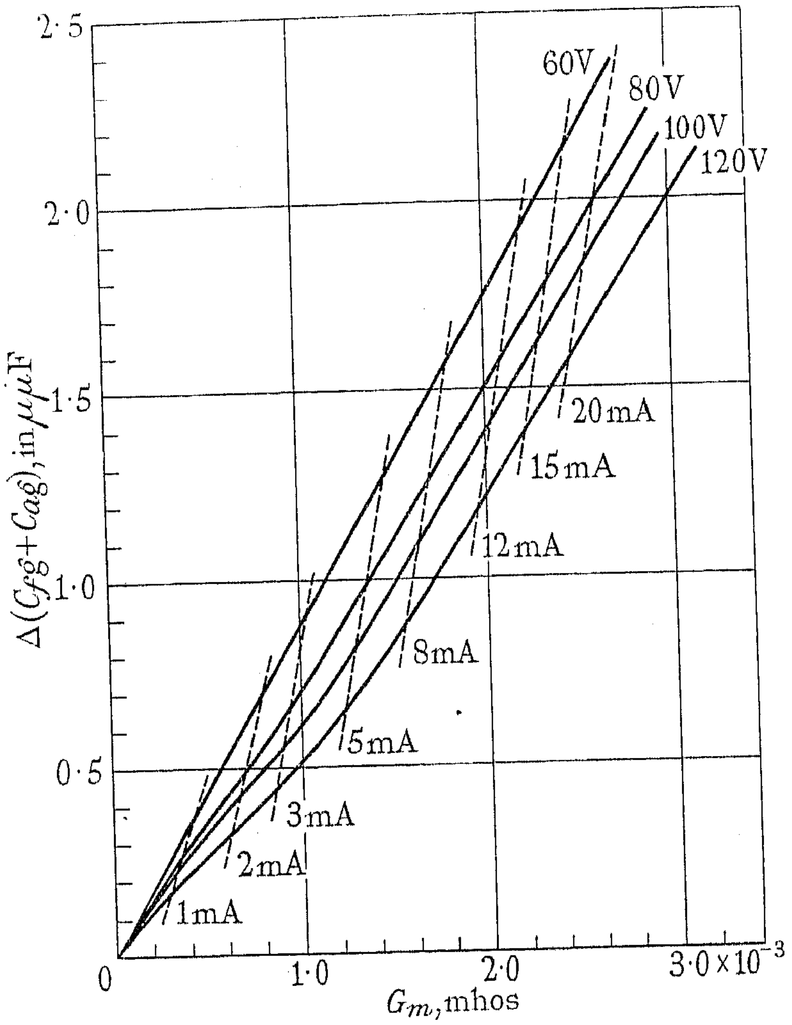

Fig. 13.—$\Delta(C_{fg} + C_{ag})$ plotted against mutual conductance, for 4XP valve with barium-oxide coating. $V_f = 4$ volts, $V_a = 60, 80, 100, 120$ volts.

The effect diminishes as the anode voltage is increased.

(d) Influence of Valve Conductances G_a and G_m

The divergence with anode voltage led to a search for a variable other than anode current, to which the effect might be more closely related. Measurements were therefore made of the anode-filament conductance (G_a) and the mutual conductance (G_m), using the same amplitude of alternating voltage as was used in the capacitance measurements on the 4XP valve mentioned above.

The curves given in Figs. 10 and 11 appeared to promise correlation, since there seemed to be a divergence with anode voltage similar to that in the case of $\Delta(C_{fg} + C_{ag})$, i.e. the conductances are larger the lower the anode voltage for a given anode current. On plotting $\Delta(C_{fg} + C_{ag})$ against G_a and G_m (Figs. 12 and 13), a divergence still remained. It therefore appears that the capacitance effect is not a simple relation of either anode current or G_a or G_m alone.

Table 3

Valve	Anode current	V_a	$\Delta(C_{fg} + C_{ag})$
	mA	volts	μμF
LS5A	20	120	$0\cdot7_1$
		150	$0\cdot6_8$
		200	$0\cdot6_3$
		250	$0\cdot5_6$
		350	$0\cdot5_0$

(5) CONCLUSION

The results given in this paper indicate that the phenomenon under review is of such a magnitude that it may have important bearing on the frequency of short-wave oscillators and upon the constancy of frequency of such oscillators. It is reasonable to suppose that the capacitance variation is more intimately associated with the valve conductances than with any other variable, but that the nature of the relation is probably complicated by the initial velocity of the electrons. The recent communication of Moullin* has thrown new light on the behaviour of the planar diode, and it is hoped that equipment now in course of assembly will assist in the investigation of time-of-transit effects in diodes as well as of the ordinary effect attributable to space charge. This and similar problems, affecting the triode also, call for a large number of observations upon a series of valves specially constructed to provide a known sequence of changes in the variables concerned. When the measurements on the diode are completed, it is proposed to undertake these further measurements.

Acknowledgments

The work described in this paper was carried out as part of the programme of the Radio Research Board and is published by permission of the Department of Scientific and Industrial Research.

REFERENCES

(1) L. Hartshorn: *Wireless Engineer*, 1931, vol. 8, p. 413.
(2) W. E. Benham: *Philosophical Magazine*, 1931, vol. 11, p. 457.
(3) E. B. Moullin: *Journal I.E.E.*, 1933, vol. 73, p. 186.
(4) G. B. Baker: *ibid.*, 1933, vol. 73, p. 196.
(5) D. W. Dye and T. I. Jones: *ibid.*, 1933, vol. 72, p. 169.
(6) E. B. Moullin: *ibid.*, 1937, vol. 81, p. 667.

* See Reference (6).

[The discussion on this paper will be found on page 20.]

DISCUSSION ON MR. IORWERTH JONES'S PAPER (SEE PAGE 11)[*]

Mr. D. A. Bell (*communicated*): It seems probable that the author was not aware of a paper published in 1935[†] which reported work on the inter electrode capacitances of valves carried out by me at Oxford University. It is very gratifying to find that those measurements, made with the simplest of apparatus, are generally confirmed by the complete range of accurate results obtained by the author at the National Physical Laboratory. The curves are of the same general shape, and two particular examples of measurements on identical types of valve may be quoted:—

(1) I found a value of $1 \cdot 0\ \mu\mu$F as the limit of $\Delta(C_{fg} + C_{ag})$ for an LS5 valve at $V_a = 210$, whereas the author gives $1 \cdot 07\ \mu\mu$F for the maximum change at $V_a = 150$.

(2) For an LS5b valve the two measurements are respectively $\Delta(C_{fg} + C_{ag}) = 1 \cdot 2\ \mu\mu$F at $V_a = 223$, and $\Delta(C_{fg} + C_{ag}) = 0 \cdot 97\ \mu\mu$F at $V_a = 150$.

The lack of exact constancy of capacitance-change for a fixed value of anode current was also illustrated in Fig. 3(*d*) of the earlier paper.

Perhaps the magnitude of the influence of filament temperature should be treated with more than the usual caution, despite the theoretical work of Moullin. For, referring to the curve for a DO24 valve in Fig. 4 of the present paper, it will be seen that above $I_f = 1 \cdot 74$, i.e. when space-charge limitation is presumably nearly complete, increasing the filament current still increases the capacitance-change only in proportion to the small growth of anode current, and shows no indication of a direct influence of temperature.

The main purpose of this communication is, however, to point out that rough results for $\Delta(C_{ag} + C_{af})$ were given in my paper; and to urge that, since results of at least qualitative significance were obtained with the crudest apparatus, experimental difficulties should not be allowed to delay the extension of accurate measurements on this important problem.

Mr. W. E. Benham (*communicated*): The author's measurements cover a large variety of valve types, and the form in which results are drawn up will appeal to those engaged in circuit design. One might perhaps have wished for a larger proportion of measurements on indirectly-heated cathode valves, as these are of particular interest in connection with mains-operated equipment.

It would, I think, have enhanced the value of the results somewhat if an indication had been given of the grid bias corresponding to the various anode currents. The point of particular interest is that corresponding to the incidence of grid current.

In Section (2)(*b*), referring to the arrangement of Fig. 2, the author points out that filament and grid are at the same alternating potential. This alternating potential is substantially zero (filament connected to screen), so that we have under consideration the value of C_{ag} under conditions for which the anode is alternating in potential, and the grid sensibly constant in potential. This condition has not hitherto received mathematical treatment, but in view of the obvious convenience of this method of measurement a brief analysis is given below.

We may conveniently begin with the appropriate "admittance theorem,"[†] writing, for the first-order admittance between grid and anode [assuming the displacement current $(i - i_c)$ all flows to the grid],

$$Y_{ga} = \frac{\bar{i} - i_c}{v_a} = pC_{ga} + \frac{i_e - i_c}{v_a} \quad . \quad . \quad (1)$$

where $p = \omega\sqrt{(-1)}$.

Here $\bar{i}$ represents the total alternating current passing between grid and anode, i_c the electron convection current at the anode (i.e. at the electrode where the alternating potential is applied), and v_a the alternating potential at the anode. The grid is assumed at zero (a.c.) potential, and the bias does not enter explicitly into the calculation. The current $\bar{i}$ is composed of the "cold" displacement current $(pC_{ga}v_a)$ and the induced current i_e, being that current flowing (in the external circuit) which is derivable from the electron convection current i_c by means of an instantaneous space-averaging process over all values i_c' of i_c between grid and anode.

A knowledge of i_e and i_c sufficiently exact for purposes of illustration is obtained in the following manner. First of all, there is a small alternating potential acting on the filament-grid region, given (nearly) by v_a/μ. This voltage may be regarded as the anode-potential fluctuation transferred to the "diode equivalent surface" lying just beyond the grid.[‡] Here we shall take the potential v_a/μ to act at a surface coinciding with the grid, and so obtain

$$(i_c)_g = g_m v_g = g_m \frac{v_a}{\mu} = \frac{v_a}{R_a} \quad . \quad . \quad . \quad (2)$$

The neglect here of finite electron transit-time in the filament-grid space can be shown to be without effect on the hot value, $\overline{C}_{ga}$, of C_{ga}. It is, however, necessary (at all frequencies) to include the effect in the grid-anode space. Thus, at any surface between grid and anode,[§]

$$i_c' = (i_c)_g e^{-p\tau_0'} - I_a \frac{\partial \tau_1'}{\partial t} = (i_c)_g e^{-p\tau_0'} - I_a \cdot p\tau_1' \quad . \quad (3)$$

where τ_0', τ_1', are respectively the d.c. and fluctuating components of electron transit-time (being that interval between the instant the electrons pass the diode equivalent surface and the instant at which the electrons reach the assumed surface). A value for $p\tau_1$ corresponding to negligible space-charge between grid and anode will be assumed for simplicity, and, since the term $(- I_a \cdot p\tau_1)$ is small in most practical cases, we will give $p\tau_1$ the approximate value corresponding to a temperature-limited planar diode, namely (putting $V_{ag} = V_a - V_g \simeq V_a$),

$$p\tau_1' = -\frac{p\tau_0'}{2} \cdot \Upsilon_3(p\tau_0') \cdot \frac{v_a''}{V_a''}$$

---

[*] Reprinted from *Journal I.E.E.*, 1938, vol. 82, p. 220.

[†] *Marconi Review*, 1935, No. 57, p. 18.

[†] See W. E. BENHAM: *Wireless Engineer*, 1936, vol. 13, p. 406.

[‡] The electrostatics of triodes is discussed in a forthcoming paper in the *Proceedings* of the Institute of Radio Engineers; and in greater detail, in Prof. Dow's new book "The Fundamentals of Engineering Electronics" (John Wiley, and Chapman and Hall).

[§] Primes indicate that the formula applies to any surface: when it is applied later to the anode the primes will be dropped.

where $\frac{v''_a}{V''_a} = \frac{v_a}{V_a}$ (nearly) and $\Upsilon_3 = \left(1 - \frac{2}{3}p\tau'_0\right)$ to sufficient accuracy for present purposes. This gives for (3), using (2),

$$i'_c \simeq \frac{v_a}{R_a}(1 - p\tau'_0) + \frac{p\tau'_0}{2}I_a\frac{v_a}{V_a} \quad . \quad . \quad . \quad (4)$$

To obtain i_e we require an instantaneous integration with respect to $x'\left(= \frac{dx'}{d\tau'_0}d\tau'_0\right)$, and after integration between grid and anode has been effected we divide by the grid-anode distance x_{ag}. It is sufficient, to our present degree of approximation, to take

$$\frac{dx'}{d\tau'_0} = \gamma\tau'_0; \quad x_{ag} = \tfrac{1}{2}\gamma\tau_0^2$$

in which γ is the acceleration (constant on our hypothesis of neglect of space charge) in the grid-anode space. We thus multiply (4) by $2\tau'_0/\tau_0^2$ and integrate with respect to τ'_0 between the limits $\tau'_0 = 0$ and $\tau'_0 = \tau_0$; obtaining, for the induced current,

$$i_e \simeq \frac{v_a}{R_a}\left(1 - \frac{2}{3}p\tau_0\right) + \frac{p\tau_0}{3}I_a\frac{v_a}{V_a} \quad . \quad . \quad (5)$$

We now drop the primes from equation (4) and subtract the resulting equation from equation (5). This gives $(i_e - i_c)$ for insertion in equation (1). Thus

$$Y_{ga} \simeq p\left(C_{ga} + \frac{\tau_0}{3R_a} - \frac{I_a\tau_0}{6V_a}\right) \quad . \quad . \quad . \quad (6)$$

If $\overline{C}_{ga}$ denote the hot value of C_{ga}, we have for $(\overline{C}_{ga} - C_{ga})$ the value

$$\delta C_{ga} = \frac{\tau_0}{6}\left(\frac{2}{R_a} - \frac{I_a}{V_a}\right) = g_m\frac{\tau_0}{6}\left(\frac{2}{\mu} - \frac{I_aR_a}{V_a\mu}\right) \quad . \quad (7)$$

The value of δC_{ag} given by equation (7) is exceedingly small, and positive. Owing to approximations made in derivation, we cannot be sure that the true value of δC_{ga} would come out positive, but we can be sure that it will remain exceedingly small. When, however, we come to consider the case where the grid electrode fluctuates in potential, the anode and filament being at constant potential, a comparatively large value of ΔC_{ga} is predicted. This case has been studied in detail by North,* but a more simple treatment is outlined below in order to show how this case differs from that examined above.

Equation (1) must be replaced by the slightly different equation

$$Y_{ga} = pC_{ga} + \frac{i_e - (i_c)_g}{-v_g}$$

in which we note that i_c must now be reckoned at the grid (i.e. where the alternating potential is applied) and also that a negative half-cycle of v_g corresponds to a positive half-cycle of grid-anode potential. The remaining equations (2a) to (5a) would be similar, but with v_a replaced by $(-v_g)$; so we remark simply that now we must take

$$\begin{aligned} i_e - (i_c)_g &= i_e - g_m(+v_g) \\ &= g_mv_g\left(1 - \frac{2}{3}p\tau_0\right) + \frac{p\tau_0}{3}I_a\frac{(-v_g)}{V_a} - g_m(+v_g) \end{aligned}$$

$$\therefore \quad \frac{i_e - (i_c)_g}{-v_g} = \frac{2}{3}p\tau_0\left(g_m + \frac{I_a}{2V_a}\right)$$

For the change in capacitance we now write ΔC_{ga}, which comes to

$$\Delta C_{ga} = \frac{g_m\tau_0}{3}\left(2 + \frac{I_aR_a}{V_a\mu}\right) \quad . \quad . \quad (7a)$$

The second term is exceedingly small, and equations (7) and (7a) give

$$\Delta C_{ga} - \delta C_{ga} = \frac{2}{3}g_m\tau_0 \quad . \quad . \quad . \quad . \quad (8)$$

$$\simeq \frac{4}{3}C_{fg}\frac{\tau_{ga}}{\tau_{fg}} \quad . \quad . \quad . \quad . \quad . \quad . \quad (8a)$$

Equation (8) may be shown to be more accurate than the rest of the analysis; this arises from the fact that the "exceedingly small" terms of equations (7) and (7a) are exactly equal, corresponding as they do to "variation time" effects in the grid-anode space.

This brings us to the interesting point that the inter-electrode capacitances are influenced to a different extent depending upon which electrodes are earthed and which are subject to alternating potentials. As is pointed out in the author's Reference (2),* "The same electrons which increase the capacity between cathode and negative grid can decrease the capacity between cathode and positive anode."

A small point arises in regard to the "hot" value of C_{af}. The cold value will have been balanced out, in the circuit of Fig. 2, by the use of a screened resistance box across the right-hand arm of the Wagner earthing device. As I understand the measurement, however, it would not be possible to balance out δC_{af} as well. One might light the filament and leave the grid floating, but then the grid would rapidly acquire a more negative potential by accumulation of electrons and there would be negligible change in C_{af}. I should like to inquire whether, referring to Section (2)(b), the author considers that δC_{af} was balanced out. It is just possible that δC_{af} is sufficiently negative to change the apparent value of δC_{ag} from slightly positive [equation (7)] to slightly negative. This would account for the negative value of ΔC_{ag} shown in Fig. 6.

In regard to Section (4)(c), it is to be noted that when V_a is increased τ_{ga} decreases somewhat more rapidly than g_m increases. The measurements are thus at least qualitatively in agreement with formulae (7) or (7a), assuming C_{fg} remains unchanged. The magnitude of the effect is such as to indicate that equation (7a) would be preferable.

Electron optical effects are likely to be of some importance in influencing inter-electrode capacitance variations,† and these are difficult to handle in this connection.

---

* D. O. North: *Proceedings of the Institute of Radio Engineers*, 1936, vol. 24, p. 123.

* W. E. Benham: *Philosophical Magazine*, 1931, vol. 11, p. 489.

† See R. F. J. Jarvis: Thesis approved for the degree of Doctor of Philosophy in the University of London, 1933, p. 65; also P. H. J. A. Kleynen: *Philips Technical Review*, 1937, vol. 2, p. 338 (particularly Fig. 8, facing p. 345).

Mr. T. I. Jones (*in reply*): It is encouraging that the publication of this paper should have brought forth contributions to the discussion of the subject from two workers in the same field.

It is true, as Mr. Bell suggests, that some of the measurements, more especially of input admittance, can be performed with simple apparatus such as tuned circuits, but the effects of drift in the frequency of the oscillator supplying the power can only be conveniently and wholly eliminated by using bridge equipment. For the separation of ΔC_{ag}, resort must be made to a bridge provided with a Wagner earthing system.

Mr. Benham's contribution deals in particular with the quantity ΔC_{ag}. The theory which he presents takes account of transit-time effects. In view of the agreement shown in Fig. 3 between the results of measurement at 100 kc. and at 1 000 kc., it is doubtful whether transit-time effects are very significant at these frequencies. The expression which he derives for $(\Delta C_{ga} - \delta C_{ga})$, however, is very interesting and may prove useful at higher frequencies.

With regard to the circuit shown in Fig. 2, any direct admittance between anode and filament should be effectively compensated by the Wagner earthing arrangement.

As regards the first point made by Mr. Benham, it should be borne in mind that the measurements were not pursued into the region of grid current, as the conductance involved was liable to affect the interpretation to be placed on changes in C_{fg}. The downward trend at the upper reaches of the curves for the lower anode voltages in Figs. 3 and 5 is probably due to the incidence of grid current.

THE APPARENT INTER-ELECTRODE CAPACITANCE OF A PLANAR DIODE.[*]

By E. B. MOULLIN, M.A., Member.

(*Paper received 9th February, 1937.*)

SUMMARY

Various experiments have suggested that the effective capacitance of a diode is probably dependent on the magnitude of the anode current: this effect, however, is not disclosed by the classic analyses of Benham and of Llewellyn. This paper shows that an analysis which ignores the emission velocity of electrons is not competent to describe the capacitance effects in a diode. A steady-state solution is found for a planar diode in which the emission velocity is not ignored. Also it is calculated that the mean-square velocity of electrons crossing the potential barrier is the same as the mean-square velocity of emission from the cathode. By considering the inertia effect of the electrons in conjunction with the displacement current at the barrier, an expression is derived for the phase angle of an electrode system. This expression shows that the phase angle is markedly dependent on the anode current. It is therefore thought that the analysis describes the basic mechanism of certain capacitance effects which have been observed in triodes.

An Appendix contains the steady-state solution of the temperature-saturated planar diode, and curves are given which show the force at the cathode and at the anode as a function of the anode current, expressed as a fraction of the space-charge limited current; also a curve which shows the transit time as a function of the anode current.

---

(1) INTRODUCTION

Experience shows that the inter-electrode capacitance of a triode changes with the thermionic current flowing in it. For example, G. B. Baker[†] has shown that the effective anode capacitance of a triode, used as a dynatron, may increase by about 1 $\mu\mu$F in a tube whose "cold capacitance" is of the order of 3 $\mu\mu$F. Similar large changes have been found in measuring the capacitance of the grid to the anode plus cathode of a triode, with negative grid. It is a problem of considerable scientific interest to discover the cause of so large a fractional change of capacitance: also the effect will some day become an important factor in the frequency stability of a valve generator. So far as the author is aware, it is not known experimentally whether the anode capacitance of a diode is a continuous function of the anode current. It is difficult to measure this capacitance, since it is shunted by a conductive path which is relatively very important save at ultra high frequencies. The author has not been able to devise a method of making the measurement. However, in order to discover the cause of the effect present in a triode, it is natural to analyse first the much simpler problem of the diode.

In any such analysis we must refer first to the classic work of W. E. Benham,[†] who showed that the net result of the space charge and of the electron inertia is to cause the capacitance of an idealized diode to be three-fifths of the cold capacitance. But it must be emphasized that this change is not a function of the anode current, provided only that this is space-charge limited. It is true that the ratio 3/5 is a limiting value of a function of the frequency; but in fact the frequency effect is unimportant until the periodic time of the alternating component of anode voltage is of the same order as the transit time of an electron from the cathode to the anode.

The author has recently derived the limiting value 3/5 by a very simple method of analysis,[‡] and reference to this will show that the phase angle between anode current and potential is independent of the mean anode current. In searching for a possible cause of such a dependence, we can but examine the idealization in the statement of the problem previously analysed, for there is no loophole in the analysis as such. Benham's analysis, and likewise the author's own version of it, postulate that the electrons leave the cathode with zero velocity, and this is contrary to reality. This is a possible reason why the analysis does not suggest the presence of the effect we are looking for, and we shall see that it is a sufficient reason. If all electrons left the cathode with the same velocity, they would all come to rest at a potential minimum near the cathode, and restart from there on their journey to the anode. In a diode with planar electrodes, the relation between force and distance would be as shown in Fig. 1. If the origin be taken at O, the potential minimum, then it is well known that

$$F = \frac{4}{3}\frac{V_a}{d}\left(\frac{x}{d}\right)^{1/3} \quad . \quad . \quad . \quad . \quad . \quad (1)$$

and

$$Ic^2 = \frac{4}{9\pi}\sqrt{\left(\frac{2e}{m}\right)}V_1^{3/2} \quad . \quad . \quad . \quad . \quad (2)$$

where V_a is the potential of the anode with respect to the minimum, and V_1 is the potential of the minimum with respect to the cathode. Since V_1 depends only on the temperature of the cathode, it follows from (2) that Ic^2 is constant. Now suppose $I = I_m(1 + M \sin pt)$, where the frequency $p/(2\pi)$ is very small compared with the reciprocal of the transit time. Then if M is small we may suppose that c fluctuates harmonically above and below a mean value and thus

$$c \simeq c_m(1 - \tfrac{1}{2}M \sin pt) \quad . \quad . \quad . \quad . \quad (3)$$

We now see why this solution cannot give an approximately correct solution for a fluctuating current. For, since the electron velocity at O is zero, the space-charge density there is infinite, and hence, as indeed follows from (1), $\partial F/\partial x$ is infinite. If we suppose the position of O fluctuates, however slowly and however little, then the force at a fixed point near it, for example its mean position, must change infinitely rapidly with time. This may be expressed alternatively as follows.

---

[*] Reprinted from *Journal I.E.E.*, 1937, vol. 81, p. 667.

[†] *Journal I.E.E.*, 1933, vol. 73, p. 196, and *Proceedings of the Wireless Section*, 1933, vol. 8, p. 187.

[†] *Philosophical Magazine*, 1931, vol. 11, p. 460.

[‡] See discussion on paper by R. W. Sloane and E. G. James, *Journal I.E.E.*, 1937, vol. 80, p. 103, and *Proceedings of the Wireless Section*, 1937, vol. 12, p. 61.

First let O be fixed. At this point the force is zero: at a point infinitesimally close to O there is a finite force. If now the curve of Fig. 1 be oscillated about its mean position, then the force at this point will change instantaneously from zero to a finite value. At the mean position $\partial F/\partial t$ must be infinite, however slowly the current is changing. Thus any change of current, however small, involves an infinite displacement current at the potential barrier and a finite displacement current at the anode. This is absurd and shows that such an approach must not be used to study fluctuating conditions in a diode.

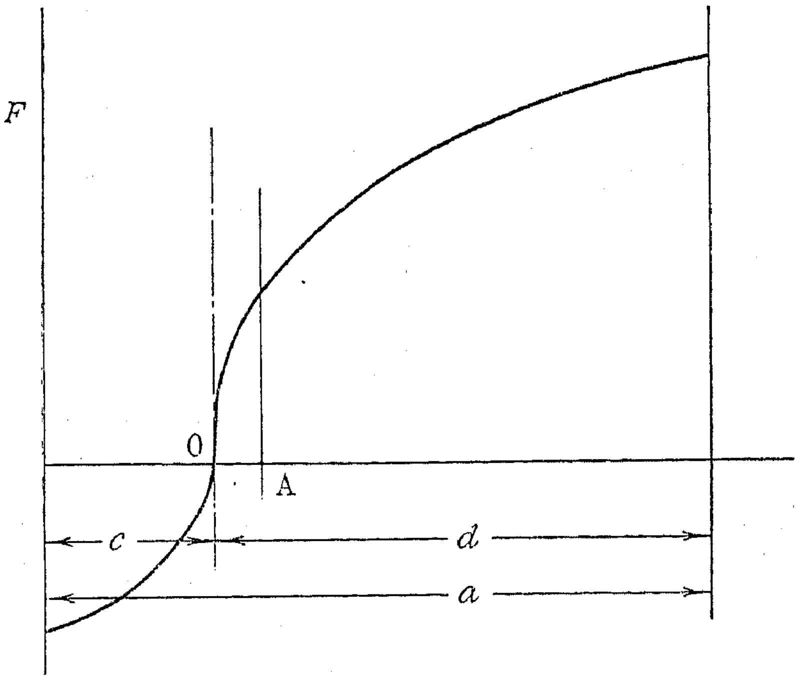

Fig. 1

(2) STEADY-STATE SOLUTION WHEN THE EMISSION VELOCITY IS NOT ZERO

It is known that the electrons leave the cathode with a variety of velocities. If there is space-charge limitation, the anode current is less than the emission from the cathode. Since some electrons return to the cathode, they must be emitted against a retarding field; and since the anode is positive to the cathode, there must be some plane at which the direction of the electric field changes sign and, consequently, passes through zero. This plane is a potential minimum: let V_1 be its potential. If an electron is emitted from the cathode with energy less than eV_1, it will not penetrate the retarding field as far as the "barrier," but will perform a short excursion and retrace its path. An electron emitted with energy greater than eV_1 will pass the barrier and have there a minimum velocity.

If the origin of co-ordinates is at the potential barrier, then we have to consider the problem of electrons leaving, with an initial velocity, from an origin at which the force is zero. The initial velocity may have any value from zero to infinity: its mean-square value is definite and will be considered in the next section. For the present we must simplify the problem by assuming that all electrons leave with the same initial velocity u_0.

Let the distance between the anode and the potential minimum be d, the potential of the anode be $(V_a - V_1)$, and the current I_a. The distribution of potential can be found by solving Laplace's equation, but it is both more simple and more instructive to consider the equation of motion of the electron. Since symmetry requires that the field shall be everywhere perpendicular to the electrodes, and since it is zero at the origin, it follows from Gauss's theorem that the force F at a distance x from the origin is 4π times the electric charge between the origin and the plane x. Let an electron reach the plane x in time t: then during this time an electric charge amounting to It has started from the origin and is situated somewhere between the origin and the plane x. Hence

$$F = 4\pi I_a t \quad . \quad . \quad . \quad . \quad . \quad . \quad (4)$$

$$\therefore \frac{d^2x}{dt^2} = \frac{4\pi e}{m} I_a t \quad . \quad . \quad . \quad . \quad . \quad . \quad (5)$$

$$\equiv A I_a t \quad . \quad . \quad . \quad . \quad . \quad . \quad (5a)$$

$$\therefore \frac{dx}{dt} = \frac{A I_a t^2}{2} + u_0 \quad . \quad . \quad . \quad . \quad . \quad (6)$$

and

$$x = \frac{A I_a t^3}{6} + u_0 t \quad . \quad . \quad . \quad . \quad . \quad (7)$$

$$= \frac{t(u + 2u_0)}{3}, \text{ from (6)} \quad . \quad . \quad (8)$$

Hence from (6), by means of (8),

$$I_a = \frac{m}{2\pi e} \frac{(u - u_0)(u + 2u_0)^2}{9x^2} \quad . \quad . \quad . \quad (9)$$

We may now relate the velocity and potential by the equation

$$e(V + V_0) = \tfrac{1}{2} m u^2$$

Hence, on substitution in (9), we obtain

$$I_a = \frac{1}{9\pi}\sqrt{\left[\frac{2e}{m}\right]} \frac{(V_a + V_0)^{3/2}}{d^2} (1 - b)(1 + 2b)^2 \quad (10)$$

where

$$b^2 \equiv \frac{V_0}{V_a + V_0}$$

Similarly, from (8),

$$T = \frac{3d}{2}\sqrt{\left[\frac{2m}{e(V_a + V_0)}\right]} \frac{1}{(1 + 2b)} \quad . \quad . \quad . \quad (11)$$

$$= \left\{\frac{3dm}{2\pi e} \cdot \frac{(1 - b)}{(1 + 2b)} \cdot \frac{1}{I}\right\}^{1/3}, \text{ from (10)} \quad . \quad . \quad (12)$$

On eliminating t between (4) and (7) we obtain a cubic equation between F and x. On making use of (9) it follows, after some reduction, that

$$\frac{x}{d} = \frac{3u_0}{u_1 + 2u_0}\left(\frac{F}{F_a}\right)\left\{1 + \frac{u_1 - u_0}{3u_0}\left(\frac{F}{F_a}\right)^2\right\} \quad . \quad (13)$$

where F_a and u_1 are respectively the force and the velocity at the anode.

In Fig. 2 is shown the curve relating F/F_a with x/d for

$u_1/u_0 = 4$, 10, 31, and infinity respectively, corresponding to $(V_a + V_0)/V_0 = 16$, 100, 1 000, and infinity. It may be seen that the initial velocity has an important effect on the shape of the force/distance curve—an effect which is still very marked even when $(V_a + V_0)/V_0 = 1 000$.

By means of (6) and (8) it is possible to express u in terms of x; the relation is

$$u^3 + 3u^2u_0 - 4u_0^3 = \frac{x^2}{d^2}(u_1^3 - 3u_1^2u_0 - 4u_0^3) \quad . \quad (14)$$

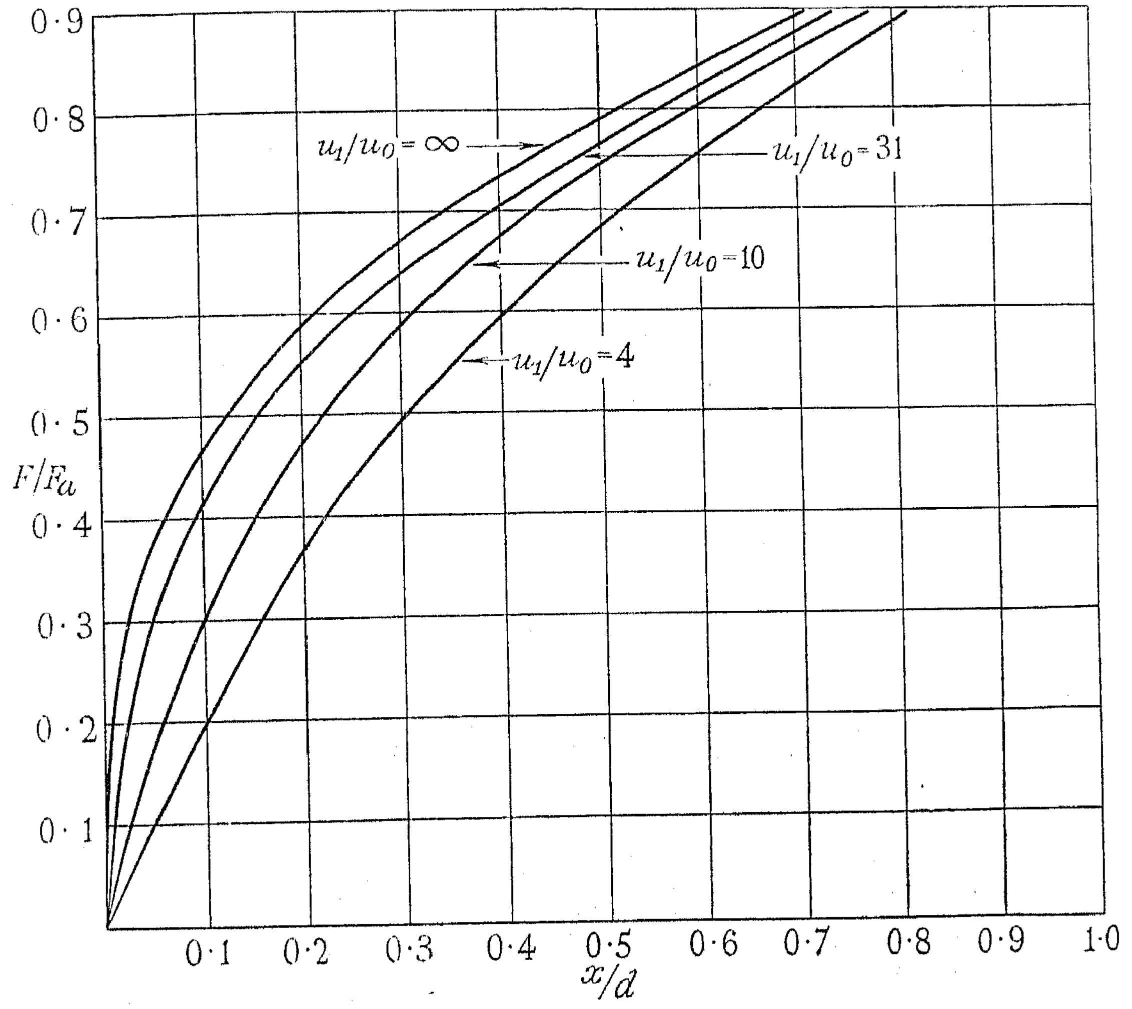

Fig. 2

Expressing u in terms of V, this becomes

$$\left(\frac{V + V_0}{V_0}\right)^{3/2} + 3\left(\frac{V + V_0}{V_0}\right) - 4 = \frac{x^2}{d^2b^3}(1 + 3b - 4b^3) \quad . \quad . \quad (15)$$

It may now appear that we have obtained a complete solution of the problem for steady conditions: this, however, is not so because the distance d between the anode and the potential barrier is unknown: we know only that it is less than a, the distance between anode and cathode. Before we can estimate $c = a - d$, we must find the relation between u_0 and the mean-square velocity of emission from the cathode.

(3) THE SQUARE VELOCITY OF EMISSION FROM THE POTENTIAL MINIMUM

If electrons are emitted from the cathode with velocities which have a Maxwellian distribution, then, of the number n which are emitted in unit time, a smaller number dn are emitted with a velocity component, normal to the surface, between u and $u + du$, where*

$$dn = n \times 2hmu\epsilon^{-hmu^2}du \quad . \quad . \quad . \quad (16)$$

where m is the mass of an electron and h is such that $hmu_2^2 = 1$, u_2^2 being the mean square velocity of emission from the cathode. If the cathode temperature be τ then $\frac{1}{2}mu_2^2 = k\tau$, where k is Boltzmann's constant.

The electrons are emitted against a retarding field which tends to slow them up: some are brought to rest and subsequently return to the cathode. Let the potential at the potential minimum be $- V_1$ with respect to the cathode. If an electron is emitted with a velocity u, it will pass the potential barrier if $\frac{1}{2}mu^2 > eV_1$. Let u_3 be the least velocity of emission which will suffice to carry an electron through the barrier and allow it to pass on to the anode. The number n_1 whose velocity exceeds u_3 may be calculated from (16) as follows:

$$n_1 = n\int_{u_3}^{\infty} 2hmu\epsilon^{-hmu^2}du$$
$$= n\Big[- \epsilon^{-hmu^2}\Big]_{u_3}^{\infty}$$
$$= n\epsilon^{-hmu_3^2}$$

Hence, if I_a be the anode current and I_e the emission current, we have the well-known equation

$$I_a = I_e\epsilon^{-hmu_3^2} = I_e\epsilon^{-eV_1/(kT)} \quad . \quad . \quad . \quad (17)$$

---

* See, for example, EUGENE BLOCH: "Thermionic Phenomena," p. 43, eqn. (16), of English translation.

Now consider an electron emitted with a velocity u greater than u_3. Its initial energy is $\frac{1}{2}mu^2$. When it reaches the potential minimum this has been reduced by an amount $\frac{1}{2}mu_3^2$. Hence

$$E_2 = \tfrac{1}{2}m(u^2 - u_3^2) \equiv \tfrac{1}{2}mv^2.$$

We require $\bar{v}^2$, the mean-square value of v^2.

Now

$$\begin{aligned}
\bar{v}^2 &\equiv \frac{1}{n_1}\int(u^2 - u_3^2)dn \\
&= \frac{2hmn}{n_1}\int_{u_3}^{\infty}(u^2 - u_3^2)u\epsilon^{-hmu^2}du, \text{ from (16)} \\
&= \frac{2hmn}{n_1}\left[-\frac{1}{2hm}\left(u^2 + \frac{1}{hm}\right)\epsilon^{-hmu^2} + \frac{u_3^2}{2hm}\epsilon^{-hmu^2}\right]_{u_3}^{\infty} \\
&= \frac{1}{hm}\frac{n}{n_1}e^{-hmu_3^2} \\
&= \frac{1}{hm}, \text{ from (17)} \\
&= u_2^2 \quad . \quad . \quad . \quad . \quad . \quad . \quad . \quad . \quad . \quad . \quad . \quad . \quad . \quad (18)
\end{aligned}$$

And thus it appears that the mean-square velocity of those electrons which pass the barrier is the same as the mean-square normal velocity of emission from the cathode. The barrier behaves as a virtual cathode at the same temperature as the real cathode, but emitting a current I_a instead of a current I_e. The retarding field is equivalent to an increase in the work function of the cathode.

(4) DISTANCE BETWEEN THE POTENTIAL MINIMUM AND THE CATHODE

Since the potential minimum may be regarded as a virtual cathode, the velocity distribution will conform with equation (16), where now n will represent the number of electrons which cross the barrier in unit time. To find the space charge at the origin we require the mean reciprocal velocity, such that

$$\begin{aligned}
\rho_0 &= I_a/\bar{u} \\
&= e\int_0^{\infty}\frac{dn}{u} \\
&= e\int_0^{\infty}2hmn\epsilon^{-hmu^2}du \\
&= 2hmI_a\sqrt{\left[\frac{\pi}{hm}\right]} \\
&= \frac{2\sqrt{\pi}I_a}{u_2}, \text{ from (18)}, \quad . \quad . \quad . \quad (19) \\
&= 2I_a\sqrt{\left[\frac{\pi m}{2eV_2}\right]}
\end{aligned}$$

Between the cathode and the barrier there are some electrons which will pass through to the anode and some which will return to the cathode with the velocity with which they departed. The distribution of charge may be regarded as a moving one which provides the current, together with a "stationary" distribution which represents the "go" and "return" electrons. The density of the "moving" electrons increases as the barrier is approached, whereas the density of the "stationary" electrons presumably decreases, since the number surviving decreases continuously as the distance increases. We can do no more than assume the total density through the region to be substantially constant and to have the value given by (19). If this were so, then in this region

$$F = 4\pi\rho_0 x$$

and $$V_1 = 2\pi\rho_0 C^2$$

or $$\begin{aligned}
c^2I &= \frac{V_1}{4\pi}\sqrt{\left[\frac{2eV_2}{\pi m}\right]} \\
&= \frac{1}{4\pi}\sqrt{\left[\frac{2e}{\pi m}\right]}\log\frac{I_e}{I_a}(V_2)^{3/2}, \text{ from (17)} \quad . \quad (20)
\end{aligned}$$

In the familiar solution which supposes that all electrons start from the cathode with energy eV_2 and are brought to rest at the barrier, we have

$$c_1^2I_a = \frac{1}{9\pi}\sqrt{\left[\frac{2e}{m}\right]}V_2^{3/2}$$

Hence $$c^2/c_1^2 = 1\cdot26\log(I_e/I_a)$$

whence $c/c_1 = 1\cdot7$ if $I_e/I_a = 10$, and $0\cdot89$ if $I_e/I_a = 2$.

Hence it seems that the assumed distribution of charge makes the distance between cathode and potential minimum not much greater than the value calculated by the classic method. It follows from (10) and (20) that

$$\frac{c}{d} = 1\cdot12\sqrt{\left[\log\frac{I_e}{I_a}\right]}\left(\frac{V_2}{V_a + V_0}\right)^{\frac{3}{4}} \quad . \quad . \quad (21)$$

We have seen in Section (3) that the mean-square velocity of departure from the barrier is equal to the mean-square velocity of emission from the cathode; hence it might appear that V_0 in (21), etc., may be equated to V_2. But (9), (10), etc., have been derived from (6) on the supposition that all electrons had the same initial velocity u_0. It remains now to decide the best value to select for u_0 in relation to the known r.m.s. velocity of departure, which does correspond to V_2. Consistent with the derivation of the distance c it is necessary to choose u_0 equal to the reciprocal of the mean reciprocal velocity of emission. Hence, from (19),

$$u_0 = \frac{u_2}{2\sqrt{\pi}}$$

and $$V_0 = \frac{V_2}{4\pi} \quad . \quad . \quad . \quad . \quad . \quad . \quad . \quad (22)$$

(5) CONDITIONS WHEN THERE IS AN ALTERNATING COMPONENT OF CURRENT

Consider the basic equation (4), namely

$$F = 4\pi it.$$

Suppose the current is increasing uniformly with time, so that $i = I'(1 + bt)$. Then if the current was I' when the electron departed, after time t the quantity of electricity behind it is $I't(1 + \frac{1}{2}bt)$. Alternatively, if the current is I_a at time t, then

$$F = 4\pi I_a t(1 - \tfrac{1}{2}bt)t \quad . \quad . \quad . \quad . \quad (23)$$

The force on an electron is less than it would be if the current had been I_a during the whole time t; hence during this time it will not have travelled so far as it would have done if the current had been steady at value I_a. Consequently, at a given distance the force is less than that corresponding to a steady current I_a, and therefore necessarily the potential is also less.

If the current is $I_a = I_m(1 + M \sin pt)$, and the initial velocity is zero, then it has been shown (see discussion on the paper by Drs. Sloane and James, *Journal I.E.E.*, vol. 80, p. 103) that when $t = 0$

$$F = F_m\left\{1 - \frac{1}{4}M\left(\frac{x}{d}\right)^{1/3} pT\right\} \quad . \quad . \quad (24)$$

and $$V_a = V_m\left\{1 - \tfrac{1}{5}MpT\right\} \quad . \quad . \quad . \quad . \quad (25)$$

where F_m is the force at distance x corresponding to a steady current I_m; V_m and T are respectively the anode potential and transit time corresponding to such a current.

It may be seen from this that the force at a given distance is less than F_m by a fractional amount which depends on x/d; but, in fact, this fractional reduction changes slowly with x/d and the average value is four-fifths of the maximum value. When the initial velocity is not zero, t cannot be expressed as an explicit function of x [see equation (7)], and consequently it is impossible to evaluate the potential algebraically. It is necessary to proceed by an approximate method and one which will put a more severe restriction on the magnitude of MpT; moreover, it does not seem possible to assess the severity of this restriction and we must be prepared to keep M very small.

If the current be I' when an electron leaves the potential barrier, then it follows that (7) becomes

$$x = \frac{AI't^3}{6}\left(1 + \frac{1}{4}bt\right) + u_0 t;$$

or, if the current be I_a at time t after departure, then

$$x = \frac{AI_a t^3}{6}\left(1 - \frac{3}{4}bt\right) + u_0 t \quad . \quad . \quad . \quad (26)$$

$$= \frac{AI_m t^3}{6}\left(1 - \frac{3}{4}pMt\right) + u_0 t \quad . \quad . \quad (26a)$$

for a sinusoidal fluctuation of current passing through its mean value I_m.

Let t be the time taken to reach a distance x when the current is passing through the value I_m, and let T_m be the time to reach the same distance when the current is steady and equal to I_m. Then

$$\frac{At^3}{6}I_m\left(1 - \frac{3}{4}pMt\right) + u_0 t = \frac{AT_m^3}{6}I_m + u_0 T_m$$

$$\therefore \quad \frac{AI_m}{6}(t^3 - T_m^3) + u_0(t - T_m) = \frac{1}{8}pMAI_m t^4.$$

Let $t - T_m = \delta T_m$. Since M is very small, t and T_m are nearly equal; hence we may write:—

$$\delta T_m(\tfrac{1}{2}AI_a T_m^2 + u_0) \simeq \tfrac{1}{8}pMAI_m T_m^4.$$

Hence, from (6) and (7),

$$\frac{\delta T_m}{T_m} \simeq \frac{3}{4}\frac{pM(x - u_0 T_m)}{u}$$

$$= \frac{3}{4}\frac{pMx}{u}\cdot\frac{u - u_0}{u + 2u_0}, \text{ from } (8) \quad . \quad . \quad (27)$$

From equation (23)

$$\begin{aligned} F &= 4\pi I_m(1 - \tfrac{1}{2}pMt)t \\ &\simeq 4\pi I_m T_m(1 - \tfrac{1}{2}pMT_m)\left[1 + (\delta T_m/T_m)\right] \\ &\simeq F_m\left[1 - \tfrac{1}{2}pMT_m + (\delta T_m/T_m)\right] \\ &= F_m\left(1 - \frac{1}{2}pM\cdot\frac{3x}{u + 2u_0} + \frac{\frac{3}{4}pMx}{u}\cdot\frac{u - u_0}{u + 2u_0}\right), \\ &\qquad\qquad \text{from (8) and (27)} \\ &= F_m\left(1 - \frac{\frac{3}{4}pMx}{u}\cdot\frac{u + u_0}{u + 2u_0}\right) \\ &= F_m\left(1 - \frac{1}{4}M\frac{u + u_0}{u}\cdot\frac{T_m}{T}pT\right) \quad . \quad . \quad . \quad . \quad (28) \end{aligned}$$

Since F/F_a is proportional to T_m/T, the value of T_m/T for a given value of x/d can be found from the family of curves shown in Fig. 2. For any stated value of u_1/u_0, it is possible to calculate u/u_0 at any value of x/d. Hence for any assigned value of u_1/u_0 it is possible to plot $\frac{u + u_0}{u}\cdot\frac{T_m}{T}\cdot\frac{F}{F_a}$ as a function of x/d. This has been done in Fig. 3 for $u_1/u_0 = 4$, 10, and infinity. To derive the anode potential it is necessary to evaluate the area under these curves. As a first approximation, however, we shall treat them as straight lines and thus obtain

$$V_a \simeq V_{ma} - \frac{MpT}{4}\cdot\frac{u_1 + u_0}{u_1}\cdot\frac{F_a d}{2}$$

It follows from (4), (8), and (9), that

$$\begin{aligned} \frac{u_1 + u_0}{u_1}F_a d &= \frac{2m}{3e}(u_1^2 - u_0^2)\frac{u_1 + 2u_0}{u_1} \\ &= \frac{4}{3}V_{ma}\frac{u_1 + 2u_0}{u_1} \end{aligned}$$

$$\begin{aligned} \therefore \quad V_a &\simeq V_{ma}\left(1 - \frac{1}{6}MpT\frac{u_1 + 2u_0}{u_1}\right) \\ &= V_{ma}\left\{1 - \tfrac{1}{6}MpT(1 + 2b)\right\} \quad (29) \end{aligned}$$

On comparing (29) with (25), it may be seen that the coefficient given here as 1/6 must in reality merge gradually into 1/5 as b tends to zero.

If in (10) we put $I = I_m(1 + M \sin pt)$, we should obtain to the first order in M,

$$V_a = V_{ma}(1 + \tfrac{2}{3}M \sin pt).$$

Hence we may write

$$V_a \simeq V_{ma}\left[1 + \tfrac{2}{3}M\left\{\sin pt - \tfrac{1}{4}pT(1 + 2b)\cos pt\right\}\right] \quad (30)$$

If the diode be represented by a resistance R shunted by a small capacitance C, then it follows from the property of such a combination that

$$CR \simeq \tfrac{1}{4}(1 + 2b)T$$

Since $$R \simeq \tfrac{2}{3}(V_{ma}/I_m)$$

$$\therefore \quad C = \tfrac{3}{8}(1 + 2b)I_m T/V_{ma}$$

$$= \frac{\frac{1}{2}(1 + 2b)^2}{1 + b} \cdot \frac{1}{4\pi d}, \text{ from (8) and (10).} \qquad (31)$$

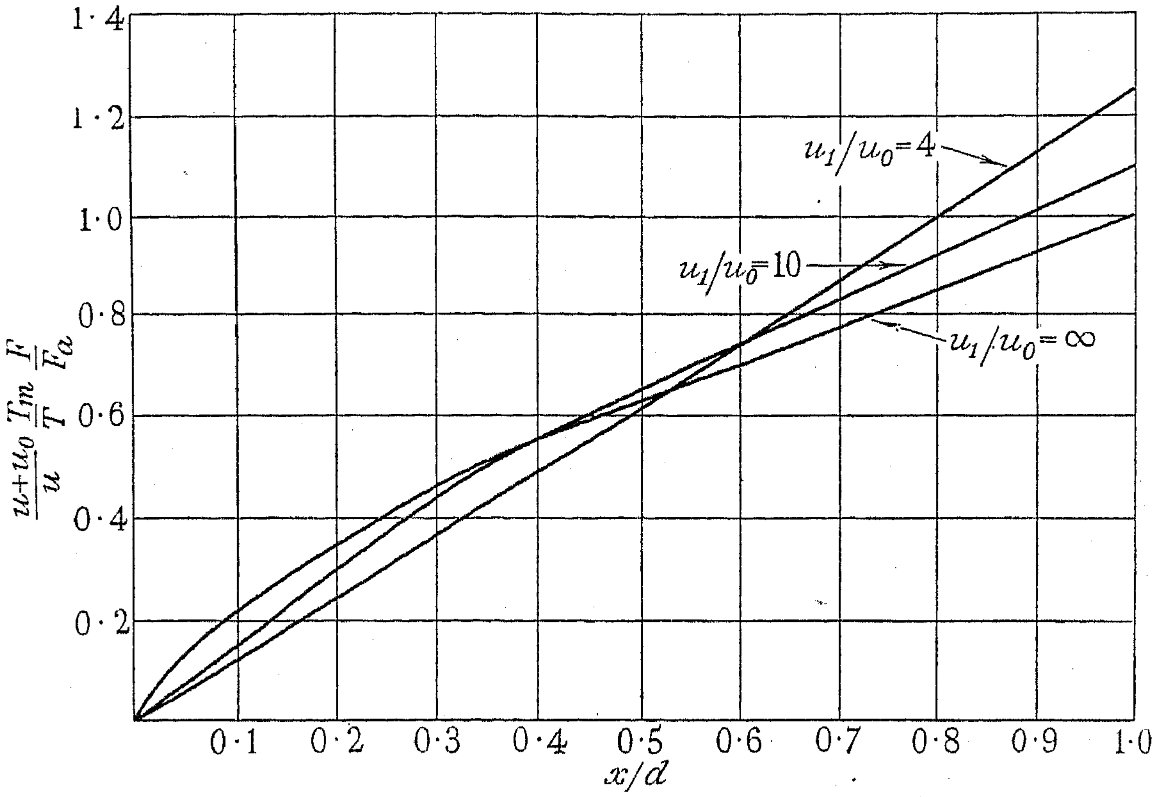

Fig. 3

If b is zero, corresponding treatment of (25) leads to

$$C = \frac{3}{5} \cdot \frac{1}{4\pi d} \quad . \quad . \quad . \quad . \quad . \quad (31a)$$

the result first pointed out by W. E. Benham.

It appears from (31) that 3/5 is a limiting lower value for the apparent dielectric constant of the space between the potential barrier and the anode. We have thus found a reason for supposing that the apparent inter-electrode capacitance of a diode will be a function of the current flowing through it; but this is by no means the whole reason, as we shall now see.

(6) THE DISPLACEMENT CURRENT AT THE POTENTIAL BARRIER

Refer now to Fig. 1, and remember that the small sinusoidal fluctuation of current causes the origin O to oscillate slightly about its mean distance c_m. From (3) and (20) it follows that, if M is very small,

$$c \simeq c_m(1 - \tfrac{1}{2}M \sin pt).$$

Consider some fixed point A, very near to the mean position of O, and let OA $= x$; then

$$x = c_m - c \simeq \tfrac{1}{2}c_m M \sin pt,$$

and $$dx/dt = \tfrac{1}{2}pc_m M \cos pt.$$

It follows from (13) that very near the origin, where F is zero,

$$F = \frac{u_1 + 2u_0}{3u_0} \cdot \frac{x}{d}F_a$$

$$= \frac{1 + 2b}{3}\left(\frac{V_a + V_0}{V_0}\right)^{\frac{1}{2}}\frac{x}{d}F_a$$

We shall now consider that, to the first order, the curve typified by Fig. 1 oscillates about its mean position unchanged in shape. Accordingly, at the fixed point A the rate of change of force is given by

$$\dot{F}_0 = \frac{1 + 2b}{3}\left(\frac{V_a + V_0}{V_0}\right)^{\frac{1}{2}}\frac{F_a}{d} \cdot \frac{dx}{dt}$$

$$= \frac{1 + 2b}{6}\left(\frac{V_a + V_0}{V_0}\right)^{\frac{1}{2}}\frac{F_a}{d}pc_m M \cos pt$$

(Note that the contribution from $\dot{F}_a$ is negligible and is zero if A is situated at O.)

In accordance with (30)

$$\dot{F}_a \simeq \tfrac{2}{3}pMF_a \cos pt$$

$$\therefore \quad \frac{\dot{F}_0}{\dot{F}_a} = \frac{1 + 2b}{4}\left(\frac{V_a + V_0}{V_0}\right)^{\frac{1}{2}}\frac{c_m}{d}$$

$$= 1{\cdot}9(1 + 2b)\sqrt{\left[\log\frac{I_e}{I}\right]}\left(\frac{V_0}{V_a + V_0}\right)^{\frac{1}{4}}$$

from (21) and (22)–(32).

This ratio will be not much less than unity until V_a/V_0 exceeds 1 000. Hence the small oscillation of the potential barrier causes the existence of a displacement current across the whole space from anode to cathode. This must have a dominant effect on the phase angle of the diode.

(7) THE FORCE/DISTANCE CURVE WHEN THE POTENTIAL BARRIER IS MOVING

Let OB, in Fig. 4, be the time/distance graph of an electron released from O with zero force but initial velocity u_0. (Fig. 2 shows such curves, though unmodified by equation (30), since the force is proportional to the time.) Then an electron reaches a distance CB in time OC.

We will now suppose that the potential barrier is moving to the left of O. Then electrons which start at a time CD after those which have reached L, will have reached a distance DE which is less than DF by the distance which the barrier has moved in time CD. The force on electrons which are at E is greater, by an amount proportional to EH, than it would be if they had been released from O.

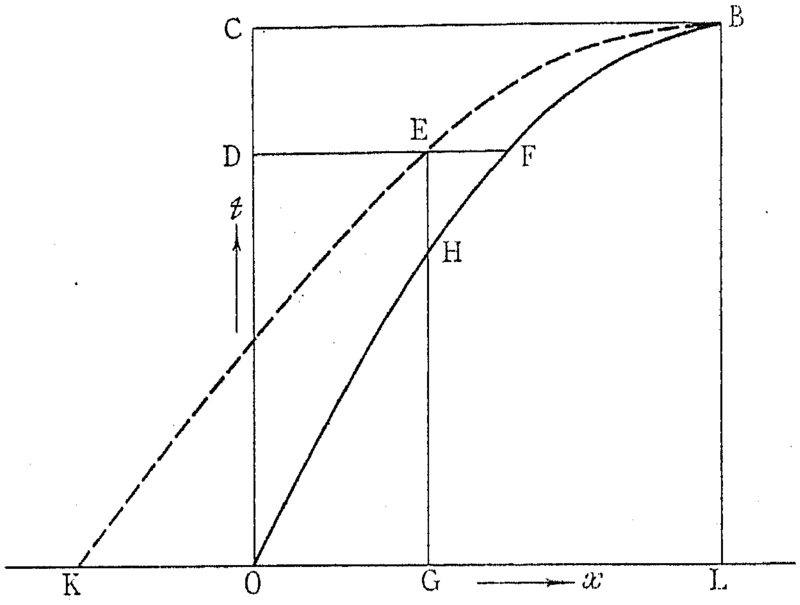

Fig. 4

Let the barrier move a distance OK in the time taken by electrons released at O to reach L. At the instant when the said electrons reach L, the potential difference between points K and L is proportional to the area under the dotted curve KEB, which is greater than the area under the curve OHB. Since the barrier will move sensibly uniformly over the period of a time of flight, it follows that an intercept such as EF is proportional to CD. Whence it follows that the area between the curves AEB and OHB is equal to ½OK × OC. It follows from Section (6) that, near the time when the current is passing through the value I_m,

$$\mathrm{KO} = \tfrac{1}{2} p c_m M T$$

Hence the increment of anode potential due to the movement of the barrier is

$$\begin{aligned}\delta V &\simeq \tfrac{1}{4} p C_m M T F_{ma} \\ &= 2\cdot5\sqrt{\left(\log\frac{I_e}{I_a}\right)}\; b^{3/2}\; \frac{(1+2b)}{(1+b)} V_{ma} p M T \qquad (33)\end{aligned}$$

We have still to allow for the effect described by equation (30). The combination of (33) with (30) leads to

$$V_a \simeq V_{ma}\left[1 + \frac{2}{3}M\left\{\sin pt + \frac{15}{4}\sqrt{\left(\log\frac{I_e}{I_a}\right)} b^{3/2} \frac{(1+2b)}{(1+b)} pT\cos pt - \frac{1}{4}pT(1+2b)\cos pt\right\}\right] \quad . \quad (34)$$

We cannot yet obtain the phase angle between the voltage and the total current, because in the last Section the expression $MI_m \sin pt$ has, in fact, stood for the conduction current at the potential barrier. When this current there passed through its mean value, there was also a displacement current, derivable from (32). In fact,

$$\begin{aligned}\frac{\dot{F}_0}{4\pi} &= \frac{1+2b}{6b}\cdot\frac{F_a}{4\pi d} p c_m M \cos pt \\ &= \frac{1+2b}{6b}\cdot\frac{c_m}{d} pTMI_m \cos pt, \text{ from (4)} \\ &= 2\cdot85(1+2b)b^{\frac{1}{2}}\sqrt{\left(\log\frac{I_e}{I_a}\right)} pTMI_m \cos pt,\end{aligned}$$

from (32) or (21)

Hence we have considered the epoch when the total current is

$$i = I_m\left[1 + M\left\{\sin pt + 2\cdot85(1+b)b^{\frac{1}{2}}\sqrt{\left(\log\frac{I_e}{I_a}\right)} pT\cos pt\right\}\right] \quad . \quad (35)$$

Hence the net phase angle of the whole system, barrier to anode, is, from (34) and (35),

$$\phi = \frac{1+2b}{4}\left[b^{\frac{1}{2}}\left(\frac{15b}{1+b} - 11\cdot4\right)\sqrt{\left(\log\frac{I_e}{I_a}\right)} - 1\right] pT \quad (36)$$

This expression for ϕ shows the possibility of a very considerable change of phase angle with current; ϕ is, however, always negative.

To find the phase angle of the diode, it is necessary also to consider the space between the barrier and the cathode. This, however, we shall not do in detail, partly because we do not really know the distribution of space charge in it—the supposition that this is uniform is little more than a guess. In cases of practical interest the potential of the barrier is a small fraction of V_a, and to include it would, in general, add only a second-order term to (34).

Suffice it then to say that, on the evidence of (36), we should expect a planar diode to have a phase angle which would change considerably as the anode potential was increased from a low value to that producing saturation.

Since there have been many approximations and simplifications in this analysis, it is not likely that equation (36) can be relied on to give results which are quantitatively correct; it is hoped, however, that it is correct qualitatively. Probably the two most important simplifications are the assumption of uniform charge density between the cathode and the barrier, and ignoring the velocity distribution of the electrons once they have left the barrier. The numerical factors, such as 15 and 11·4 in (36), must be appreciably dependent on both these simplifications. Also b is defined in terms of the supposedly uniform velocity with which the electrons leave the barrier: it is related to the mean-square velocity of emission from the cathode by equation (22). This equation contains the factor 4π, whose validity or appro-

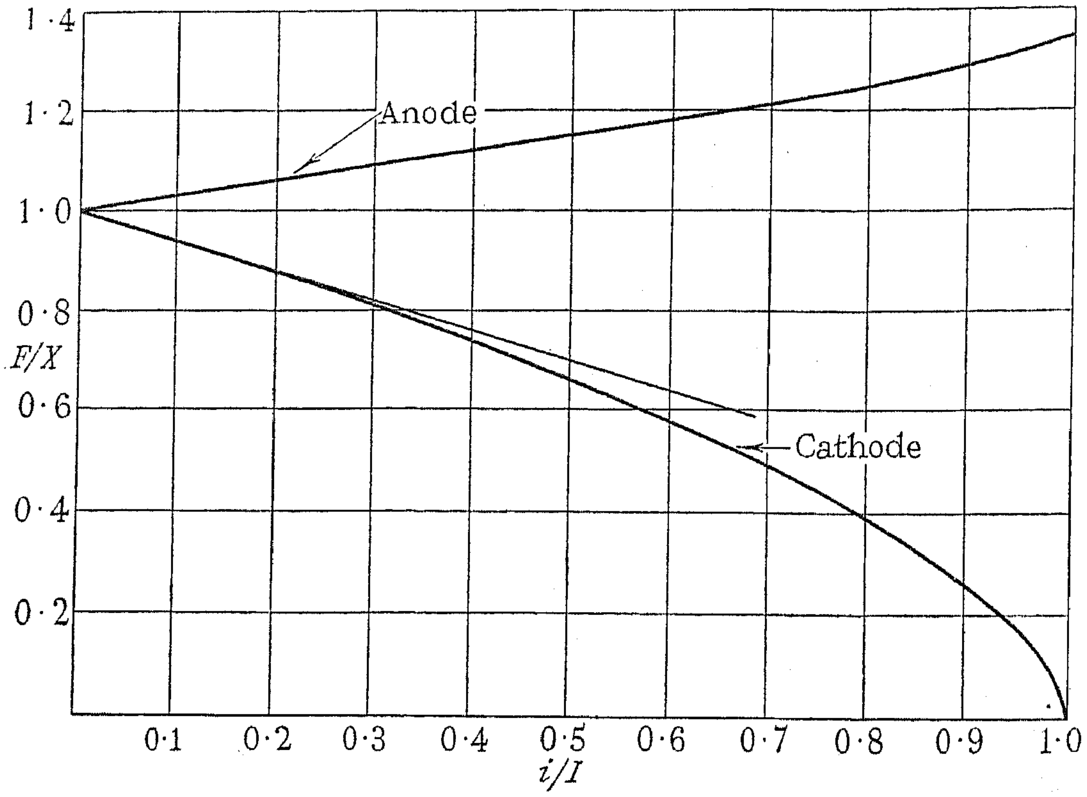

Fig. 5

priateness is open to argument. Thus in practice the factor b could not be evaluated with certainty.

Furthermore, planar diodes do not exist. A cylindrical electrode system would no doubt introduce in (36) a factor depending on the ratio of the radii. If, however, an equation corresponding to (36) could be derived for cylindrical electrodes, it would no doubt be of the same general form. The chief, perhaps the only, interest of (36) is to show the possibility of very great changes in the apparent capacitance of a thermionic tube as the anode current is increased from a small value up to saturation.

APPENDIX

In the course of investigating the problem which occupies the main part of this paper the author has also been led to investigate the distribution of force, potential, etc., in a temperature-limited diode. The solution of this problem may have been published previously, but he is not aware that it has been. At any rate the solution does not seem to be well known and, as it is brief, it seems appropriate to add it as an appendix to this paper.

The solution can be derived by eliminating t from equations similar to (4), (5), and (6), except that now there is a force F_0 at the cathode. Here, however, it is more direct to derive it as a solution of Laplace's equation. (For this solution the author wishes to acknowledge his indebtedness to Professor D. R. Hartree, F.R.S.) This equation for a planar diode is well known to be:—

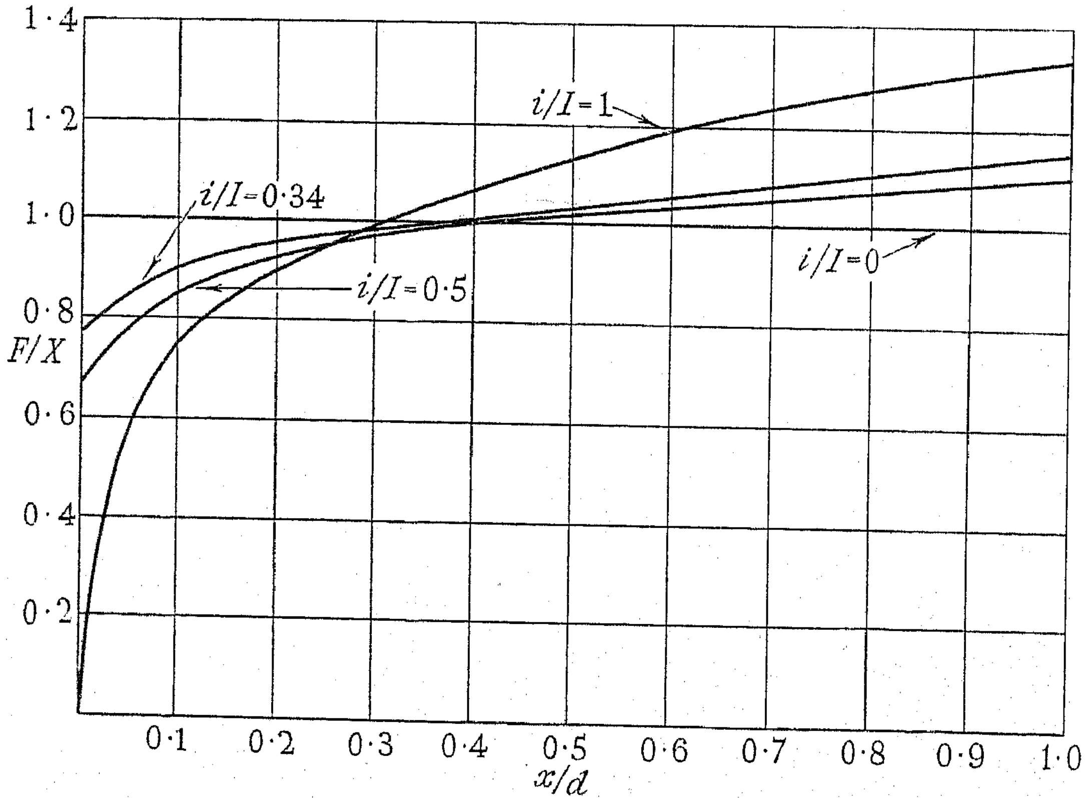

Fig. 6

$$\frac{\partial^2 V}{\partial x^2} = 4\pi\sqrt{\left[\frac{m}{2e}\right]}V^{-\frac{1}{2}}i \equiv kV^{-\frac{1}{2}}i$$

$$\therefore \left(\frac{\partial V}{\partial x}\right)^2 - F_0^2 = 4kiV^{\frac{1}{2}} \quad . \quad . \quad . \quad . \quad (37)$$

where F_0 is the field at the cathode, from which the electrons emerge without velocity. If I is the space-charge-limited current corresponding to anode potential V_a and electrode separation d, then it follows from (37) that

$$\frac{16}{9}V_a^{3/2} = 4kId^2$$

Using this equation to eliminate k from (37), we have

$$\left(\frac{\partial V}{\partial x}\right)^2 = F_0^2 + \frac{16}{9}\alpha^2X^2\left(\frac{V}{V_a}\right)^{\frac{1}{2}} \quad . \quad . \quad (38)$$

where $\alpha^2 \equiv i/I$ and $X \equiv V_a/d$.

On substituting $V/V_a = Z$ and $x = yd$, we obtain

$$\left(\frac{\partial Z}{\partial y}\right)^2 = \left(\frac{F_0}{X}\right)^2 + \frac{16}{9}\alpha^2Z^{\frac{1}{2}}$$

$$\equiv \frac{16}{9}\alpha^2(Z^{\frac{1}{2}} + a)$$

where $$a = \frac{9}{16\alpha^2}\left(\frac{F_0}{X}\right)^2$$

$$\therefore \frac{\partial Z}{\partial y} = \frac{4}{3}\alpha(Z^{\frac{1}{2}} + a)^{\frac{1}{2}} \quad . \quad . \quad . \quad . \quad (39)$$

$$\therefore y\alpha = \frac{3}{4}\int\frac{dZ}{(Z^{\frac{1}{2}} + a)^{\frac{1}{2}}} + \beta$$

$$= 3\int(\theta^2 - a)d\theta + \beta$$

where $$\theta^2 \equiv (Z^{\frac{1}{2}} + a)$$

$$= (\theta^3 - 3a\theta) + \beta$$

$$= (Z^{\frac{1}{2}} + a)^{\frac{1}{2}}(Z^{\frac{1}{2}} - 2a) + 2a^{3/2},$$

since $$Z = 0,\ y = 0$$

or $$Z(Z^{\frac{1}{2}} - 3a) = \alpha y(\alpha y - 4a^{3/2}) \quad . \quad . \quad . \quad (40)$$

When $y = 1$, $Z = 1$,

$$\therefore a = 2a^{3/2} - (2a - 1)(a + 1)^{\frac{1}{2}} \quad . \quad . \quad (41)$$

This is an equation relating i/I with F_0/X, and thus allows us to find the field at the cathode when the current is any assigned fraction of the space-charge-limited current for the given anode potential.

If $a >> 1$, i.e. i/I is very small, then

$$\frac{4}{3}\alpha a^{\frac{1}{2}} \simeq 1 - \frac{1}{3a} + \frac{3}{16a^2}$$

$$\left.\begin{aligned} \therefore \frac{F_0}{X} &\simeq 1 - \frac{16}{27}\frac{i}{I} \\ \text{similarly} \qquad \frac{F_a}{X} &\simeq 1 + \frac{8}{27}\frac{i}{I} \end{aligned}\right\} \quad . \quad . \quad . \quad . \quad (41a)$$

The curves of Fig. 5 show F_0/X and F_a/X as functions of i/I and are derived from equations (39) and (41). It is perhaps interesting to find that F_0/X is still as much as 66 per cent when the current is half the saturation value. The four curves of Fig. 6 show field strength plotted as a function of distance for $i/I = 0$, $0\cdot34$, $0\cdot5$, and 1.

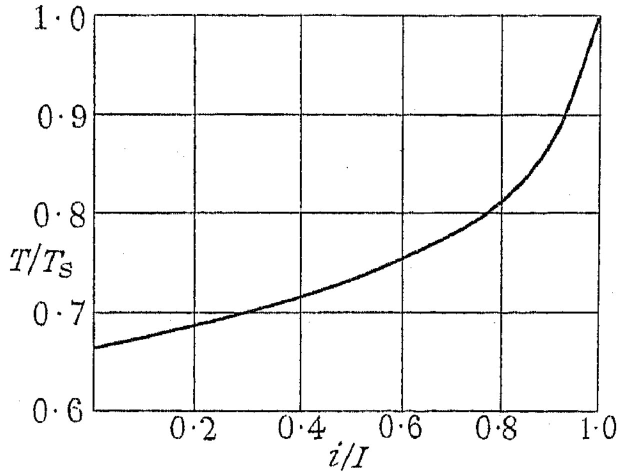

Fig. 7

Since the transit time is given, from (4), by the relation

$$T = \frac{\text{charge in transit between electrodes}}{\text{current}}$$

it follows readily that

$$\frac{T}{T_s} = \frac{4}{3}\frac{X}{(F_a + F_0)} \quad . \quad . \quad . \quad . \quad . \quad (42)$$

where T_s is the transit time when there is space-charge limitation. Fig. 7 shows T/T_s plotted as a function of i/I.

DISCUSSION.*

Mr. W. E. Benham (*communicated*): The author's contribution to the theory of valve circuits is directed towards explaining the variations in hot capacitance in a diode valve as a function of the space current. In Section (1), he says that he is not aware that experimentally the anode capacitance is a continuous function of the anode current. If he will refer to pages 482–489 of my paper in the *Philosophical Magazine* (1931, vol. 11) he will, however, find that such is the case. A resonance method was used for measurements on diode capacitances, in view of the exceptionally heavy damping. As I had succeeded in measuring diode capacitances by this method, though not without some difficulty, the same method was used for experiments on triodes. A more accurate method was adopted at a later date for triode capacitances, but my published measurements using a resonance method may be taken as accurate to $0\cdot1$ $\mu\mu$F and give some general indication of the effects studied. It should be mentioned that ΔC changes from negative to positive in a diode as emission limitation sets in. Fig. 13 of my paper does not show this effect, as the region investigated corresponds to infra-saturation. A number of curves taken in 1928 did, however, show the effect, also ΔC_{fg} was found to be negative for a temperature-limited triode. For various reasons these results were not published at the time, but they now receive confirmation in the light of North's and of Bakker and de Vries's* extensions of Müller's theory.† In regard to the ideal theoretical value of 3/5, on page 487 I pointed out that this value was only intended to apply at one point of the characteristic. Fig. A shows a typical diode characteristic and also the ideal 3/2 power law. The point where the analysis neglecting initial velocities approaches reality is indicated by a cross and may be referred to as the Langmuir point. Müller‡ has dealt with the region to the right of the Langmuir point and his analysis gives, inter alia, variations of capacitance in this region. The d.c. results given by Mr. Moullin in the Appendix will be of value in providing quantitative interpretation of Müller's important work, as also will the work of R. Cockburn (in course of publication).§ The region to the left of the Langmuir point can only be exactly explained by a very complete investigation of the potential minimum. I am not in agreement with Mr. Moullin that equations (1) and (2) of his paper are well known, nor do I think we can employ them here. Fig. 1 and equation (1) show an infinity in ρ which is, of course, purely mythical, since the electron velocity at O is not zero. On page 27 Mr. Moullin uses the symbol b for something quite different from its meaning on page 24. This makes his analysis very confusing. His conclusion in Section (6), to the effect that the displacement current at the potential minimum is nearly equal to that at the anode, is at variance with the views I expressed in a recent paper.* My view still is that the displacement current is zero (or very small) at the mean position of the potential minimum, but that the alternating current at the cathode consists of some displacement current, plus convection current arising from electrons returning from the potential minimum. No alternating convection current is carried by *outgoing* electrons at infinitesimal distance from the cathode, owing to the inability of the electrons (in view of their inertia) to respond instantaneously to the alternating field in which they find themselves immediately on emerging from the cathode. These 1934 views do not conflict with my 1928/31 assumption that the convection current at the cathode was equal to the total current, since this hypothesis merely corresponded to assuming that the potential minimum coincided with the cathode. In the space-charge limited diode, the electric field undergoes a much greater change (for a given anode potential) as we pass from cathode to anode, than in a space-charge saturated condition, and the hot capacitance would therefore be expected to differ somewhat from that given by simple theory.

---

* Reprinted from *Journal I.E.E.*, 1938, vol. 82, p. 219.

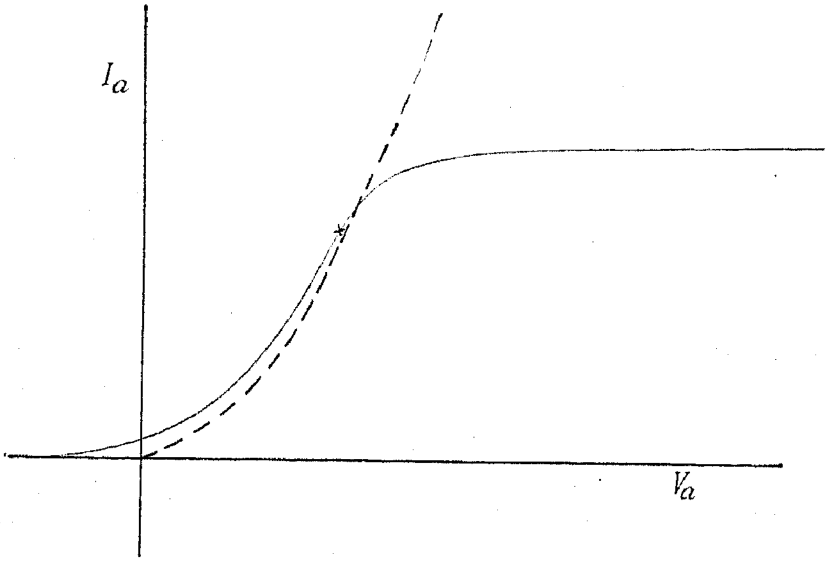

Fig. A

Mr. E. B. Moullin (*in reply*): Surely equations (1) and (2) are extremely well known: they follow directly from any solution of the space-charge-limited condition in which electrons cross the barrier with zero velocity. I agree they cannot be accepted: this long and laborious paper has been written only because they cannot be accepted as representing a real diode in the problem investigated here. Surely this is made clear in Section (1) of the paper. I agree that it is unfortunate I have used the symbol b in the equation $i = I'(1 + bt)$ near the beginning of Section (5). If Mr. Benham will replace b where it appears in Section (5) up to and including equation (26) by b' I think all confusion will be avoided.

I am interested to know that Mr. Benham still considers the displacement current to be very small at the mean position of the barrier. The analysis of this problem is very complex and it is possible that I have taken some inappropriate boundary condition. The steps leading up to my conclusions in Section (6) are straightforward. I hope that Mr. Benham will later point out the place where I have taken the step which leads me to conclusions different from his, and that he will then discuss critically the validity or invalidity of it.

---

* C. J. Bakker and G. de Vries: *Physica*, 1935, vol. 2, p. 683. D. O. North: *Proceedings of the Institute of Radio Engineers*, 1936, vol. 24, p. 108.

† Johannes Müller: *Hochfrequenztechnik und Elektroakustik*, 1933, vol. 41, p. 156.

‡ *Loc. cit.*

§ See also *Proceedings of the Physical Society*, 1935, vol. 47, p. 810.

* See also *Proceedings of the Physical Society*, 1935, vol. 47, p. 8.

AN IMPROVED MEDIUM-WAVE ADCOCK DIRECTION-FINDER[*]

By R. H. BARFIELD, M.Sc., Associate Member, and R. A. FEREDAY, Ph.D.

[From the Radio Department, National Physical Laboratory.]

(*Paper first received 16th March, and in final form 29th May,* 1937.)

SUMMARY

This paper describes a medium-wave Adcock direction-finder capable of working over the wavelength range 750 to 2 000 metres (frequency 400 to 150 kc.) with a pick-up factor between 3 and 5 metres. Under favourable conditions a bearing can be taken on a field strength of 10 microvolts per metre with a swing of less than 1°. When the field strength is 1 microvolt per metre the corresponding swing is ± 10°. The standard-wave error is less than 1° as measured on a wavelength of 1 760 metres (frequency 170 kc.), and this may most probably be taken to be representative of its value over the whole range. The instrumental error after balancing is less than 1°, but no information is at present available as to how long the balance remains constant.

The instrument may therefore be said to constitute a practical development of the balanced-coupled Adcock system, retaining all the advantages of that type as regards polarization error but with a greatly enhanced pick-up factor compared with that of the early experimental model, which makes the apparatus capable of taking bearings with field strengths as low as 1 microvolt per metre, and with an instrumental accuracy as good as that of a loop-type Bellini–Tosi direction-finder.

INTRODUCTION

In an earlier paper[†] an account was given of an investigation limited to a study of the principles underlying the design of spaced vertical aerials or Adcock direction-finders. This work dealt chiefly with the factors determining polarization error and pick-up factor rather than with the details of design of practical direction-finders. The present work continues from the point where this investigation left off and describes the development of a practical and efficient direction-finder based on the principles laid down in the earlier investigation.

Attention was given in the design to the attainment of (1) very small polarization error, (2) high pick-up factor, (3) small instrumental error. These are dealt with in full under separate sections, but the methods of attaining these ends are briefly stated below.

(1). The balanced-coupled aerial system was employed, which was the type found, in the earlier investigation, to give the lowest polarization error.

(2). The pick-up factor was made as large as possible by (*a*) employing multi-wire aerials of high capacitance, (*b*) arranging for the resonating frequency of the aerials to be just below the lowest frequency in the wave range, (*c*) arranging for the resonating frequency of the secondary circuit to be just above the highest frequency in the wave range.

(3). The instrumental error was reduced to its lowest possible value by the provision of trimming condensers on the transformer primaries, the balancing being carried out by injection into each aerial from a centrally placed local generator by means of temporarily laid-out feeders.

REDUCTION OF POLARIZATION ERROR

To be completely free from polarization error, an Adcock aerial system must have zero response to horizontal fields. This can only be achieved by paying careful attention to the nature of the connecting links between the aerials. Of the many methods possible, the balanced-coupled system has been found most satisfactory for reducing this pick-up to a minimum.

The circuit diagram showing the position of the balancing condensers is seen in Fig. 1, and the transformer construction in Fig. 2. The secondary winding is carried in a screw thread on the outside of an ebonite cylinder. After insulation by a layer of silk, a layer of copper foil is wound over the winding to form a screen between it and the primary winding. The slotted former for the primary winding is a " push fit " over the flanges on the secondary bobbin. By adopting this form of construction the inter-winding capacitance is reduced to less than 10 $\mu\mu$F.

The screen is connected to the centre of the primary and ensures that the currents induced in the feeders by the horizontal e.m.f. pass into the aerial circuit at a known point and thus correct for the effect of non-uniformly-distributed capacitance between the windings.

The feeders (described below) are unscreened and raised above the ground. The use of buried, screened feeders, though more convenient in many ways, is not desirable. There is some risk that the polarization error would be re-introduced by the proximity of the feeder earthing-points to the earth of the aerials, and also it would not be so easy to work near resonance in the secondary circuit.

A measurement was made of the standard-wave error of the system by comparing the e.m.f.'s which had to be injected into the horizontal and vertical members respectively to give the same output from the receiver. The measurements indicated a standard-wave error of the order 0·2°. This is an order of magnitude too small to be measured by the injection method employed, so that it is difficult to assign a definite figure for the performance of the system; it seems probable, however, that the standard-wave error is not actually in excess of

---

[*] Reprinted from *Journal I.E.E.*, 1937, vol. 81, p. 676.

[†] *Journal I.E.E.*, 1934, vol. 76, p. 423, and *Proceedings of the Wireless Section*, 1935, vol. 10, p. 55.

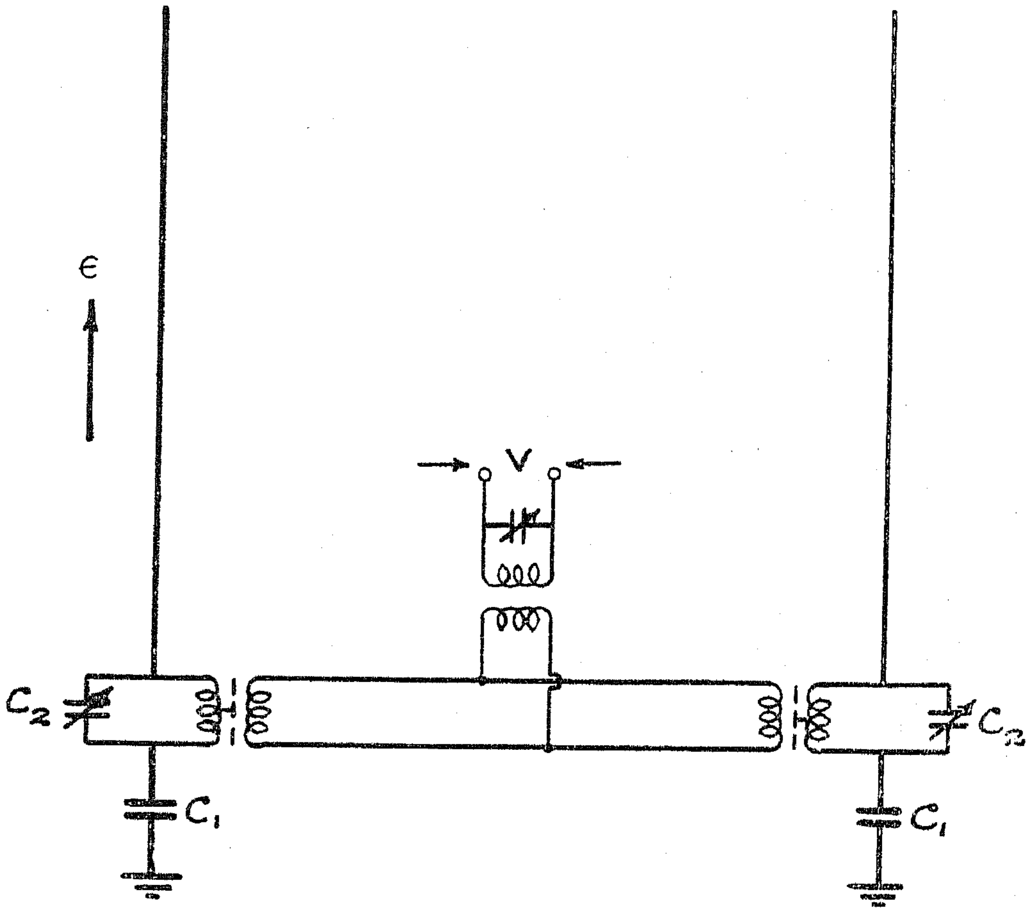

Fig. 1.—Circuit diagram showing position of balancing condensers.

C_1 = Aerial balancing condenser.
C_2 = Fine-balancing condenser.

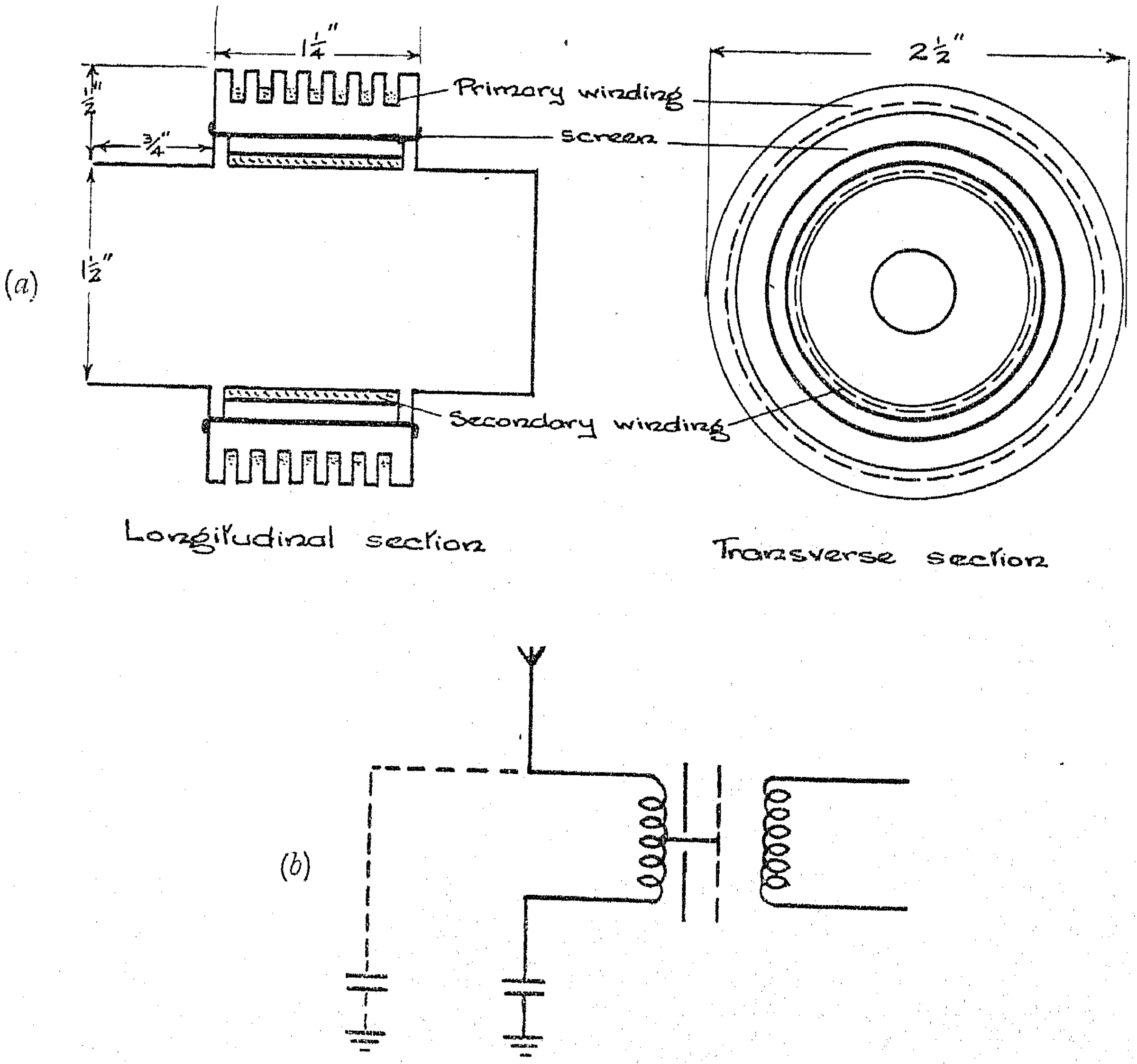

Fig. 2.—Aerial-transformer details.

(a) Details of transformer construction.
(b) Balanced transformer with aerial balancing condenser.

1°. Confirmation of this improvement was provided by a series of observations made of the bearings of the Kalundborg broadcasting station under conditions of night effect, which indicated a somewhat better performance than the best attained with the experimental model described in a previous paper.*

PICK-UP FACTOR

If ϵ is the field strength in volts per metre and V is the p.d. in volts across the grid circuit of the first amplifying valve, the pick-up factor is defined as V/ϵ and is therefore expressed in metres (see Fig. 1).

It has been shown that the factor is proportional to the effective height of the aerials, approximately proportional to the aerial spacing, and inversely proportional to the impedance of the aerial circuit. It has been further shown that for an untuned aerial circuit the pick-up factor is nearly proportional to the capacitance of the aerials. For this reason high-capacitance multi-wire cage-type aerials were employed, consisting of eight wires 60 ft. high suspended from an octagonal former of 4 ft. side fixed at the top of the tower. In this way the wooden tower was surrounded by wires—an arrangement which has the added advantage that the screening effect of the wires reduces the influence that any irregularities or differences in the woodwork of the tower might have on the balancing of the aerial system. The capacitance of each aerial of this type was found to be 510 $\mu\mu$F, as against 130 $\mu\mu$F for a single wire, thus giving a gain in pick-up factor of approximately 4 times.

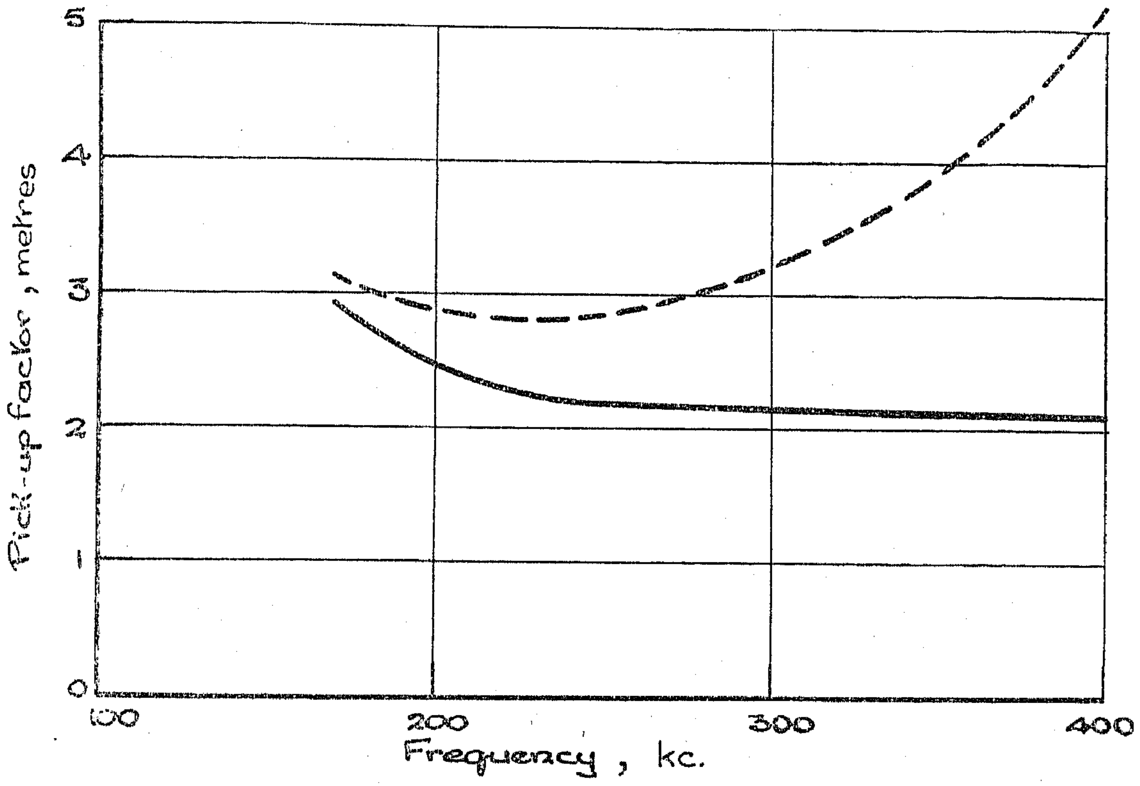

Fig. 3.—Pick-up factor as function of frequency.

———— Lines untuned.
— — — — Lines partially tuned by 0·004-μF condenser.

It would be very difficult in practice to work with tuned aerials. It is, however, of material advantage to have the natural frequency of the aerial circuits falling not far beyond the working range, so that the approach to resonance is limited by the difficulty of maintaining electrical equivalence of the opposite aerials forming a pair throughout a frequency band in the neighbourhood of resonance. It is advantageous to have the resonance point at the lower end of the frequency band in order that, on receding from resonance, the decrease in pick-up factor due to the increase in aerial impedance shall be compensated for by the increase in pick-up factor due to the increase of the ratio of aerial spacing to wavelength.

If the resonance is near the upper end, the two effects add together and a very rapid change in pick-up factor with frequency results.

Owing to the fairly wide frequency range which the system is intended to cover, the effect of such an aid to increased sensitivity will not be felt equally over the whole band. Having arranged, however, that at the low-frequency end of the range the pick-up factor was increased by approach to resonance of the aerial circuit, it was found that a corresponding increase at the high-frequency end could be secured by arranging that the circuit comprising coupling-transformer secondaries, transmission lines, and goniometer field coil, should resonate just beyond the working range at the high-frequency end. This resonance was easily controlled by a small condenser across the line.

In Fig. 3 the full-line curve shows the variation of pick-up factor with frequency with the lines untuned. The broken-line curve shows the effect of a suitable degree of partial tuning of the lines and represents the pick-up factor curve for the completed system. The value is then seen to lie between 2·5 and 5·5 metres, and for comparison it may be noted that the pick-up factor of a highly efficient multi-turn tuned coil 1 square metre in area will be of the order of 15 metres over the same frequency range. By restricting the working range and allowing a correspondingly closer approach of aerial and line resonances, the pick-up factor may be increased, and values up to 15 metres have been measured. The performance of the system on weak signals is of course largely dependent on the sensitivity and noise level of the receiver with which it is used. In conjunction with a Marconi DFG8 receiver, it was found possible to obtain first-class bearings (i.e. having a swing of ± 0·5°) with a field strength of 10 microvolts per metre. With a 1 microvolt per metre steady field, bearings could be taken with a swing of ± 10°.

---

* *Loc. cit.*

METHOD OF REDUCING INSTRUMENTAL ERROR

The accurate performance of any Adcock system depends upon exact equivalence of the four component aerials, and recent theoretical study* of the behaviour of a system in which the aerials differ slightly in characteristics has made it possible to lay down quantitative requirements as to the permissible tolerance for a given degree of accuracy. For a short-wave system where the ratio of spacing to wavelength may be kept comparatively large, it may be possible to construct aerials and transformers so nearly alike that no balancing adjustment is necessary, but for medium or long waves this is not the case.

Taking 1° maximum instrumental error as a desirable ideal to aim at, it was found that with the wavelength range and spacing of the present system a set of aerials erected with reasonable care to ensure similarity did not fulfil the necessary conditions, so that some fine balancing control was needed by which a final adjustment might be made after erection.

A full control of aerial capacitance and resistance may be effected by a small variable condenser across the transformer primary and a variable resistance in the earth lead. Except in a case of bad out-of-balance on the fixed installation, the condenser alone was found to give sufficient control; but during development the need was found for inclusion of both capacitance and resistance, in order to secure the necessary degree of balance, and this was taken as an indication of a serious initial discrepancy, the source of which had to be determined and removed.

Two alternative methods of setting the fine-balance condensers and measuring the degree of balance attained were used.

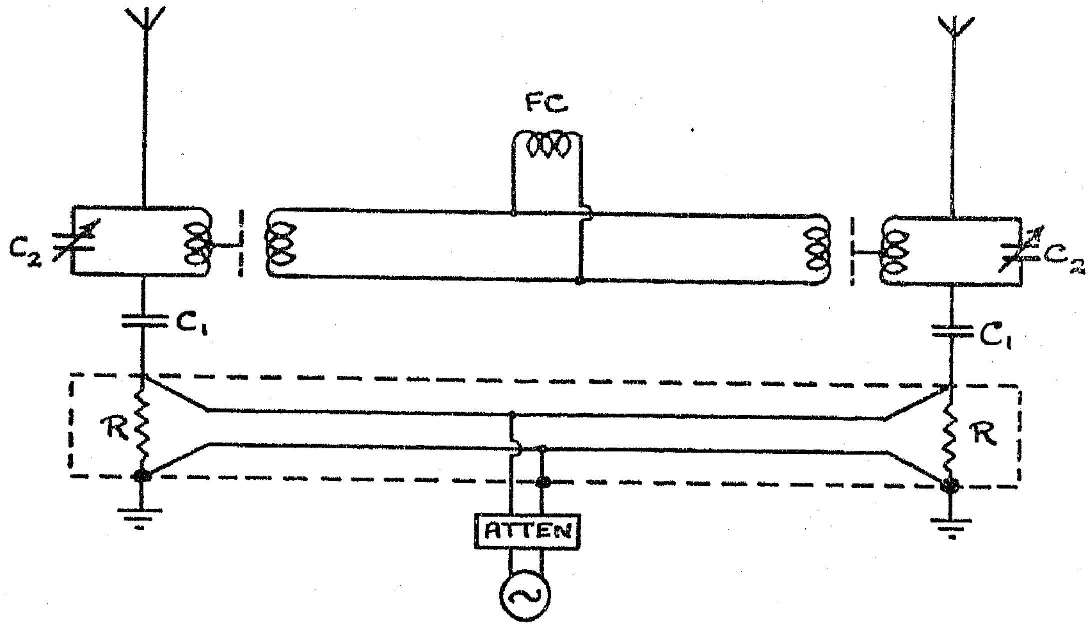

Fig. 4.—Fine-balance arrangement (injection from central oscillator).

FC = Field coil. R = Injection resistance (500 ohms).
C_1 = Aerial balance condenser (500 $\mu\mu$F).
C_2 = Fine-balance condenser (30 $\mu\mu$F).

In the first method (see Fig. 4) a small e.m.f. is injected into each of the aerials to be compared; the source of e.m.f. is a central oscillator, feeding through an attenuator and a pair of matched screened transmission lines to 500-ohm resistances at the base of each aerial. By careful matching of these lines and of the resistances, equality of the voltages injected into the aerials is ensured; also, since the attenuator impedance of 10 ohms is shunted across each injection resistance, very slight disturbance of the constants of the aerials is assured. An e.m.f. is injected in this way, and its amplitude adjusted so that it gives normal output from the receiver. The injection leads and resistance of one aerial are then removed, and the attenuation increased to reduce the receiver output to the previous level. From the two attenuator settings the relative outputs from one aerial and from the balanced pair are thus immediately known.

In the second method, one Adcock pair is connected normally to the receiver and a signal is radiated from one aerial of the other pair by energization from a small oscillator located at its base. If the pair is completely balanced no signal will be received, and the comparison of the actual receiver output under these conditions with that when one aerial is disconnected gives a measure of the degree of balance.

Results obtained by the two methods show satisfactory agreement. If the balancing adjustment is made at a frequency far removed from the resonant frequency of the aerials, it will be found to hold good over a wide frequency band. In the present case, however, the frequency range with which we are concerned is near to the aerial resonant frequency and, the balancing adjustment having been made at one frequency, it is found that the degree of balance is poorer at any other frequency, since the manner of variation of aerial characteristics with frequency near to resonance is not the same for each aerial. For frequencies nearer to resonance the degree of balance falls off rapidly. For frequencies farther from resonance there is a smaller drop, followed by a rise as the frequency becomes so far removed from resonance that small differences in aerial characteristics are no longer important.

---

* R. H. Barfield and W. Ross: "A Short-Wave Adcock Direction-Finder" (see page 39).

It was found that, with the lower working frequency limit set at 150 kc., the aerials could be allowed to resonate at about 120 kc. A higher frequency made it impossible to maintain a sufficiently good balance, and a lower frequency was undesirable owing to the resulting drop in pick-up factor.

Owing to the rapid falling-off of balance toward the resonant frequency, it was necessary to effect the balancing adjustment at the low-frequency end of the working range. Fig. 5 shows the degree of aerial balance obtained over the working range (150–400 kc.) when adjusted for best balance at 160 kc. It also shows the degrees of balance necessary to ensure instrumental errors of less than 0·5°, 1°, and 2° respectively for downcoming waves not steeper than 45°; an accuracy of less than 1° error is realized over practically the whole range.

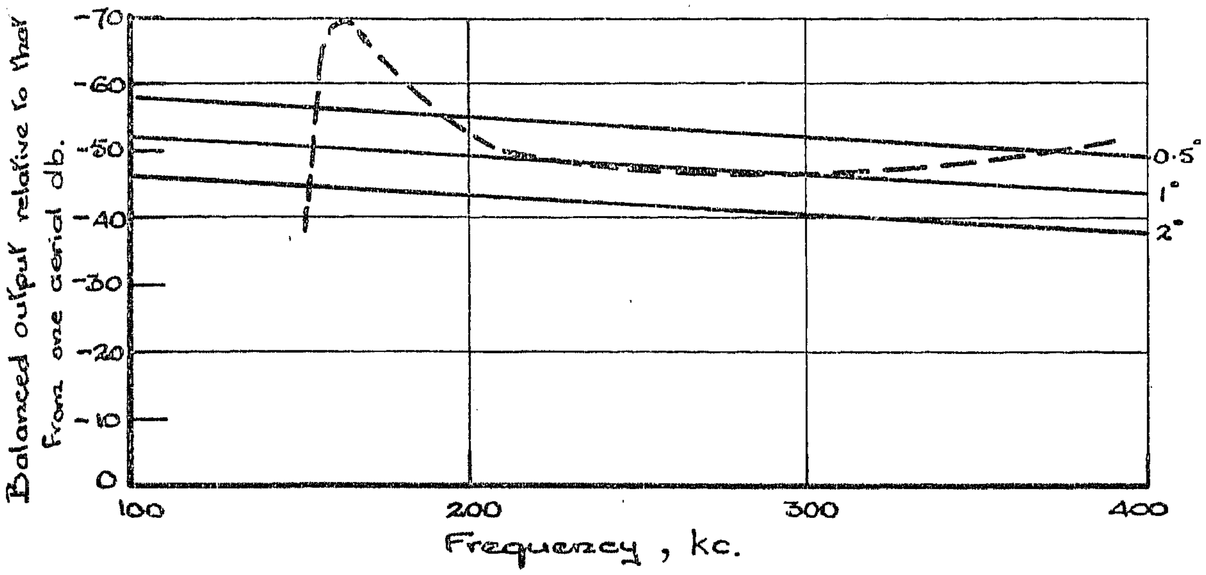

Fig. 5

— — — Degree of balance over range 150–400 kc. when adjusted for best balance at 160 kc.
——— Minimum balances for degree of accuracy shown (waves not steeper than 45°).

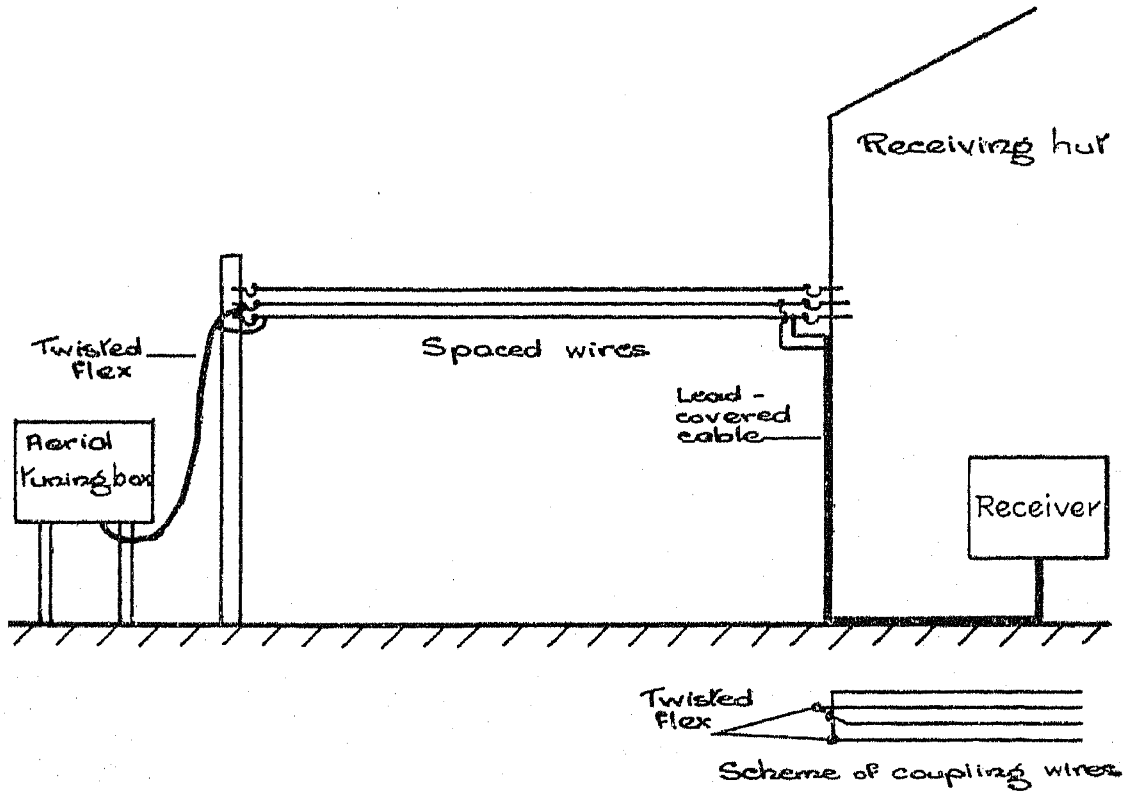

Fig. 6.—General layout of feeder system.

CONSTRUCTIONAL DETAILS OF AERIAL SYSTEM

The Adcock aerials are spaced out at the corners of a square of 100 metres diagonal. Each consists of a light wooden tower supporting eight wires which, hanging at the corners of a regular octagon of 4 ft. side, form a vertical cage aerial. The wires are brought together at the lower end and led into a weatherproof box at the base of the mast which houses the aerial coupling-circuit components.

Connection between the aerials and the central receiv ing hut is effected by transmission lines supported on poles at 8 ft. above ground. These lines, which terminate at the walls of the hut, whence lead-covered cables connect to the receiver, are arranged according to a well-known method. Each line consists of four wires (of No. 18 S.W.G. hard-drawn copper) spaced so that in a section of the line they appear at the corner of a square of 6 in. diagonal (see Fig. 6). At each extremity of the line the diagonally-opposite wires are connected together to form one conductor. It will be seen that each pair of diagonally-opposite wires may then be regarded as equivalent to a single conductor passing through the centre of the square, and hence the whole system to a pair of coincident " go " and " return " wires along the axis of symmetry, so that the whole should be non-receptive and non-radiating.

CONCLUSIONS

The apparatus described constitutes a medium-wave Adcock direction-finder capable of working over the wavelength range 750–2 000 metres with a pick-up factor between 3 and 5 metres. Under favourable conditions a bearing can be taken on a field strength of 10 microvolts per metre with a swing of less than 1°. When the field strength is 1 microvolt per metre the corresponding swing is ± 10°.

The standard-wave error is less than 1° as measured at 170 kc., and this may most probably be taken to be representative of its value over the whole range. The instrumental error after balancing is less than 1°, but no information is at present available as to how long the balance remains constant.

The instrument may therefore be said to constitute a practical development of the balanced-coupled Adcock system, retaining all the advantages of that type as regards polarization error, but with a greatly enhanced pick-up factor compared with that of the early experimental model, which makes the apparatus capable of giving bearings with field strengths as low as 1 microvolt per metre and with an instrumental accuracy as good as that of a loop-type Bellini–Tosi direction-finder.

Acknowledgments

The work was undertaken as part of the programme of the Radio Research Board and is published by permission of the Department of Scientific and Industrial Research. The authors desire to acknowledge the contribution made to this work by Mr. H. Page, who was responsible for carrying the development to the stage at which the complete system was erected in the preliminary form. They are also indebted to Messrs. G. H. Calver and R. E. Burgess for assistance in connection with the experimental work.

A SHORT-WAVE ADCOCK DIRECTION-FINDER[*]

By R. H. BARFIELD, M.Sc., Associate Member, and W. ROSS, M.A.

[From the Radio Department, National Physical Laboratory.]

(*Paper received* 17*th June*, 1937.)

SUMMARY

This paper gives full details of the construction and performance of a short-wave aural Adcock direction-finder of the coupled type with a working wavelength range of from 35 to 70 metres (frequency 8·6 to 4·3 Mc.). It describes how the design of the instrument is based on the principles brought to light in an earlier investigation. It deals with its design in respect of polarization error, pick-up factor, and instrumental error, and describes experiments by which these properties were measured. The values obtained for these were as follows: standard-wave error, 3° to 8°; pick-up factor, 4·5 to 6 metres; instrumental error, 2° to 3° at maximum.

The apparatus is considered to constitute a satisfactory direction-finder from a practical point of view, though it will be possible in future models, one of which is already under construction,[†] to take advantage of the experience gained to obtain an instrument with lower instrumental and polarization errors and higher pick-up factor.

INTRODUCTION

The short-wave Adcock direction-finder described below embodies a specially designed radiogoniometer with aural indication. The development of the apparatus arises directly out of the investigation, described in an earlier paper, into the principles underlying the design of Adcock direction-finders.[‡] This work dealt with the various modifications of Adcock's principle of spaced vertical aerials, and showed in a quantitative manner how the performance of each type depended on many different factors, such as the height and spacing of the aerials in relation to the wavelength, the conductivity of the soil, and particularly the arrangement of the horizontal feeders connecting the aerials to the receiving apparatus. Attention was directed, in the first place, to the influence of these factors on the polarization errors of the system, specified by means of a defined quantity to which the name " standard-wave error " was given; and, in the second place, to the efficiency of the aerial system as a receiver of wireless energy, expressed in terms of a defined quantity called the " pick-up factor."

It was therefore possible to design an instrument satisfactory in the above respects without much further experimental or development work. The production of an apparatus suitable for making a series of accurate observations over a prolonged period, however, necessitated attention being given to certain other features in the design. These are of a less fundamental nature, but bear directly on the accuracy of the instrument. The most important of these is the problem of instrumental error, that is to say, of the error which results from departure from symmetry of the system or from exact similarity of those parts which are supposed to be identical with one another. A section of the paper has been devoted to a discussion of the theoretical aspects of this problem and to a description of the experiments carried out to determine the instrumental error.

POLARIZATION ERROR

Reduction of polarization error to a minimum in an Adcock direction-finder depends entirely on the method of connecting together the four aerials. The various ways in which this can be done, together with the relative merits of each, have been fully described in a previous paper.[†] In the particular installation here described the method known as the " coupled system " was chosen as being most satisfactory for the purpose in hand. It is true that the balanced coupled type has been shown to be capable of giving lower polarization errors than the coupled type: the short-wave Adcock system here described, however, employs an aerial circuit which, at one end of the frequency band, works near its resonance point. Under these conditions the balancing impedance would not be a pure capacitance but would require an inductance and possibly a resistance. The design, testing, and construction, of these complex balancing impedances would have required a considerable amount of further development work which, at the time the direction-finder was required, it was not possible to undertake. Performance in respect of polarization error was thus sacrificed to obtain simplicity of construction.

The circuit arrangement is shown in Fig. 1, and details of the transformers are indicated in Fig. 2. The principle on which the system works has already been given, and it will suffice to say here that it is essential that the capacitance between the transformer windings shall be low. The aerial circuit is extended inwards towards the centre for a length of 5 ft., to a point just underneath the corner of the operating hut, at which the transformer is situated, the earth wire being brought back to the earthing system directly under the aerial. By this arrangement the length of the secondary circuit is reduced. This increases the impedance of the screening boxes regarded as open horizontal aerials, thus minimizing the current flowing in them and the consequent risk of coupling between them and the aerials, which is a factor contributing to the polarization error. The transformers are not helically wound, but are made up of a number of separate rings connected alternately in series in the manner shown in Fig. 2. By this means the two ends of one transformer winding have approximately equal capacitance to the other winding. The feeders connecting the secondary windings of the transformers are constructed of stretched wires spaced 2 in. apart on light wooden beams and are placed inside screening tubes consisting of wire netting stretched round a wooden framework of 1 ft. square box section. The feeder wires are approximately 12 in. above the ground.

---

[*] Reprinted from *Journal I.E.E.*, 1937, vol. 81, p. 682.

[†] This new system has now been completed. As a result of minor modifications in design the following performance has been attained: Standard-wave error, 1° to 4°; pick-up factor, 4 to 10 metres; instrumental error, 2½° (maximum).

Other improvements have also been introduced, such as the provision of switches enabling lining-up tests to be made quickly and as a matter of routine and the addition of a sense-finding device operating on a new principle.

[‡] R. H. BARFIELD: "Some Principles Underlying the Design of Spaced-Aerial Direction-finders," *Journal I.E.E.*, 1935, vol. 76, p. 423, and *Proceedings of the Wireless Section*, 1935, vol. 10, p. 55.

[†] *Loc cit.*

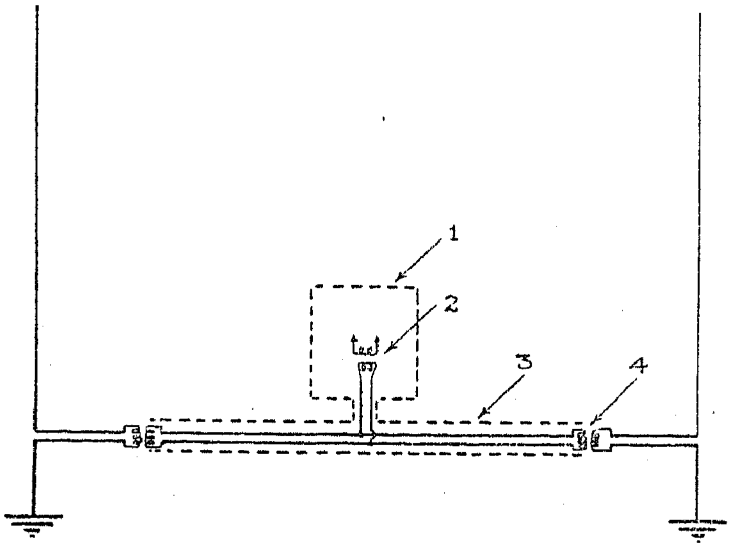

Fig. 1

1. Screening cage (6-ft. cube). 2. Goniometer.
3. Feeder screen. 4. Aerial transformer.

An elevated transmitter with rotating aerials similar to that described in the paper already referred to, and erected on a 70-ft. tower at a distance of about 150 ft. from the aerial system, was used for the purpose of measuring the standard-wave error of the system. The results of a series of measurements are shown in Table 1. These results indicate a standard-wave error varying from 3° at the short-wave end of the band to 8° at the long-wave end. Although the standard-wave error at the upper end of the wave band is rather high, being one quarter that of a loop direction-finder, a large number of observations have tended to confirm that it is low enough for practical purposes, having regard to the other types of variation which the waves are liable to undergo.

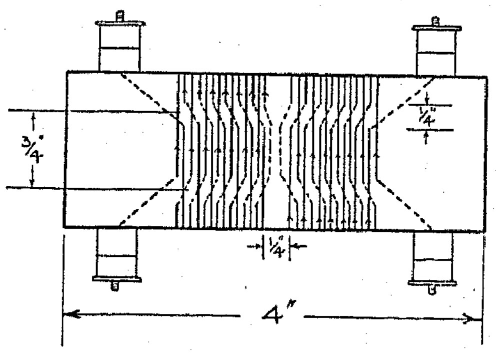

Fig. 2

Self-inductance of each winding, 7 μH.
Mutual inductance of each winding, 1·3 μH.
Capacitance between windings, 2·9 μμF.

Further tests were made by means of this elevated transmitter to ascertain the effect on the polarization error of the large screening cage (6-ft. cube) erected inside the operating hut at the centre of the system and housing the operator, goniometer, and receiving apparatus. No change in polarization error was observable. The effect of inserting, between the primary and secondary windings of the transformers, screens which were earthed at points immediately under the transformers, was also investigated by this method. These also were found to have no influence on the polarization error.

PICK-UP FACTOR

The pick-up factor of a coupled Adcock system has been shown to be proportional to the effective height of the aerials, the spacing between the aerials, and the admittance of the aerial circuit. It also depends on the electrical constants of the transformers, feeders, and circuits between the goniometer and the amplifier. It is defined as the quotient of the output in volts across the first grid circuit of the amplifier and the field strength in volts per metre. The height of the aerials in the case of short waves is limited by the necessity for a loading inductance in the form of the primary of the aerial transformer.

Since the system is to cover a band of wavelengths the aerial circuit cannot be tuned; it might be tuned at one wavelength in the band, but this is inadvisable because of the difficulty of maintaining phase balance with several tuned circuits. The aerial impedance, however, can be kept as low as possible by arranging that the aerial circuit shall resonate at a point just outside the working wavelength band.

Table 1

Wavelength metres	Frequency Mc.	Standard-wave error degrees
64·0	4·7	8·2
59·5	5·05	7·4
53·5	5·6	4·8
41·7	7·2	4·7
37·0	8·1	3·1

In this system the aerial circuit is tuned to a wavelength just above the longest wavelength of the band. In this way the decrease in pick-up, caused by the increase in aerial impedance on receding from resonance in the direction of shorter waves, is compensated for by an increase in pick-up due to the increase in the spacing factor (2π × spacing)/wavelength. At the lower end of the wavelength range the tendency for the pick-up factor to fall off is compensated for by arranging the resonance of the secondary circuit just outside the lower end of the wavelength band.

The search-coil circuit, which is the first tuned circuit in the series between the aerial and the amplifier, is coupled by means of a screened transformer to the first grid circuit of the amplifier (see Fig. 3). The ratio of the p.d. across the first grid circuit to the e.m.f. induced in the search coil must be made as large as possible by careful design. In the present installation a value for this factor between 30 and 40 was obtained for the working wavelength-range.

The pick-up factor of the installation has been determined experimentally by injecting a high-frequency voltage into one aerial of one of the aerial pairs and measuring the voltage developed across the first grid circuit of the amplifier, with the search coil in the position of maximum coupling with the field coil. From the results of this measurement and a knowledge of the spacing and effective height of the aerials the pick-up factor may be calculated. The effective height of the aerials was taken as half the true height, this assumption being as good as the accuracy of the high-frequency measurements justified. The results obtained for different wavelengths are given in Table 2, where p is the pick-up factor in metres.

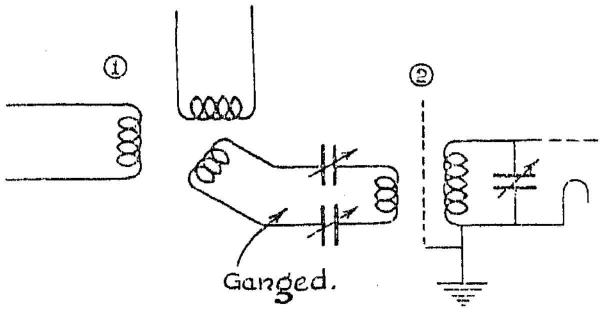

Fig. 3

1. Goniometer.
2. Screened input transformer.

Table 2

λ	p
metres	metres
70	5
	5
50	5·5
	4·5
40	5·5
	5
36	6

These values of pick-up factor may be compared with that of 3 to 5 obtained on medium wavelengths of 750 to 3 000 m.

INSTRUMENTAL ERROR

The fundamental principle of direction-finders using fixed aerials in conjunction with some form of goniometer is that the relative magnitudes of the signals induced in two aerial systems, usually placed at right angles to each other, are compared by means of the goniometer, this comparison enabling the direction of arrival of the signal to be determined. It follows that any error introduced in the relative amplitudes or phases of the signals from the two aerial systems will give rise to errors in bearing, or flatness of the bearing, or both.

The following notation will be used:—

A, B, C, D = the four aerials of the direction-finder.

ψ = direction of arrival of wave relative to plane of one pair of aerials, namely the pair AB.

ϵ = error in bearing due to lack of balance in the aerial system.

ϵ_0 = that portion of ϵ which is due to relative errors in the mean outputs from the two aerial pairs (see definition of δ_0 below).

K = ellipticity, i.e. ratio of minor axis of ellipse to major axis for the resultant magnetic field in the goniometer or trace on oscillograph screen.

K_0 = that portion of K which is due to relative phase error between the mean output from the two aerial pairs (see definition of ϕ_0 below).

δ_1 = fractional difference in amplitude of the signal from one aerial of the pair AB relative to that from the other aerial when equal and co-phasal electromagnetic fields exist at all four aerials.

δ_2 = ditto for pair CD.

δ_0 = fractional difference in amplitude between the mean amplitude of the signals in the pair AB relative to the mean amplitude for the pair CD in the above circumstances (δ_0 gives rise to the quantity ϵ_0).

Δ = total fractional error in amplitude of the output from one aerial pair relative to that from the other, for signals from any direction.

ϕ_1 = phase difference between signals from the two aerials of the pair AB when equal and co-phasal fields exist at all four aerials.

ϕ_2 = ditto for pair CD.

ϕ_0 = phase difference between the mean of the signals in the pair AB relative to the mean of the signals in the pair CD in the above circumstances (ϕ_0 gives rise to the quantity K_0).

Φ = total phase error in the output from one aerial pair relative to output from the other pair for signals from any direction.

d = distance between the aerials in a pair.

λ = wavelength.

S = angular spacing of the aerials for a ground wave $= 2\pi d/\lambda$.

θ = angle of incidence of wave (relative to vertical).

$S_1 = 2\pi d \sin \theta/\lambda$.

r_1 = ratio of amplitude of signal obtained from pair AB connected in opposition to amplitude of signal obtained when the pair are connected in conjunction across some common impedance when equal and co-phasal fields exist at both aerials.

r_2 = ditto for pair CD.

ψ' = angle whose tangent is equal to ratio of amplitude of signal from pair CD to amplitude of signal from pair AB (see Appendices).

ψ'' = inclination of major axis of ellipse, i.e. apparent bearing (Appendices only).

The following equations, connecting certain of the above quantities, can be obtained by elementary analysis, and are true so long as Δ and Φ are assumed reasonably small compared with unity:—

$$K = \tfrac{1}{2} \tan \Phi \sin 2\psi \quad . \quad . \quad . \quad (1)$$

$$\tan \epsilon = \tfrac{1}{2}\Delta \sin 2\psi \quad . \quad . \quad . \quad . \quad . \quad (2)$$

If Δ and Φ are zero, then ϵ and K are also zero and the bearing is sharp and correct. In an aural system, K is related to the swing necessary in taking a bearing. In a visual system it is observed directly.

Equations (1) and (2) may be used to calculate the permissible tolerance in the various parts of the aerial system, since they give Φ and Δ in terms of the permissible error e and the permissible ellipticity (flatness) K.

(a) Systems Employing Two Pairs of Spaced Aerials in Planes at Right Angles to each other

The above results apply to any systems employing two aerial arrays at right angles to each other. It will now be shown that, in the special case in which each aerial array consists of a pair of spaced aerials connected in opposition, the quantities Δ and Φ (and therefore ϵ and K) depend on the characteristics of the separate aerials. It is supposed that the spacing between the aerials is small compared with the wavelength, but the results given are substantially true for spacings up to a quarter of a wavelength.

Let the four aerials be referred to as A, B, C, and D; AB being one pair, CD the other pair. Let there be a fractional difference in the amplitude of A relative to B of amount δ_1, and a relative phase-difference ϕ_1; let there also be relative amplitude and phase differences between the signals from C and D of amounts δ_2 and ϕ_2 respectively; further, let there be a fractional difference δ_0 between the mean of the amplitudes of A and B and the mean of the amplitudes of C and D, and a corresponding phase-difference between these means of amount ϕ_0, when exactly equal and co-phasal fields exist at all four aerials.

It can be shown (see Appendices) that when a signal arrives from a direction ψ relative to pair AB then the resulting bearing-error and ellipticity are given by

$$\tan \epsilon = \frac{\phi_1}{S} \sin \psi + \frac{\phi_2}{S} \cos \psi + \frac{\delta_0}{2} \sin 2\psi \quad . \quad (3)$$

$$K = \frac{\delta_1}{S} \sin \psi + \frac{\delta_2}{S} \cos \psi + \frac{\phi_0}{2} \sin 2\psi \quad . \quad (4)$$

(b) Practical Determination of Instrumental Accuracy

The quantities δ_1, δ_2, δ_0, ϕ_1, ϕ_2, ϕ_0 are determined by variations in the constants of the various parts of the aerial systems and associated feeders. They are difficult to determine directly, but the following method has been developed to determine the instrumental accuracy of a given system.

By some convenient method, it is arranged to inject exactly equal and co-phasal signals into all four aerial circuits. The aerials in each pair are first connected across a common impedance such as a goniometer field coil so as to oppose each other, and then reversed so as to be in conjunction. The ratio of the magnitudes of the resultant signals obtained in the common impedance (measured at the output from the associated amplifier) can easily be shown to be given by

$$r_1 = \tfrac{1}{2}\sqrt{(\delta_1^2 + \phi_1^2)} \quad . \quad . \quad . \quad . \quad (5)$$

for the pair AB, and

$$r_2 = \tfrac{1}{2}\sqrt{(\delta_2^2 + \phi_2^2)} \quad . \quad . \quad . \quad . \quad (6)$$

for the pair CD.

From these expressions it is not possible to determine δ_1 and ϕ_1 separately or δ_2 and ϕ_2 separately, but inspection of equations (3) and (4) shows that the maximum possible bearing error will be obtained by supposing that δ_1 and δ_2 are zero and that $\phi_1 = 2r_1$ and $\phi_2 = 2r_2$, while the maximum possible ellipticity is given by putting $\phi_1 = \phi_2 = 0$ and $\delta_1 = 2r_1$, $\delta_2 = 2r_2$. Thus measurement of r_1 and r_2 enables outside limits to be estimated for the instrumental accuracy of the direction-finder. It is possible that the most probable instrumental performance is given by assuming $\delta_1 = \phi_1 = \sqrt{2}r_1$ and $\delta_2 = \phi_2 = \sqrt{2}r_2$.

δ_0 and ϕ_0 can be observed directly in the following way. With equal signals injected into all four aerials, the members of each pair are connected so as to be in conjunction and each pair is connected to its appropriate field-coil or amplifier. The bearing indicated ought to be exactly at 45° relative to the direction of one field coil (or axis, in the case of an oscillograph) and should be perfectly sharp (a line, in the case of the visual system). Any departure from these conditions is due to the existence of δ_0 and ϕ_0. Suppose the bearing differs from 45° by ϵ_0 and has an ellipticity K_0, then we have the relations

$$\tan \epsilon_0 = \frac{\delta_0}{2} \text{ and } K_0 = \frac{\phi_0}{2}$$

In order to eliminate errors arising in the goniometer itself, the 45° position used in this test should be the bearing indicated when exactly equal e.m.f.'s are applied to both field coils.

In a visual system employing separate amplifiers it is possible to eliminate the effects of δ_0 and ϕ_0 by adjustments to the gain and phase-shift of the associated amplifiers so as to make the trace in the above circumstances take the form of a line at 45°.

Having measured r_1, r_2, ϵ_0, K_0, we have the following results for the maximum possible instrumental error and ellipticity:—

$$\epsilon = \frac{2r_1}{S} \sin \psi + \frac{2r_2}{S} \cos \psi + \epsilon_0 \sin 2\psi \quad . \quad . \quad (7)$$

$$K = \frac{2r_1}{S} \sin \psi + \frac{2r_2}{S} \cos \psi + K_0 \sin 2\psi . \quad . \quad (8)$$

Equations (7) and (8) can be used to determine the accuracy of a given system. Owing to the impossibility of separating out δ_1 and ϕ_1 from r_1, δ_2 and ϕ_2 from r_2, they only specify the maximum possible values of ϵ and K for the system. Moreover, it is impossible to attach a sign to r_1 and r_2; thus it is impossible to use these equations to plot out an instrumental calibration for the system. They will, however, show the manner in which the error will vary with azimuth.

If it is possible, by making preset adjustments to some of the constants of the aerials and feeder systems, to control the values of r_1 and r_2, ϵ_0 and K_0, equations (7) and (8) will determine the values of these quantities to be aimed at if the instrumental error is not to exceed a given value.

It should be noted that since S is the "angular" spacing, the values of r_1 and r_2 required for a given instrumental accuracy depend upon the wavelength, and, moreover, since the effective distance between the aerials depends on the angle of incidence of the wave, r_1 and r_2 will also vary with angle of incidence. In fact, if the waves considered are not travelling along the ground we must take for S the value S_1.

The formulae given do not include any errors arising in the goniometer, nor any octantal errors which will also be present if the spacing of the aerials is a large fraction of the wavelength, but refer solely to errors due to lack of perfect symmetry in the aerial system.

(c) Experimental Determination of Instrumental Accuracy of Short-Wave System at Sunnymeads

In order to determine the accuracy of the short-wave direction-finder at Sunnymeads, the following method was employed.

A wire-netting cage was built exactly at the centre of the system to house the goniometer, the receiving amplifier, and the observer. The dimensions of the cage were approximately 6 ft. × 6 ft. × 6 ft. Preliminary tests were made to ensure that the erection of this cage did not in itself introduce any errors, by calibrating the direction-finder by means of a local oscillator on the ground at about 100 yards radius on one or two wavelengths with and without the cage in position. By means of a local elevated oscillator it was also verified that the cage did not in any way affect the polarization error of the system for downcoming, partially horizontally-polarized waves. A small oscillator was then placed on the roof of the cage, having a short vertical aerial as radiator. This oscillator could be located exactly at the geometrical centre of the system to within 1 in. or less. It was assumed that under these conditions the central oscillator would induce exactly equal and co-phasal e.m.f.'s in all four aerials.

The quantities referred to as r_1, r_2, ϵ_0, and K_0, were determined as described above, on several wavelengths within the working range of the direction-finder. From these results it was possible to estimate the magnitude of the maximum instrumental error of the system on these wavelengths, by finding in each case the maximum value of the expression (7) above. These measurements, of course, assume that the radiation from the central oscillator is quite symmetrical, and this seems a reasonable assumption since great care was taken to ensure perfect symmetry by having the cubical cage, as well as the oscillator, exactly at the centre of the system.

As a check on the accuracy of the measurements, the balance between a pair of aerials was measured by radiating a signal into them from an oscillator placed on the ground at about 100 yards from the system and equidistant from the two aerials of the pair under consideration. The measurements agreed substantially with those obtained by means of the central oscillator.

If the formulae given in (7) and (8) are examined it is seen that the instrumental error will vary with the azimuth ψ, and in fact there is one value of ψ for which its absolute value reaches a maximum. In what follows it is this maximum value of the error which will be mentioned, and it is to be understood that for most directions the error will be considerably less than this maximum.

Between the wavelengths 45 metres and 65 metres the maximum error did not exceed 3°, and for most of this range the value was 2°. The resonance of the aerial primary circuits occurred in the neighbourhood of 80 metres, and as this wavelength was approached the balance between the aerials fell off rapidly, resulting in a rapid increase in instrumental error in this neighbourhood. Thus, at 70 metres the maximum instrumental error was about 4°, at 75 metres it was of the order of 10°, and at 80 metres it reached the value of 40°. Beyond 80 metres the degree of balance rapidly improved once more, and at 85 metres the error was about 14°. There was some evidence that the improvement would be continued, but measurements were not made at wavelengths greater than 85 metres.

A subsidiary resonance in the transmission lines was found to occur in the neighbourhood of 34 metres, and, while the balance between the individual members of each aerial pair remained good in this region, the balance of the one pair relative to the other pair was disturbed and as a result the quantity ϵ_0 increased rapidly and changed sign discontinuously as the point of resonance was traversed. As a result, the maximum instrumental error in the neighbourhood of 34·5 metres was of the order of 15°, but at 30 metres balance was again much better and the error was of the order of 5°.

These results show that over the range of wavelengths 40 to 70 metres the maximum possible error was 4° and the probable instrumental error less than this. The error as determined by the above experiments is entirely due to the mis-matching or "out of balance" of the aerials and their associated circuits. It takes no account of errors due to the goniometer or of the "octantal" aerial-spacing error, nor do the measurements described in this section enable the direction-finder to be calibrated for this instrumental error. The goniometer was found, when tested at 800 cycles per sec., to have a maximum error of less than $\frac{1}{4}$°. The octantal error (in degrees) is very approximately obtained by the formula $23\cdot 5\,(d/\lambda)^2$, where d is the aerial spacing. This gives a maximum error of about 1° at the lower end of the wavelength range and of about $\frac{1}{4}$° at the upper end.

It can be shown that the use of a goniometer having two separate search coils, one coupled to each field coil and the two joined in parallel, can give rise to an octantal type of error. An analysis of the circuit of such a goniometer reveals that the magnitude of this error depends on the ratio of the square of the maximum mutual reactance between one search coil and field coil to the product of the impedance of one of the search coils alone and the series impedance of the field-coil circuit. When the latter impedance is high, as is normally the case, the error is negligible; but in the neighbourhood of a series resonance of the field-coil circuit the impedance of this circuit falls and the error here referred to may attain considerable size (10° or more at maximum). It is, of course, constant so long as the parameters of the various circuits remain constant and does not vary with such variables as the angle of incidence of the wave. It could therefore be allowed for by calibration of the apparatus, but can be avoided by arranging to have no series resonance of the field-coil circuits within or close to the working range.

In the system described, octantal errors due to this cause were encountered in the neighbourhood of the resonance of the secondary circuits of the aerial feeder system, i.e. at the shorter wavelengths. In the working range the error did not exceed about 3° and in practice was allowed for by calibration of the direction-finder.

CONSTRUCTION

The construction of the aerial system may be understood from Fig. 4 and the following details. The aerials, which are 30 ft. high and spaced 30 ft. apart, are constructed of $1\frac{1}{2}$-in. diameter water pipe in two 15-ft. lengths. They are supported halfway up by a wooden bracket fixed to the outside of the hut and raised on large porcelain insulators.

The earth connections under each aerial consist of four cylinders made from tinned iron sheet 9 in. in diameter and 3 ft. 6 in. long, sunk into the ground with their axes vertical and spaced 2 ft. apart. The horizontal feeders between pairs of opposing aerials are in four lengths—a primary and a secondary section for each aerial. They each consist of a pair of No. 18 S.W.G. hard-drawn copper wires spaced 2 in. apart, stretched on a length of 3 in. × 2 in. timber, and held $1\frac{3}{4}$ in. above the top surface of the timber by means of barrel-type porcelain insulators which rest in grooves at each end of the beam. The primary feeders are 4 ft. 6 in. long, and the secondary 9 ft. 6 in. long; they are screened by means of a wire-netting cage of 1 ft. square box section, and 10 ft. long. The height of both sets of feeder wires above the ground is approximately 1 ft. The screening system of the feeders and the wire-netting cage are connected to an earth pin at the centre of the system.

The aerial-coupling transformers are mounted on the outer end of the beam supporting the secondary feeder, and are surrounded by the wire-netting screening cage already referred to. The connections between the secondary circuits and the goniometer field coils are made by means of vertical feeders consisting of stretched wires inside $1\frac{1}{2}$-in. diameter brass tubes, with a flexible link of screened twin flex from the top of each tube to the goniometer field-coil plug.

Great care was taken in the design, construction, and testing of each link in this feeder chain to ensure that the matching between the corresponding portions for the opposing aerials should be as perfect as possible.

The operating hut is 15 ft. square, the aerials being erected on the extensions of its diagonal lines. At its centre is a wire-netting cage (6 ft. × 6 ft. × 6 ft.), and this contains all the receiving apparatus together with the operator. The screening systems of the horizontal and vertical feeders are bonded together and to this cage. The local radiating source with its short vertical rod aerial is placed on the top of the cage at its centre, which is accurately arranged to be at the true centre of the aerial system.

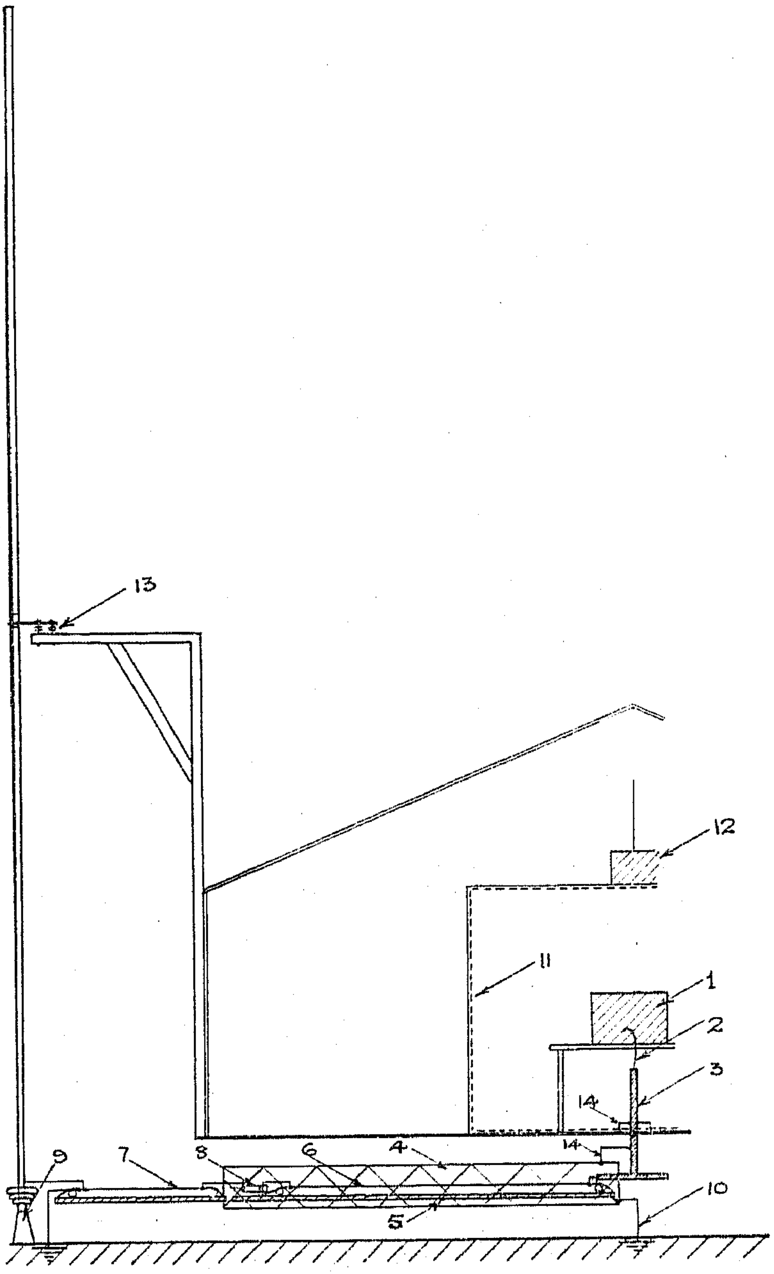

Fig. 4

1. Receiver and goniometer.
2. Screened flexible connection.
3. Vertical feeders in brass tube.
4. Feeder screen.
5. Wooden beam supporting stretched feeders.
6. Secondary feeder.
7. Primary feeder.
8. Aerial transformer.
9. Aerial-supporting insulator.
10. Earth connection for screening system.
11. Screening cage (6-ft. cube).
12. " Line-up " oscillator and aerial.
13. Aerial-supporting insulator.
14. Bonding connections.

The operating hut is raised on piles to a height of 2 ft. 6 in. above the ground to allow of the feeders being led underneath the hut, and this lower space is protected from the weather by skirting boards fixed between the bottom edges of the hut and the ground.

GONIOMETER

The goniometer was specially designed and constructed for the installation, and differs in several respects from standard practice. Its general arrangement is shown in Fig. 5. The goniometer has two search coils mounted one above the other on the same spindle, which is hollow and carries the leads from the search coils (in parallel with each other) to the slip-rings. Two field coils are wound on cylindrical coaxial formers and are placed in separate screened compartments. There is a screen, in the form of a cage of bare wire, between the search coil and the field coil. The field coils are wound in two halves on the former, which is itself divided into two hemi-cylinders, these being detachable together with half of the screen which is mounted on the inside. In this way access may be obtained to the search coils for inspection or test after the goniometer has been completed.

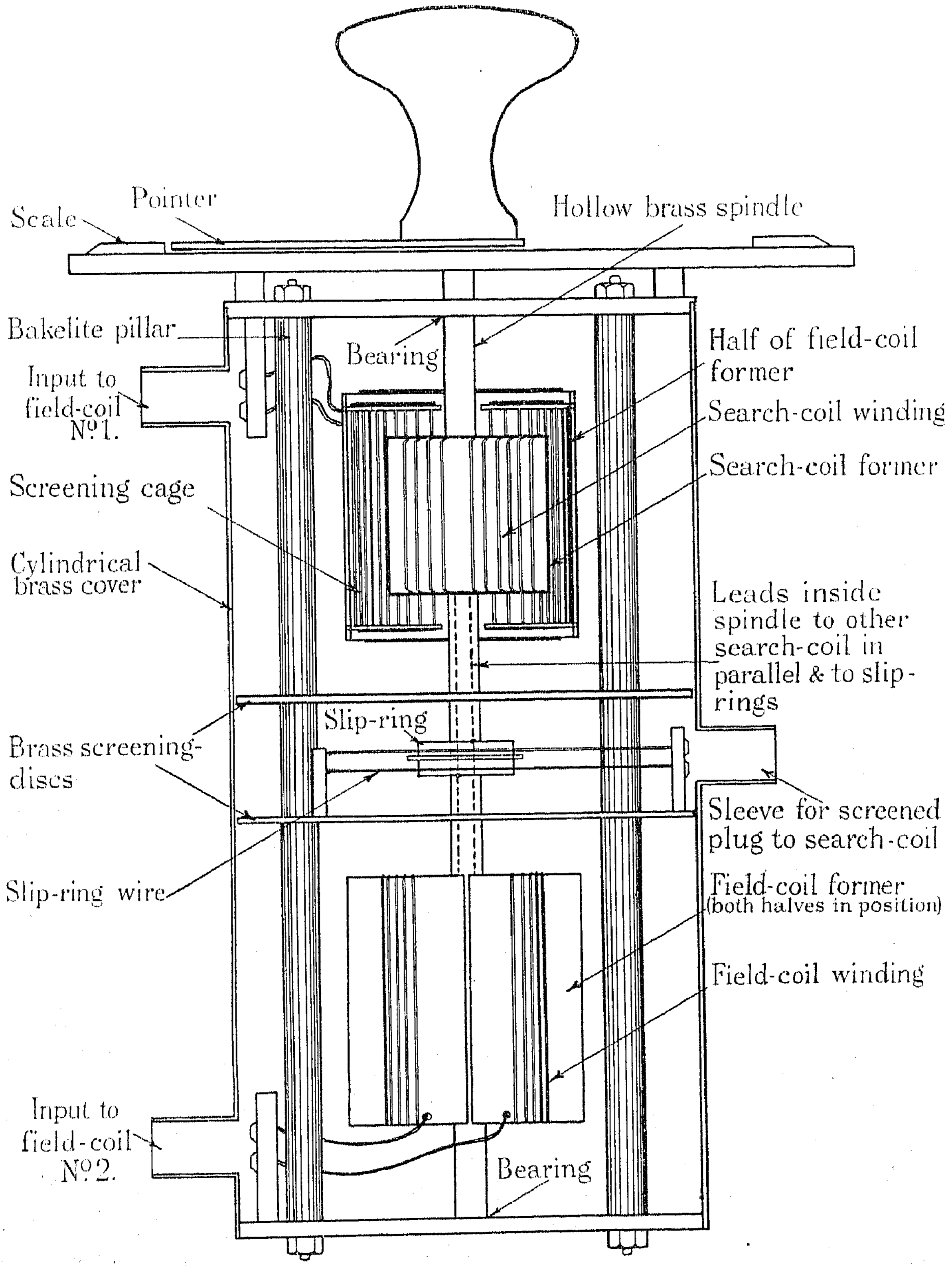
Scale
Pointer
Hollow brass spindle
Bakelite pillar
Bearing
Input to field-coil No. 1.
Half of field-coil former
Search-coil winding
Search-coil former
Screening cage
Cylindrical brass cover
Leads inside spindle to other search-coil in parallel & to slip-rings
Slip-ring
Brass screening-discs
Sleeve for screened plug to search-coil
Slip-ring wire
Field-coil former (both halves in position)
Field-coil winding
Input to field-coil No. 2.
Bearing

Fig. 5.—Goniometer with half of upper field-coil removed.

The whole assembly is carried on a framework consisting of an upper, a lower, and two centre brass discs supported on four bakelite pillars. The search-coil spindle passes through the centre of the discs, the bearings being carried on the upper and lower discs. The slip-rings occupy the space between the two central discs, which serves as a separate screened compartment for the search-coil output leads. The field-coil cylinders, carrying the electrostatic cage screen, are fixed by brackets to the upper and lower discs. The whole assembly is enclosed in a brass cylindrical cover concentric with the spindle, search coils, and field-coil formers. This cylinder is 6 in. in diameter and 12 in. long, and on it are mounted three screening sleeves for the input plugs to the field coils and search coils respectively.

The input leads are plugged into sockets mounted on the upper and lower discs, and these sockets are connected by very short flexible leads to the field-coil windings. The output socket is mounted on one of the central discs and is connected directly to the slip-ring " brush," which consists of twin phosphor-bronze wires running in grooves in the slip-rings and stretched tight by steel springs.

Since there are no terminals or sockets or connections of any kind fixed to the cover, it can be removed without making any disconnection. The scale is engraved on a brass ring 1 ft. in diameter; this is mounted on a plate of bakelite, 1 ft. square, fixed to the top disc. The pointer is fixed to the spindle, which projects through the top disc by an amount sufficient to carry it and the ebonite tuning-knob.

ACKNOWLEDGMENTS

The work described above formed part of the programme of the Radio Research Board, and this paper is published by permission of the Department of Scientific and Industrial Research. The authors wish to express their indebtedness to Mr. L. H. Bainbridge-Bell, M.A., and Mr. H. Page, B.Sc., for the design of the special radiogoniometer described in the paper.

APPENDIX I

Suppose the signal output from one aerial pair CD has phase and amplitude errors relative to that from the other pair of amount Φ and Δ respectively. Define the angles ψ' and ψ'' as follows:—

$$\tan \psi' = \frac{\text{Amplitude of signal from pair CD}}{\text{Amplitude of signal from pair AB}}$$

$$\therefore \tan \psi' = (1 + \Delta) \tan \psi \quad . \quad . \quad . \quad . \quad . \quad . \quad . \quad (9)$$

where ψ is the azimuth of the signal relative to the pair AB.

Let ψ'' = inclination of the major axis of the elliptical field in the goniometer, or the trace on oscillograph screen, relative to some fixed axis in the goniometer or oscillograph which corresponds to the direction of the plane of AB.

ψ'' is thus the apparent or observed bearing. It can easily be shown, from the geometry of ellipses, that

$$\tan 2\psi'' = \tan 2\psi' \cos \Phi \quad . \quad . \quad . \quad . \quad . \quad (10)$$

$$\tan \Phi \quad = \frac{2K}{1 - K^2} \frac{1}{\sin 2\psi''} \quad . \quad . \quad . \quad (11)$$

From (10) it is easily deduced that, providing Φ is small, we can write $\psi'' = \psi'$.

If we also assume that Δ is small compared with unity, then the difference between ψ' and ψ is also small, and we can write $\psi' = \psi$ in equation (11) and hence from (9) and (11) deduce equations (1) and (2).

APPENDIX II

Consider the case $\delta_1 = \delta_0 = \phi_1 = \phi_2 = \phi_0 = 0$, but $\delta_2 \neq 0$. It can be shown that

$$\tan \Phi = \frac{\delta_2}{S \sin \psi} \quad . \quad . \quad . \quad . \quad . \quad (12)$$

$$\Delta = 0 \quad . \quad . \quad . \quad . \quad . \quad . \quad . \quad . \quad (13)$$

Equation (13) is not true near $\psi = 0$.

These equations assume S sufficiently small for the following equations to hold for all values of ψ:—

$$\cos \frac{S \sin \psi}{2} = 1$$

$$\sin \frac{S \sin \psi}{2} = \frac{S \sin \psi}{2}$$

Substituting from (12) and (13) in equations (1) and (2), we get

$$\epsilon = 0 \quad . \quad . \quad . \quad . \quad . \quad . \quad . \quad . \quad . \quad (14)$$

$$K = \frac{\delta_2}{S} \cos \psi \quad . \quad . \quad . \quad . \quad . \quad (15)$$

We shall show that these equations are still true near $\psi = 0$.

As ψ tends to 0, the e.m.f.'s in C and D are nearly co-phasal and their difference is a small vector 90° out of phase with either of them, providing $\delta_2 = 0$. If $\delta_2 \neq 0$ it is easy to see that this small vector representing the difference between the e.m.f.'s in C and D undergoes a phase-shift Φ and is increased in length by a fractional amount Δ (not necessarily small). We have the following approximate but fairly accurate relation:—

$$\cos \Phi = \frac{1}{1 + \Delta} \quad . \quad . \quad . \quad . \quad . \quad (16)$$

Also, as before,

$$\tan \psi' = (1 + \Delta) \tan \psi$$

or, since ψ' and ψ are both small,

$$\psi' = (1 + \Delta)\psi$$

Substitution in equation (10) (Appendix I) gives

$$\psi'' = (1 + \Delta)\psi \frac{1}{1 + \Delta} = \psi$$

Now

$$\epsilon = \psi'' - \psi$$

$$\therefore \qquad \epsilon = 0 \quad . \quad . \quad . \quad . \quad . \quad . \quad . \quad . \quad (17)$$

Since $\epsilon = 0$ we can write $\psi'' = \psi$ (accurately) in equation (11). Thus

$$K = \tfrac{1}{2} \tan \Phi \sin 2\psi$$

Also equation (12) still holds near $\psi = 0$, and hence we have

$$\epsilon = 0 \quad . \quad . \quad . \quad . \quad . \quad . \quad . \quad . \quad (14)$$

$$K = \frac{\delta_2}{S} \cos \psi \quad . \quad . \quad . \quad . \quad . \quad (15)$$

still true where ψ is small.

These equations thus hold for all values of ψ.

APPENDIX III

Suppose $\delta_1 = \delta_2 = \delta_0 = \phi_1 = \phi_0 = 0$, but $\phi_2 \neq 0$. (It should be noted that we assume that $\phi_2 \neq 0$ in such a way that ϕ_0 does equal zero. This is always possible.) It can be shown that the result is a fractional error in the amplitude of the signal from the pair CD relative to that from the pair AB of amount

$$\Delta = \frac{\phi_2}{S \sin \psi} \quad . \quad . \quad . \quad . \quad . \quad (18)$$

This will be small compared with unity except near $\psi = 0$, and so may be substituted in equation (2) to obtain

$$\tan \epsilon = \frac{\phi_2}{S} \cos \psi \quad . \quad . \quad . \quad . \quad (19)$$

Near $\psi = 0$ we should have a phase difference equal to $S \sin \psi$ between the outputs from the two aerials C and D. In place of this we have a phase difference

$$S \sin \psi + \phi_2$$

Since ψ is assumed to be small, we can write this in the form

$$S\left(\psi + \frac{\phi_2}{S}\right) \text{ approximately}$$

The result is equivalent to the case in which $\psi_2 = 0$ but the signal arrives from a direction $\left(\psi + \frac{\phi_2}{S}\right)$ instead of ψ. That is, the quantity ϕ_2 has introduced an error in bearing of amount $\epsilon = \phi_2/S$, which is precisely the value to which the expression for ϵ in equation (19) tends as ψ tends to zero. Equation (19) thus holds for all values of ψ.

THE REFLECTION COEFFICIENT OF THE EARTH'S SURFACE FOR RADIO WAVES[*]

By J. S. McPETRIE, Ph.D., B.Sc., Associate Member.

[From the National Physical Laboratory.]

(*Paper first received* 28*th April, and in final form* 20*th September*, 1937.)

SUMMARY

Curves are given from which, by two interpolations, the reflection coefficient of the ground can be determined for any angle of incidence or any value of dielectric constant and conductivity of that surface. Curves are given for the two cases in which the electric vector of the incident radiation is polarized in and perpendicular to the plane of incidence respectively, so that the reflection coefficient can also be determined for any state of polarization.

INTRODUCTION

The solution of many of the problems relating to the propagation of radio waves necessitates a knowledge of the magnitude of the reflection occurring at the earth's surface. For frequencies within the visible spectrum the distance of any object or receiver from a reflecting surface is so great compared with the wavelength of the radiation that at the point at which reflection occurs the incident radiation may be assumed to be plane. The reflection occurring under such conditions is given by the well-known Fresnel equations. In the case of the propagation of radio waves along the earth's surface, however, the distance between the transmitter or receiver and that surface may be very small compared with the wavelength. The radiation incident on the earth's surface is then no longer plane, and care must be taken in the application of the results obtained from the simple ray theory.

The conditions required for the ray theory to apply may be stated roughly as follows:—

(1) If the radiation incident on the earth's surface (or any other reflector) is polarized so that the electric vector is perpendicular to the plane of incidence, the ray theory may be applied for practically all heights of the receiver or transmitter, provided the effects of refraction in the atmosphere and diffraction round the earth's surface may be neglected.

(2) If the radiation is polarized with the electric vector in the plane of incidence, the ray theory applies only to cases in which either or both the transmitter and the receiver are at heights above the earth comparable with the wavelength. This limitation to the applicability of Fresnel's equations occurs because (as was first shown by Sommerfeld[†]), for this type of polarization, a wave, usually known as the surface wave,[†] is propagated along the earth's surface and the formula for the propagation of this wave is not deducible from the ordinary ray theory. For high angles of incidence or elevated transmitter and receiver, Fresnel's equation can still be used as the surface wave is confined to regions near the ground.

Even with the above limitation to the applicability of the ray theory, the reflection coefficient of the ground as determined from the theory is often required in radio problems. Fresnel's equations in their usual form are such, however, that the calculation of the reflection coefficient, which at best is laborious, must be made for each particular problem. It is shown in this paper[‡] how, by a series of interpolations, the reflection coefficient of the ground can readily be determined without recourse to computation for all angles of incidence, all states of polarization of the incident radiation, and all values of ground constants, met with in practice.

DESCRIPTION OF METHOD

The reflection coefficient at the earth's surface is complex and may conveniently be represented in the form $(K + jK')$. The magnitudes of the two rectangular components K and K' are functions of the dielectric constant (κ), the ratio of the conductivity of the ground (σ) to the frequency (f) of the radiation considered, and also of the angle of incidence. The reflection coefficient is also a function of the state of polarization of the radiation incident on the earth's surface. This latter complication is readily overcome by resolving the radiation into its respective components polarized in and perpendicular to the plane of incidence. In this paper, the reflection coefficient has been calculated for these two states of polarization.

The usual method for determining the reflection coefficient for a particular case is to calculate from Fresnel's equations the two rectangular components of the coefficient for the appropriate values of the dielectric constant and of the ratio of conductivity to frequency. As the effects of these two functions on the coefficient are difficult to assess separately, a series of values of both must be taken in order to determine possible limits in the value of the reflection coefficient. For the general determination of the reflection coefficient it is much more convenient to make the calculation assuming κ as constant and the ratio σ/f as parameter in turn. When such a calculation is made for a given angle of incidence a series of interesting curves can be drawn as shown in Fig. 1. In this figure the horizontal axis represents the in-phase component K, and the vertical axis the in-quadrature component K', of the reflection coefficient. The point of intersection of any two curves determines both K and K', so that the length of the vector to the point of intersection gives the magnitude of the reflection coefficient and the angle which it makes with the horizontal axis gives the change of phase occurring on reflection, for the ground constants represented by the common values of κ and σ/f of the intersecting curves. The reflection coefficient for the same angle of incidence for any values of k and σ/f not given directly by the curves in Fig. 1 can be obtained by interpolation. If a series of curves such as those in Fig. 1 are calculated for a sufficient number of angles of incidence, the reflection coefficient for any values of κ and σ/f can be obtained by a second interpolation for all angles of incidence.

---

[*] Reprinted from *Journal I.E.E.*, 1938, vol. 82, p. 214.

[†] *Annalen der Physik*, 1909, vol. 28, p. 665.

[†] Recently, American workers—for example, Wise (*Bell System Technical Journal*, 1937, vol. 16, p. 35)—have questioned the existence of Sommerfeld's surface wave: nevertheless, they agree that the simple ray theory cannot be applied to cases in which the transmitter and receiver are near the ground.

[‡] Since the preparation of this paper, another graphical method for determining the reflection coefficient of the ground has been described by Burrows (*Bell System Technical Journal*, 1937, vol. 16, p. 45).

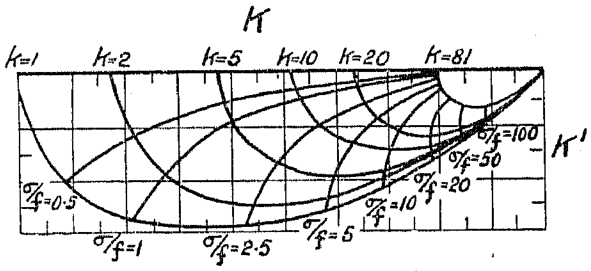

Fig. 1.—Curves giving the in-phase (K) and the in-quadrature (K') components of the reflection coefficient for a given angle of incidence and various values of the ground constants.

This method has been followed in the paper for the two cases of radiation polarized respectively in and perpendicular to the plane of incidence. By resolving the polarization of the incident radiation into these two components, therefore, the reflection coefficient can be found for any values of ground constants or angles of incidence; conversely, if in any problem the reflection coefficient and phase-change on reflection are known, the ground constants can be determined directly from the curves. The curves are instructive also in showing the different effects of change in dielectric constant or conductivity of the reflecting surface. The values of dielectric constant have been limited to those between 1 and 81, the latter representing the conditions for water. No values for ionized media ($\kappa < 1$) have been included, as the present study is limited to reflection from the earth's surface.

RADIATION POLARIZED WITH ELECTRIC FIELD PERPENDICULAR TO PLANE OF INCIDENCE

If the reflection coefficient for horizontally-polarized waves is designated $(K_p + jK_p')$, the values of K_p and K_p' are given by

$$K_p = \frac{\cos^2\theta - (c^2 + d^2)}{\cos^2\theta + (c^2 + d^2) + 2c\cos\theta} \quad . \quad . \quad (1)$$

$$K_p' = \frac{-\,2d\cos\theta}{\cos^2\theta + (c^2 + d^2) + 2c\cos\theta} \quad . \quad . \quad (2)$$

in which θ (the angle of incidence on the ground) and c and d are given by

$$c = +\frac{1}{\sqrt{2}}\sqrt{\left\{\sqrt{\left[(\kappa - \sin^2\theta)^2 + 4\frac{\sigma^2}{f^2}\right]} + (\kappa - \sin^2\theta)\right\}} \quad (3)$$

$$d = -\frac{1}{\sqrt{2}}\sqrt{\left\{\sqrt{\left[(\kappa - \sin^2\theta)^2 + 4\frac{\sigma^2}{f^2}\right]} - (\kappa - \sin^2\theta)\right\}} \quad (4)$$

where κ represents the dielectric constant of the ground, σ the conductivity in electrostatic units, and f the frequency of the radiation.

The positive direction of the reflected wave as given by equations (1) and (2) is assumed (as shown in Fig. 2) to be the same as that of the primary radiation.

Equations (1) and (2) have been used, in the manner described in the previous Section, to obtain the curves given in Fig. 3, representing the reflection coefficient for angles of incidence of 0°, 20°, 40°, 50°, 60°, 70°, and 80° respectively. It will be seen that for given ground-constants the reflection coefficient increases as the angle of incidence increases, becoming unity for all ground constants for an angle of incidence of 90°. As the vector representing the reflection coefficient lies in the second quadrant, there must be an advance of phase on reflection of between 90° and 180° for horizontally-polarized waves.

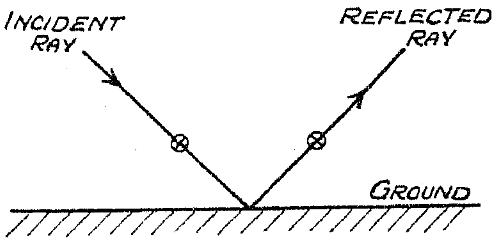

Fig. 2.—Diagram showing relative directions of electric field in incident and reflected rays for cases given in Fig. 3.

RADIATION POLARIZED WITH ELECTRIC FIELD IN PLANE OF INCIDENCE

For this type of polarization the components K_i and K_i' of the reflection coefficient $(K_i + jK_i')$ are given by

$$K_i = \frac{\left(\kappa^2 + 4\frac{\sigma^2}{f^2}\right)\cos^2\theta - (c^2 + d^2)}{\left(\kappa^2 + 4\frac{\sigma^2}{f^2}\right)\cos^2\theta + (c^2 + d^2) + 2\cos\theta\left(\kappa c - 2d\frac{\sigma}{f}\right)} \quad (5)$$

$$K_i' = \frac{-\,2\cos\theta\left(\kappa d + 2c\frac{\sigma}{f}\right)}{\left(\kappa^2 + 4\frac{\sigma^2}{f^2}\right)\cos^2\theta + (c^2 + d^2) + 2\cos\theta\left(\kappa c - 2d\frac{\sigma}{f}\right)} \quad (6)$$

in which the symbols have the same significance as in equations (1) and (2). The positive direction of the electric field in this case is shown in Fig. 5. The curves given in Fig. 4 have been calculated for angles of incidence of 0°, 20°, 40°, 50°, 60°, 70°, and 80°. It will be seen that for zero angle of incidence the reflection

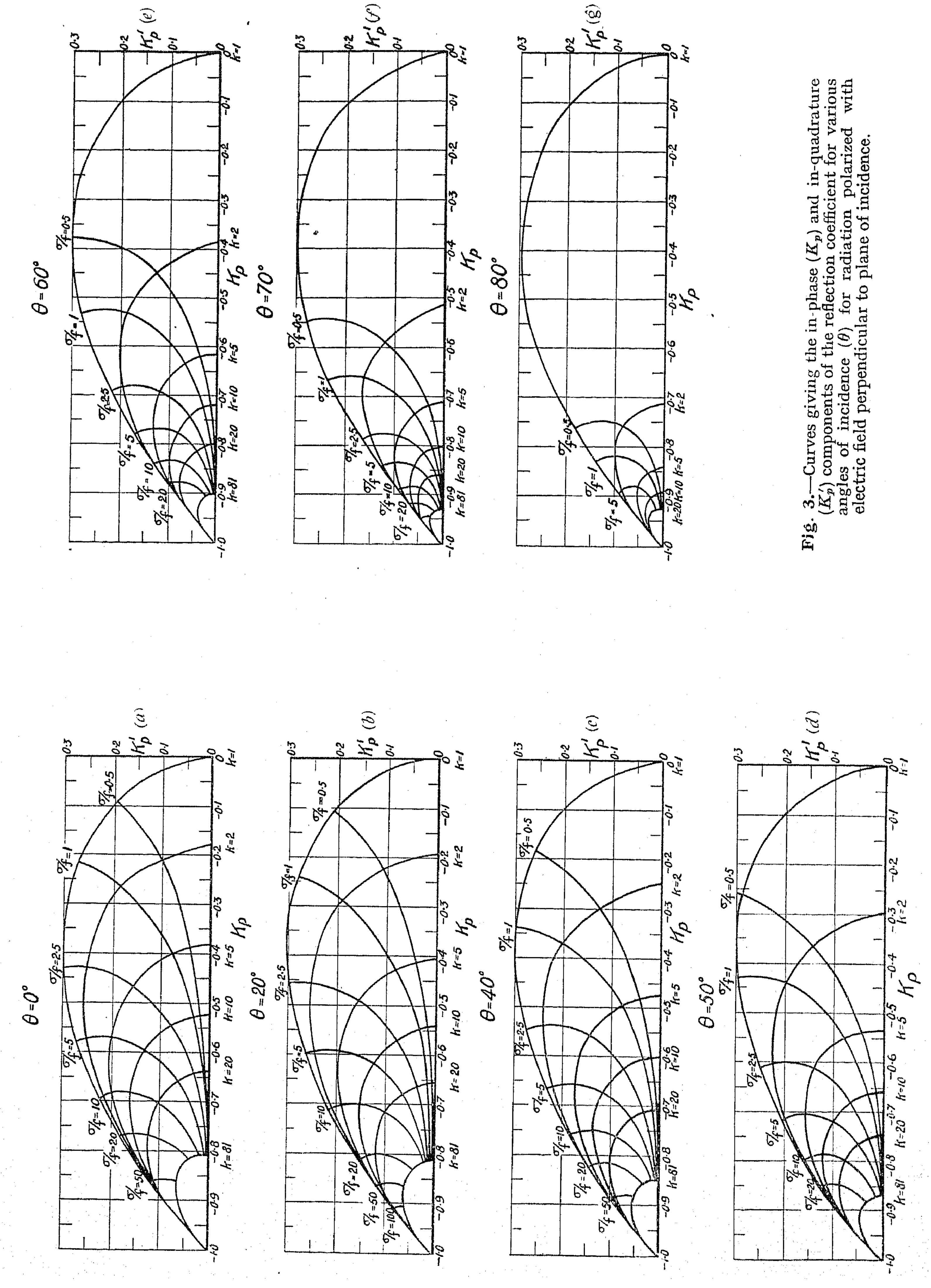

Fig. 3.—Curves giving the in-phase (K_p) and in-quadrature (K_p') components of the reflection coefficient for various angles of incidence (θ) for radiation polarized with electric field perpendicular to plane of incidence.

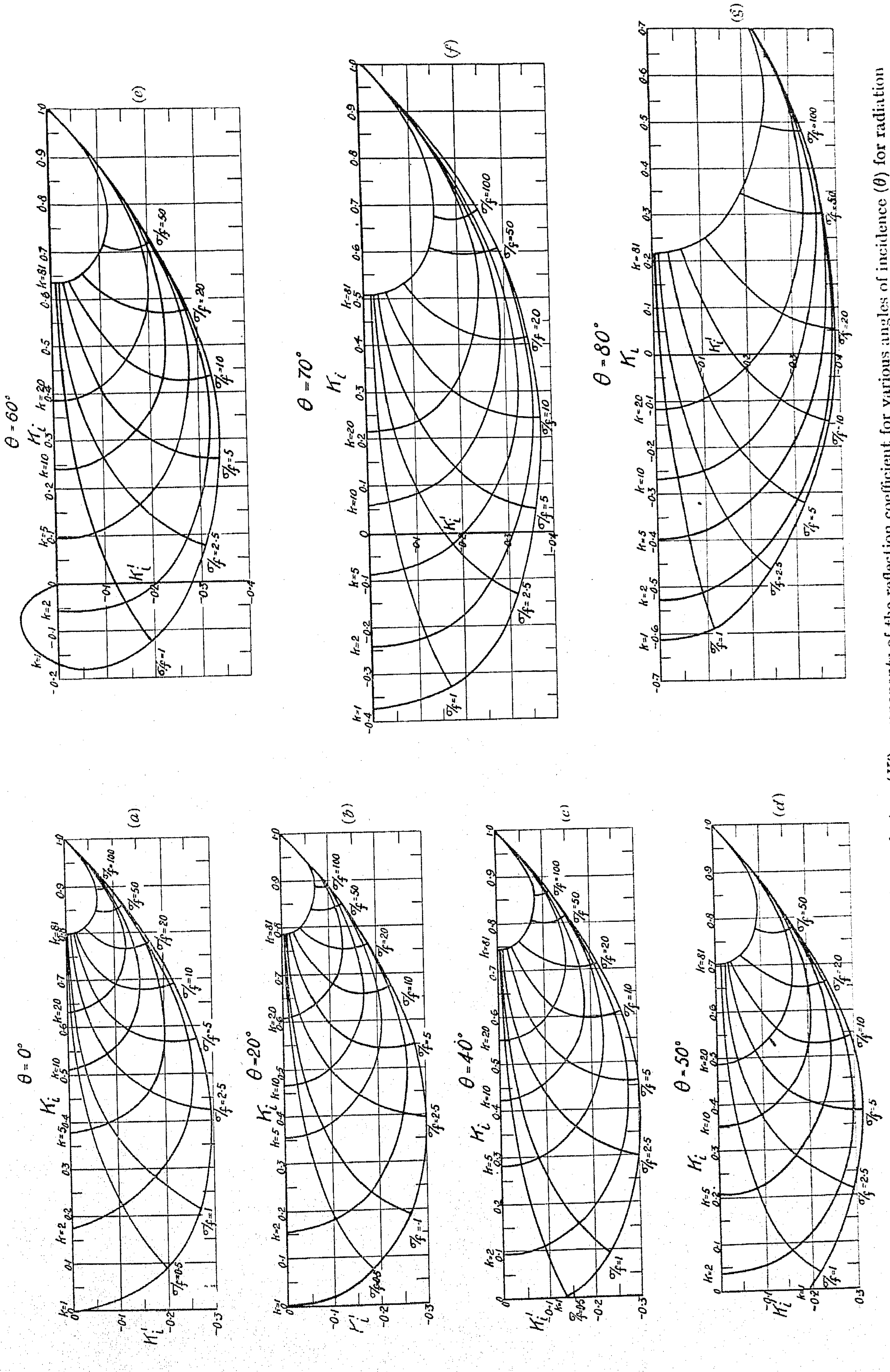

Fig. 4.—Curves giving the in-phase (K_i) and in-quadrature (K_i') components of the reflection coefficient for various angles of incidence (θ) for radiation polarized with electric field in plane of incidence.

coefficient has the same magnitude as for horizontally-polarized waves at the same angle, but that there is a change in phase of 180° between the two cases. The reflection coefficient should be identical for this case of normal incidence, and the apparent discrepancy arises from the assumption as to the positive direction of the reflected waves as given in Figs. 2 and 5. It will be seen that, as with horizontally-polarized waves, the reflection coefficient tends to unity as the angle of incidence approaches 90°. The reflection coefficient of a body having zero conductivity and unity dielectric constant is zero for all angles of incidence. The curve for this value of dielectric constant is similar to that for the other values of dielectric constant until the reflection coefficient lies in the third quadrant. When this occurs the curve for unit dielectric constant does not terminate on the axis of abscissae but crosses it into the second quadrant and spirals back in that quadrant to the origin. This part of the curve is limited to small conductivities and, as it is of no practical importance in the present problem, it has not been included in any of the diagrams, except Fig. 4(*e*); here it is given only to show the result obtained with such a reflector.

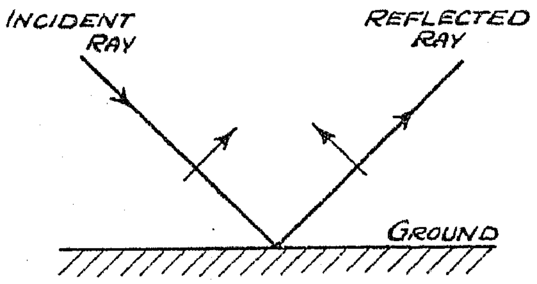

Fig. 5.—Diagram showing relative directions of electric field in incident and reflected rays for cases given in Fig. 4.

EXAMPLES OF USE OF METHOD

The curves given in the paper may be used in two ways: firstly, to find the reflection coefficient at any angle of incidence when the ground constants are known; or, secondly, to determine the ground constants if the reflection coefficient is known. As an example of the use of the first method, suppose the reflection coefficient and phase-change on reflection are required for vertically-polarized waves at a frequency 4×10^6 cycles per sec. for an angle of incidence of 45°, the dielectric constant and conductivity of the ground being respectively 15 and 10^8 e.s.u.* The appropriate value of σ/f is, therefore, 25. Reference to Fig. 4(*d*) shows that the values of K_i and K'_i for the given values of κ and σ/f are approximately 0·735 and − 0·16 respectively for an angle of incidence of 40°, while Fig. 4(*e*) shows them to be 0·685 and − 0·18 for an angle of incidence of 50°. Assuming that the rate of change of both components is approximately linear over the range 40° to 50°, the values at an angle of incidence of 45° become 0·71 and − 0·17. These values represent, therefore, the two components of the reflection coefficient, giving 0·73 for the magnitude of the coefficient and − 13° for the phase-change. The coefficient could, of course, have been determined without resolving it into its two components. The actual method adopted depends to a large extent on personal preference. Calculating the magnitudes of K_i and K'_i directly from equations (5) and (6) gives the same values for K and K_i, so that the accuracy of the method of interpolation in the particular example given is amply sufficient.

If the reflection coefficient were given as 0·73 and the phase-change as − 13° for an angle of incidence of 45°, the ground constants could be determined by reversing the above procedure.

An example of the application of the method to the determination of the electrical constants of the ground from an experimental determination of the reflection coefficient at normal incidence has already been given by the author.*

CONCLUSIONS

The curves given in the paper enable the reflection coefficient for any angle of incidence, any state of polarization of the radiation, and any electrical constants of the ground, to be determined by, at most, two interpolations; conversely, the ground constants can be found from the curves if the reflection coefficient and phase-change on reflection are known for any angle of incidence at the earth's surface. In addition, the curves are instructive in that they show how small changes in dielectric constant or conductivity affect the reflection conditions for any angle of incidence.

ACKNOWLEDGMENTS

The work described in this paper has been carried out as part of the programme of the Radio Research Board, and acknowledgment is due to the Department of Scientific and Industrial Research for granting permission for publication. The author is also indebted to Dr. R. L. Smith-Rose for suggesting this investigation and for advice on the method of presentation of the paper, and to Mr. B. J. Byrne for assistance in the computing work involved.

---

* The electrical constants of different types of ground surface at radio frequencies have been determined by R. L. Smith-Rose (*Journal I.E.E.*, 1934, vol. 75, p. 221, and *Proceedings of the Wireless Section*, 1934, vol. 9, p. 293). His paper also includes an extensive bibliography on the subject.

* *Proceedings of the Physical Society*, 1934, vol. 46, p. 637.

THERMAL FLUCTUATIONS IN COMPLEX NETWORKS.*

By F. C. WILLIAMS, M.Sc., D.Phil., Graduate.

(*Paper first received* 16*th March and in final form* 24*th July*, 1937.)

SUMMARY

This paper is concerned with the thermal fluctuations generated in networks containing reactance as well as resistance. Earlier work is reviewed, and it emerges that Moullin and Ellis were unable to interpret Nyquist's equation for a network at uniform temperature by their method of representation. An alternative method is suggested in which each element of resistance is replaced by a fluctuation generator in series with the element of resistance. The fluctuation voltage appearing between any two points in a linear network with any temperature distribution is then evaluated. This general expression is shown to be in agreement with Nyquist's result if the temperature is uniform. It is also shown that the relevant values of resistance in these formulae are the equivalent power-loss resistances and not the metallic resistances.

There follows a description of experimental tests which are regarded as satisfactory verification of the method of representation adopted and of the values of resistance used.

The noise/signal ratio existing between any two points in the generalized network is then discussed, and is shown to be incapable of exceeding the value obtaining in the arm in which the signal is introduced. General recommendations for optimum noise/signal ratio are given.

A few special cases are then considered. It is shown that in radio reception a resonant circuit is preferable to a band-pass filter as a coupling between aerial and amplifier. In the former case an analysis of the optimum coupling between aerial and circuit is given which takes account of the fluctuations generated in the amplifier itself. A simple practical method of obtaining the optimum conditions is outlined.

Fluctuations in long cables are briefly discussed. It is shown that temperature conditions in the vicinity of the receiving end only need be considered. The use of transformers or resonant circuits to couple the cable to an amplifier is governed by the same recommendations as for aerial-amplifier coupling.

(1) INTRODUCTION

It is well known that there exists across the extremities of a resistor a fluctuation voltage which is dependent on the absolute temperature of the resistor. Such fluctuations have been ascribed to the thermal agitation of the electrons contained in the resistor, and have been the subject of considerable investigation, both analytical and experimental.

Thus Johnson,† Nyquist,‡ and Moullin and Ellis,§ have all shown that the mean-square thermal agitation voltage developed across a resistance R can be expressed in the form:—

$$|v|^2 = 4Rk\tau df \quad . \quad . \quad . \quad . \quad . \quad (1)$$

where $|v|^2$ is the mean-square value of those harmonic components of the total fluctuation voltage which have frequencies within the range df, k is Boltzmann's gas constant, and τ is the absolute temperature of the resistance.

Johnson has tested this expression by deducing a value for k from observations of the fluctuation voltage appearing across metallic and electrolytic resistors. Moullin and Ellis† made a similar series of measurements of k using a highly refined technique by which the probable error was reduced to about 1 per cent, but confined their attention to metallic resistances. In all cases good agreement with the accepted value was found.

Nyquist extended his analysis to the general case of fluctuations in a network of impedances containing reactive as well as resistive components. He showed that if $(r + jx)$ is the impedance between any two points in the network at the frequency f, then the mean-square value of the fluctuation voltage between the limits f and $(f + df)$ is given by the equation

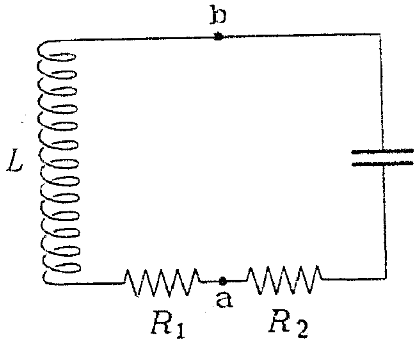

Fig. 1

$$|v|^2 = 4rk\tau df \quad . \quad . \quad . \quad . \quad . \quad (1a)$$

So far as the author is aware this expression has not been tested experimentally.

Moullin and Ellis‡ have stated that they cannot understand Nyquist's proof and have given an example in which, according to their interpretation of thermal fluctuations, equation (1*a*) is at fault. They considered the circuit shown in Fig. 1, which represents a resonant circuit having resistances R_1 and R_2 in series with the inductance and capacitance arms respectively. They calculated the fluctuation voltage appearing between the points *a* and *b* by their own method and also by means of Nyquist's equation. The two methods agreed only when R_2 was zero.

A knowledge of the thermal fluctuations to be antici-

---

* Reprinted from *Journal I.E.E.*, 1937, vol. 81, p. 751.

The earlier portions of the paper were the result of research work carried out during the author's tenure of the Ferranti Scholarship.

† See Bibliography, (1). ‡ *Ibid.*, (2). § *Ibid.*, (3).

† See Bibliography, (4).

‡ *Ibid.* (3).

pated in complex networks such as filter circuits is of considerable importance in many branches of communication engineering, and the present paper is devoted to a discussion of these conflicting views and to the provision of a general formula for estimating the thermal fluctuations generated in any network. The concluding sections discuss the application of the formula to practical cases.

(2) ANALYTICAL DISCUSSION

Experimental measurements have been confined almost entirely to the potential difference developed by thermal agitation disturbances across the extremities of a resistor, comparison with analysis being made by means of equation (1). Yet it appears from the Moullin–Ellis derivation of equation (1) that this equation refers rather to the effective e.m.f. of thermal agitation acting round the complete *LCR* circuit which, inevitably, is associated with the resistance. Since the value of the e.m.f. depends only on the resistance, and not on the inductance and capacitance, it is usual to associate thermal agitation voltages with the resistance; whether such association has any physical significance remains in doubt. It appears probable, however, from the form of the equation, that the thermal agitation disturbances in any circuit might be most conveniently evaluated by associating a hypothetical fluctuation generator with every element of resistance in the circuit; the e.m.f. of the fluctuation generator being given by equation (1) and being supposed concentrated, for convenience.

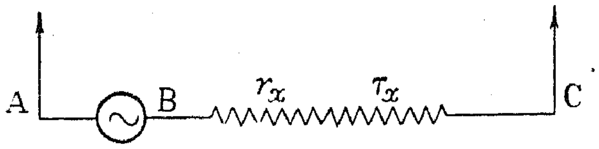

Fig. 2

Under such circumstances, every element of resistance in the circuit would be replaced by the combination shown in Fig. 2. The fluctuation generator is supposed such that it maintains a mean-square p.d. given by

$$|v|^2 = 4r_x k\tau_x df$$

between the points A and B, where τ_x is the absolute temperature of the typical resistance r_x. Since the generator is merely a convenient representation of a distributed effective e.m.f., it must be supposed that A and C are the only points available for external connection, and hence that the generator cannot be isolated from its associated resistance r_x.

It may be noted that rigorous physical support for this representation is not attempted. It is put forward as a convenient analytical representation whose ultimate justification must rest upon experimental evidence. That it is valid for sensibly isolated resistances is evident from results already quoted; its validity in more general circuits will be established later in the present paper.

With representation as defined above, it is shown in Appendix 1 that the fluctuation voltage appearing between any two points A and A′ in a network of linear impedances is given by the equation

$$|v|^2 = Z^2_{AA'}4kdf\sum\frac{r_x\tau_x}{Z^2_{Ax}} \quad . \quad . \quad . \quad (2)$$

where $|v|^2$ = mean-square fluctuation voltage within the frequency range df; Z_{Ax} = modulus of the transfer impedance from the hypothetical generator in series with the typical resistance r_x to a short-circuit across the points A, A′; $Z_{AA'}$ = modulus of the network impedance from A to A′; τ_x = absolute temperature of the typical resistance r_x.

Also, if the impedance from A to A′ is $(r + jx)$, then it is shown in Appendix 2 that

$$r = Z^2_{AA'}\sum\frac{r_x}{Z^2_{Ax}} \quad . \quad . \quad . \quad . \quad . \quad (3)$$

It follows from equations (2) and (3) that, if the network is at the uniform temperature τ, then

$$|v|^2 = 4rk\tau df$$

the result which was obtained by Nyquist [equation (1*a*)].

Nyquist's result for a general network is therefore consistent with the accepted expression relating to simple resistances, provided that that expression is interpreted as has been described above, and provided also that the network is composed only of linear impedances. This last proviso was not apparent from Nyquist's proof. Accordingly, Llewellyn* applied Nyquist's result to a network containing a thermionic valve, and put forward the hypothesis that thermal fluctuations were generated in the anode-slope resistance of the valve. This hypothesis has since been disproved experimentally,† thus supporting the view that equation (1*a*) refers only to linear networks.

The integrations performed in the derivation of Moullin and Ellis were possible only when the resistance was regarded as independent of frequency. Accordingly, they were unable to decide from their analysis whether the relevant value of resistance in the above formulae was the metallic resistance or the equivalent power-loss resistance. The expression for r obtained in Appendix 2 is the equivalent power-loss resistance. It follows that an experimental check of equation (1*a*) or (2) will not only verify the validity of the method of representation adopted, but will also determine which is the relevant value of the resistance in those formulae. An exhaustive experimental investigation was therefore undertaken and is described in the succeeding sections.

(3) EXPERIMENTAL VERIFICATION

The apparatus used in making the measurements about to be described was similar to that mentioned in previous papers relating to shot effect.‡ A 6-stage amplifier was used which employed resistance-capacitance coupling. Each stage was separately screened, and the amplifier was further subdivided into three sections by further screening boxes which enclosed the necessary battery supplies. An attenuator with logarithmic grading was included between the second and third stages of amplification, and a resonant filter having adjustable parameters between the fourth and fifth stages. The calibration system was similar to that used by Moullin and Ellis, and is fully described in their paper.§ The amplifier was capable of giving a maximum voltage amplification of about 10^8 and was completely stable.

[*] See Bibliography, (9).

[†] *Ibid.*, (5), (6).

[‡] *Ibid.*

[§] *Ibid.*, (4).

(4) MEASUREMENTS WITH METALLIC RESISTANCES

The first series of measurements was made with a non-inductive wire-wound resistor. They were made in order to check the performance of the amplifier and to permit the use of the resistor for calibration purposes in later experiments. The resistor used had a value of 10 070 ohms and was tapped at 5 485 and 1 850 ohms. It had been used successfully in the measurement of shot voltages up to frequencies of about 400 kc.* Such high frequencies are not approached in the present research.

The circuit used in these tests is shown in Fig. 3, the harmonic calibration voltage being introduced at S. One end of S was connected to earth as shown, and all other apparatus was earthed at this point. Such earth connection has been found to reduce spurious input voltages to a minimum.

The deflection due to shot effect in the amplifier was first observed by connecting the amplifier input terminal to earth. The resistance was then introduced and the added deflection due to thermal fluctuations noted. A sinusoidal voltage of suitable magnitude and frequency was next introduced at S and the further increase in deflection was observed. The ratio of these last two increments of deflection gives a measure of the effective series e.m.f. of thermal agitation which is independent of any unavoidable capacitance shunt imposed by the amplifier. The experimental correction for this capacitance adopted by Moullin and Ellis is therefore unnecessary. The frequency/response curve of the amplifier was delineated and applied to the formulae in a manner which has been fully described elsewhere.†

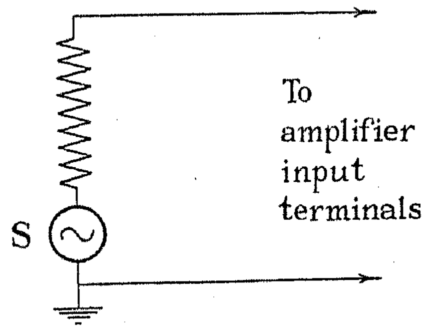

Fig. 3

The results were used to determine a value for Boltzmann's constant, k, and were expressed in terms of the ratio k'/k, k' being the value determined by experiment. In all, 28 values of k' were obtained using filters with resonant frequencies spread over the audio-frequency band. The mean value of k'/k was 1·007, individual results varying between 0·95 and 1·06.

These results were felt to be a sufficient check of the accuracy of measurement obtained with the apparatus, and to justify the use of the resistance for calibration purposes. Experiment also showed that the input impedance of the amplifier was high enough to be neglected.

(5) THERMAL FLUCTUATIONS IN RESONANT CIRCUITS

It has been stated in Section (1) that Moullin and Ellis were unable to agree with Nyquist's prediction of the thermal fluctuations generated in a resonant circuit which included resistance in the condenser arm. The circuit shown in Fig. 4 was therefore set up to differentiate between the alternative formulae. The resistance could be included in either the inductance or the capacitance arm, or could be equally divided between the two arms, by connecting one of the points a, b, c, to earth.

According to Nyquist, the agitation voltage should be given in all circumstances by equation (1a). The values of r (denoted by r_a, r_b, and r_c) relevant to connection being made to a, b, or c, were therefore calculated. For simplicity it was assumed that the equivalent loss resistance of the coil and condenser, a series resistance of 104 ohms at resonance, was constant and added to the inserted metallic resistance of 896 ohms, which was accordingly assumed to have a value of 1 000 ohms and to be centre-tapped. With these assumptions the calculated values of r_a, r_b, and r_c, are shown by the dotted curves of Fig. 5.

A sharply tuned resonant filter of adjustable resonant frequency was incorporated in the amplifier in order to obtain a measure of r_a, r_b, and r_c at various frequencies by fluctuation measurements. Values were obtained by comparing the output deflection due to the resonant circuit with that obtained from the calibrating resistance. The results are shown by the plotted points in Fig. 5, through which mean lines have been drawn.

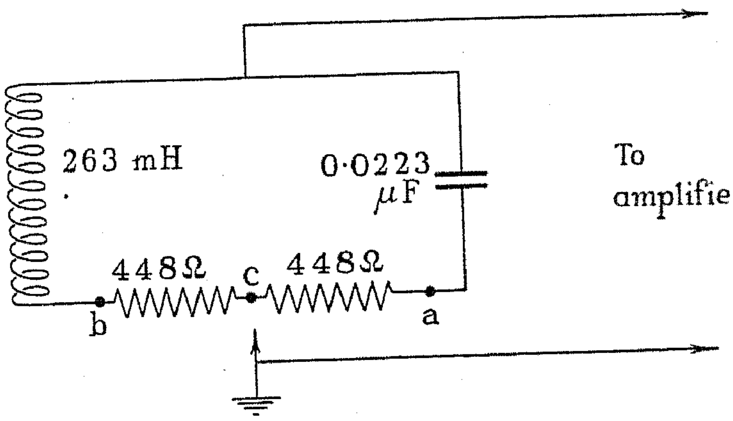

Fig. 4

Experiment is found to be in good agreement with prediction except in the vicinity of resonance, where the experimental values are about 8 % low. This discrepancy is ascribed to the finite band width of the amplifier response curve; for it can be shown that in the region of the resonant frequency experimental results are low on that account by a fractional amount approximately equal to the ratio of the filter power factor to the test-circuit power factor. In these experiments the ratio was 6 %. The maintained discrepancies found on the skirts of the curves can be explained in terms of the residual losses in the coil and condenser. The average ratio of the predicted to the experimental values of r_a, r_b, and r_c, for all experimental points on the figure are 1·02, 0·96, and 1·005 respectively. Thus experiment supports Nyquist's equation. The values predicted by the equation of Moullin and Ellis* lie very close to the curve of r_a, differing by a maximum of + 8 % at the resonant frequency. Experiment therefore fails to confirm their equation.

---

* See Bibliography, (7).

† *Ibid.*, (3), (4), (5), (6).

* See Bibliography, (3), p. 334.

(6) FLUCTUATIONS IN BAND-PASS FILTERS

The next series of experiments was made with a band-pass filter. The circuit of the filter used is shown in Fig. 6. The two branches of the filter were carefully matched. The calculation of the equivalent series resistance of such a filter is laborious, and measured values were therefore used. The "three voltmeter" method was adopted, the arrangement of the connections being such that the amplifier could be connected across the filter, across a known resistance in series with the filter, or across a sinusoidal source supplying current to the series combination of filter and resistance. The source was of adjustable frequency and yielded deflections great compared with those due to fluctuation voltages. The equivalent series resistance of the filter was deduced by drawing the vector triangle corresponding to the square roots of the three deflections obtained. The values obtained from these measurements are shown by the dotted curve of Fig. 7.

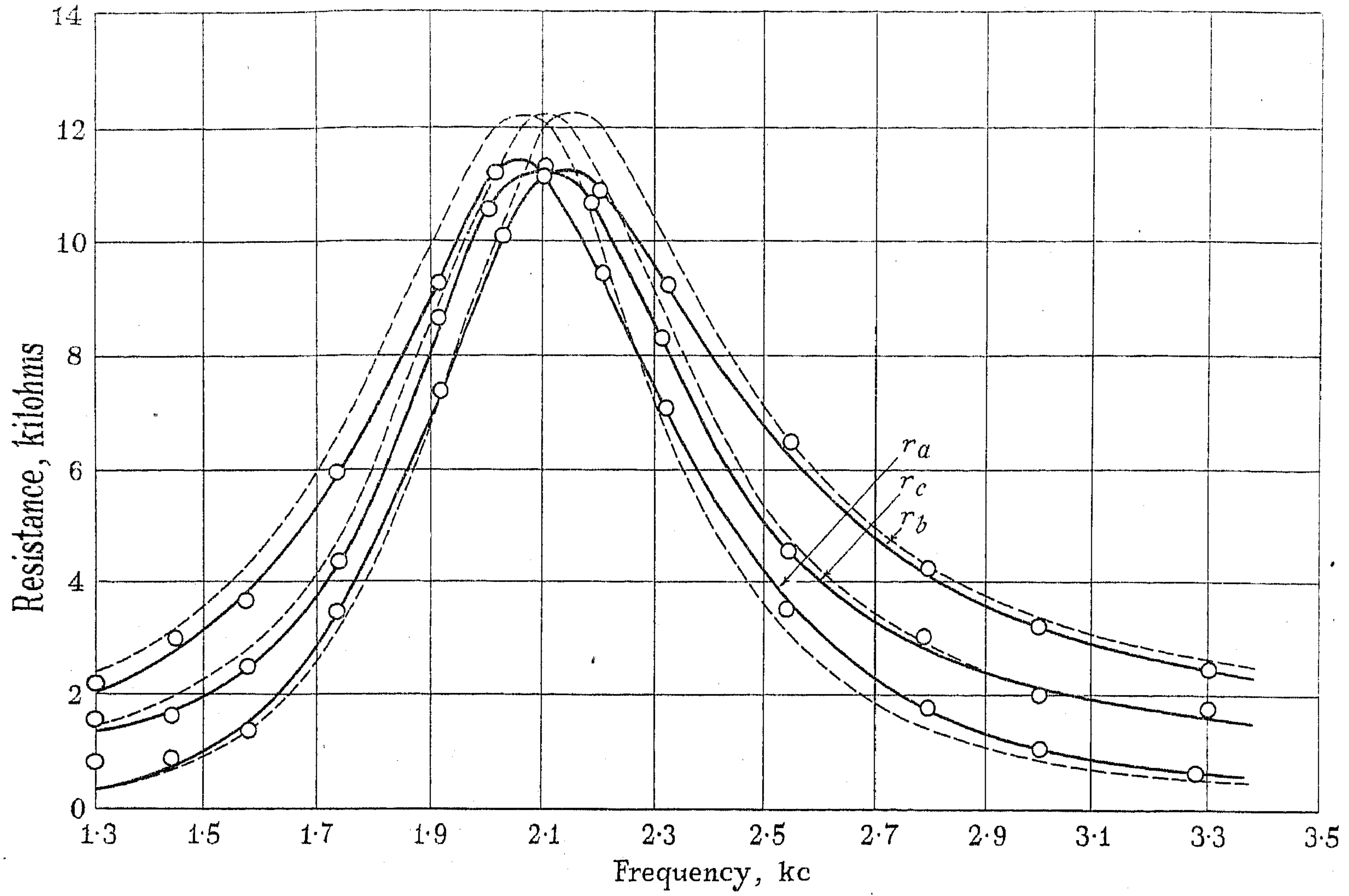

Fig. 5.—Equivalent resistance of resonant circuit as a function of frequency and disposition of resistance. Dotted curves show calculated values; plotted points have been deduced from fluctuation measurements.

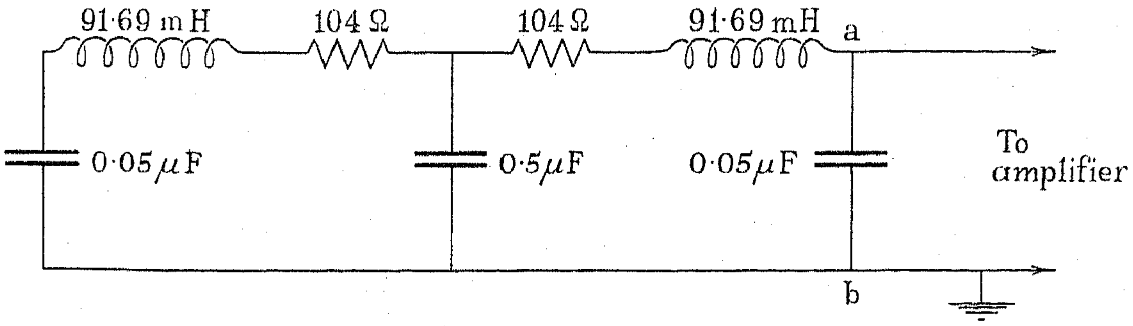

Fig. 6

The fluctuation voltage appearing between the points a and b (Fig. 6) was then measured and expressed as before in terms of the metallic resistance required to give an equal deflection. The results are shown by the plotted points in Fig. 7. Agreement between the two methods of measurement is good except that the fluctuation measurements do not show the sharply-defined peaks and trough shown by the alternative method. This discrepancy is again ascribed to the finite band width to which the amplifier responds, and as before is of the type and order to be expected.

The experiments so far described relate to circuits in which the bulk of the losses could be ascribed to metallic resistances. In many practical circuits losses due to eddy currents, hysteresis, or poor dielectrics, are predominant. The next section describes some measurements made under such circumstances.

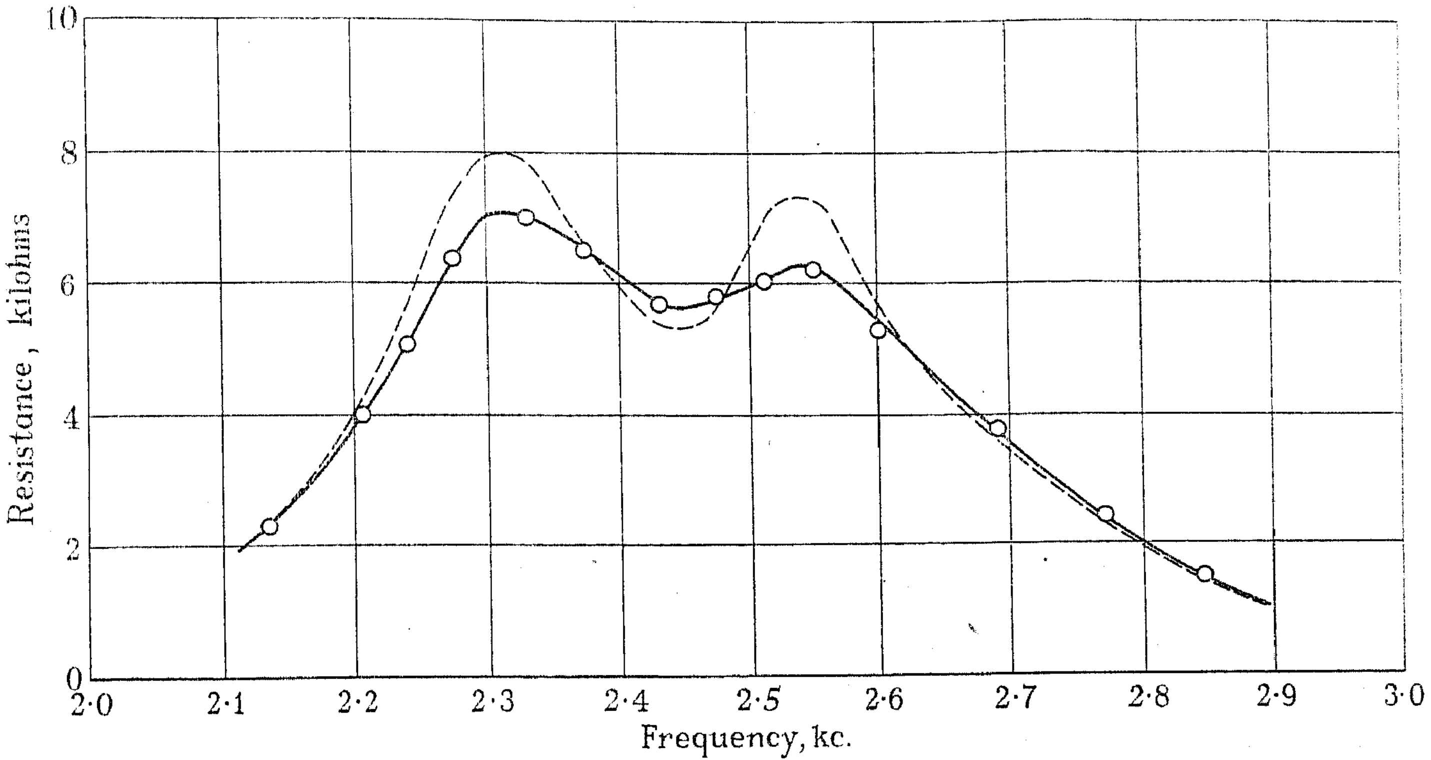

Fig. 7.—Equivalent resistance of a band-pass filter as a function of frequency. Plotted points have been deduced from fluctuation measurements; dotted lines show values obtained by the three-voltmeter method.

(7) THERMAL FLUCTUATIONS IN NON-METALLIC RESISTORS

The first series of measurements were made with an iron-cored coil having a very small air-gap. The copper losses in this coil were negligible compared with the iron losses. The coil was shunted by a small condenser in series with a resistance of 895 ohms. The combination yielded a fairly symmetrical resonance curve which corresponded to a total effective series resistance of about 2 000 ohms. In the absence of the added resistance the band width was not sufficiently greater than that of the filter incorporated in the amplifier.

Measurements of effective series resistance were made by the two methods described in the last section, fluctuation measurements again being shown by the plotted points. The results are shown in Fig. 8. Agreement is again good, the mean ratio of the results obtained by the two methods being 1·008.

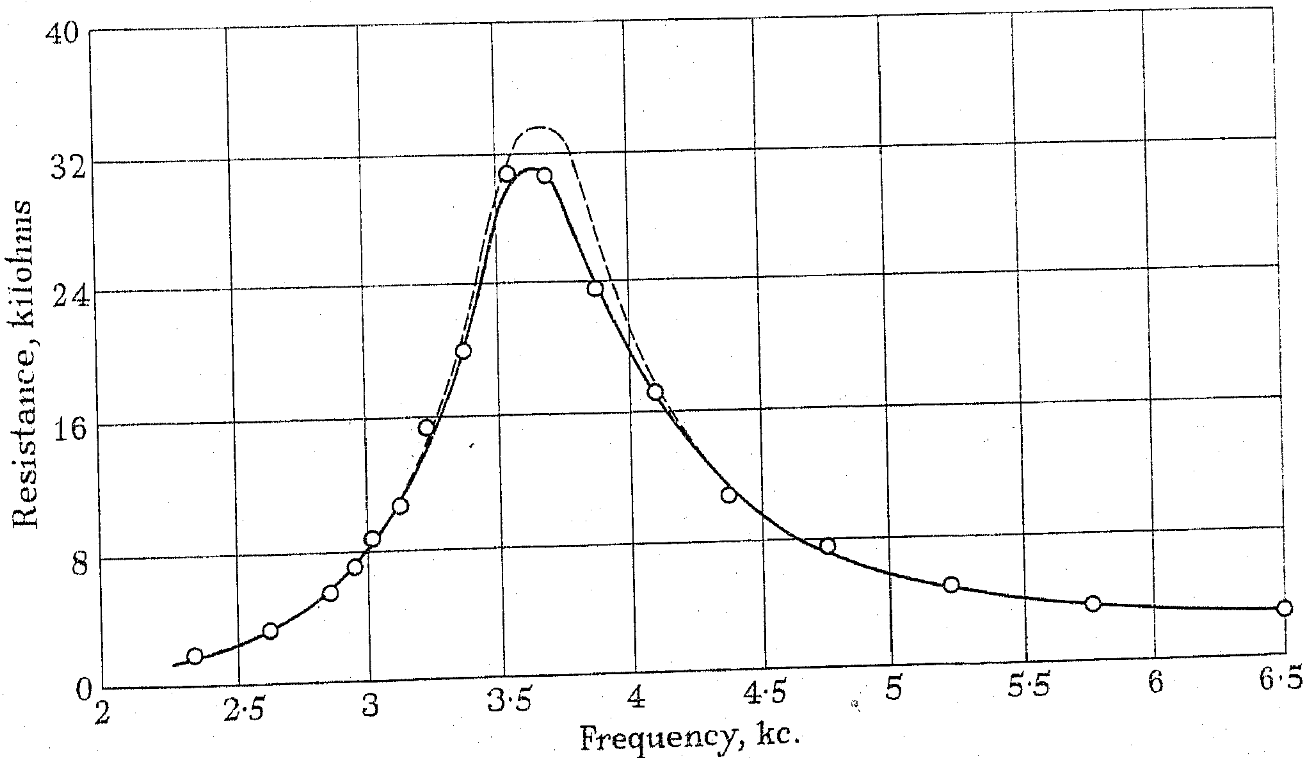

Fig. 8.—Equivalent resistance of a circuit containing iron losses as a function of frequency. Plotted points have been deduced from fluctuation measurements; dotted lines show values obtained by the three-voltmeter method.

Experiments were also made with a small condenser immersed in a polar dielectric. The substance used, namely Permitol, has been thoroughly examined by Jackson,* who gives the power factor as about 10 % at 6 000 cycles per sec. and 16° C. Several measurements were made at frequencies between 6 000 and 8 000 cycles per sec., but in this case the condenser was used alone as its value was so small as to render it unsuitable for inclusion in a resonant circuit. It was found that resistance values deduced from fluctuation measurements were about 10 % in excess of those obtained by the three-voltmeter method. This is believed to be due to errors in the latter measurement; for the comparatively high ratio of reactance to resistance reduces the accuracy of the method.

Measurements were also made, for another purpose, with a liquid resistance containing a concentration of virus. The method of comparison was similar to that used in the last tests, but the reactance was now negligible. The results obtained from the two methods of resistance measurement differed by less than 1%.

The degree of agreement obtained in all the experiments is felt to be sufficient to verify equation (1*a*), and to show that the relevant value of resistance in this equation is the equivalent power-loss resistance. The general expression, equation (2), relating to networks in which the temperature is not uniform, has not been tested. The experimental difficulties of such a test are considerable and the equation is not of such great practical importance as equation (1*a*). However, the method of representation adopted in the proof of equation (1*a*) given in this paper has been justified, and there appears little reason to doubt the validity of the general equation. Llewellyn† has deduced a formula for the thermal agitation voltage developed by two resistors at different temperatures connected in parallel. His expression can readily be deduced from equation (2) and has been tested experimentally by Moullin and Ellis.‡ They found approximate agreement only, and an exhaustive check is to be undertaken shortly.

NOISE/SIGNAL RATIO

It follows from equation (2) and the derivation given in Appendix 1 that if a signal of sinusoidal wave-form and mean square value e^2 be introduced in the nth branch of a general network, then

$$\frac{|v|^2}{v_s^2} = \left(\frac{Z_{AA'}}{Z'_{AA'}}\right)^2 4kdf\frac{\Sigma r_x \cdot \tau_x/Z^2_{Ax}}{e^2/Z'^2_{An}}$$

where v_s^2 is the mean-square signal output at the points A, A′ and the dashes indicate values of impedance relevant to the frequency of the signal.

If the overall frequency response of the apparatus considered is limited at a later stage to a small finite frequency band δf, the values of the impedances will be sensibly constant within that range; whence, with uniform temperature distribution, we have

$$\frac{|v|^2}{v_s^2} = 4k\tau\delta f\left(\frac{r_n + Z^2_{An}\Sigma r_x/Z^2_{Ax}}{e^2}\right) \quad \text{(omitting } n\text{)}$$

The first term within the brackets is proportional to the (Noise/Signal)^2 ratio in the arm in which the signal is introduced. It follows that the signal/noise ratio cannot be raised above the level obtaining in that arm. This result is perhaps obvious on physical grounds, but the author has previously experienced some difficulty in reconciling it with Nyquist's equation, which bears no obvious relation to conditions in the input arm.

This limiting value of signal/noise ratio is approached when the second term within the brackets is negligible compared with r_n. It follows from equation (3) that such is the case when the resistive component of the impedance from A to A′ is sensibly independent of the resistance values in arms other than the nth: that is, when the terminals A, A′ are heavily loaded by the nth arm. This condition can often be attained in practice, and a few special cases are considered in the following sections.

(9) THE INPUT CIRCUIT OF RADIO RECEIVERS

The aerial is usually coupled to the first amplifying valve through a resonant circuit. Many different circuits are used, but it is sufficient to consider that shown in Fig. 9. The resonant circuit losses are represented by the shunt resistance r_b.

If the associated amplifier responds only to a narrow band of frequencies δf, situated about the resonant frequency of the circuit, it follows from equation (2) that the relevant portion of the thermal agitation fluctuation appearing between A and A′ is

$$|v|^2 = Z^2_{AA'}4k\tau\delta f\left(\frac{r_a}{Z^2_{Aa}} + \frac{1}{r_b}\right)$$

The total fluctuation output of the receiver is closely equal to the sum of the thermal fluctuations in the first

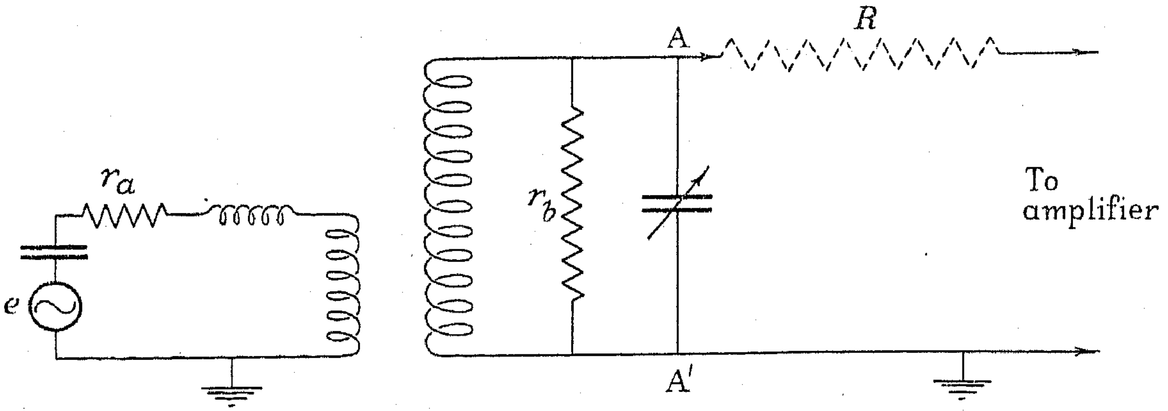

Fig. 9

---

* See Bibliography, (8).

† *Ibid.*, (9).

‡ *Ibid.*, (3).

circuit and the shot fluctuations in the first valve. Pearson* has shown that shot fluctuations can be conveniently represented by an equivalent resistance producing thermal fluctuations in the grid circuit. The total fluctuation output of an amplifier, apart from that due to thermal agitation in the input circuit, can be similarly represented. This equivalent resistance R must be regarded as connected between the circuit and the grid of the first valve, as shown by the dotted lines of Fig. 9. The total fluctuation output referred to the grid of the first valve is then

$$|v|^2 = 4k\tau\delta f Z^2_{AA'}\left(\frac{r_a}{Z^2_{Aa}} + \frac{1}{r_b} + \frac{R}{Z^2_{AA'}}\right)$$

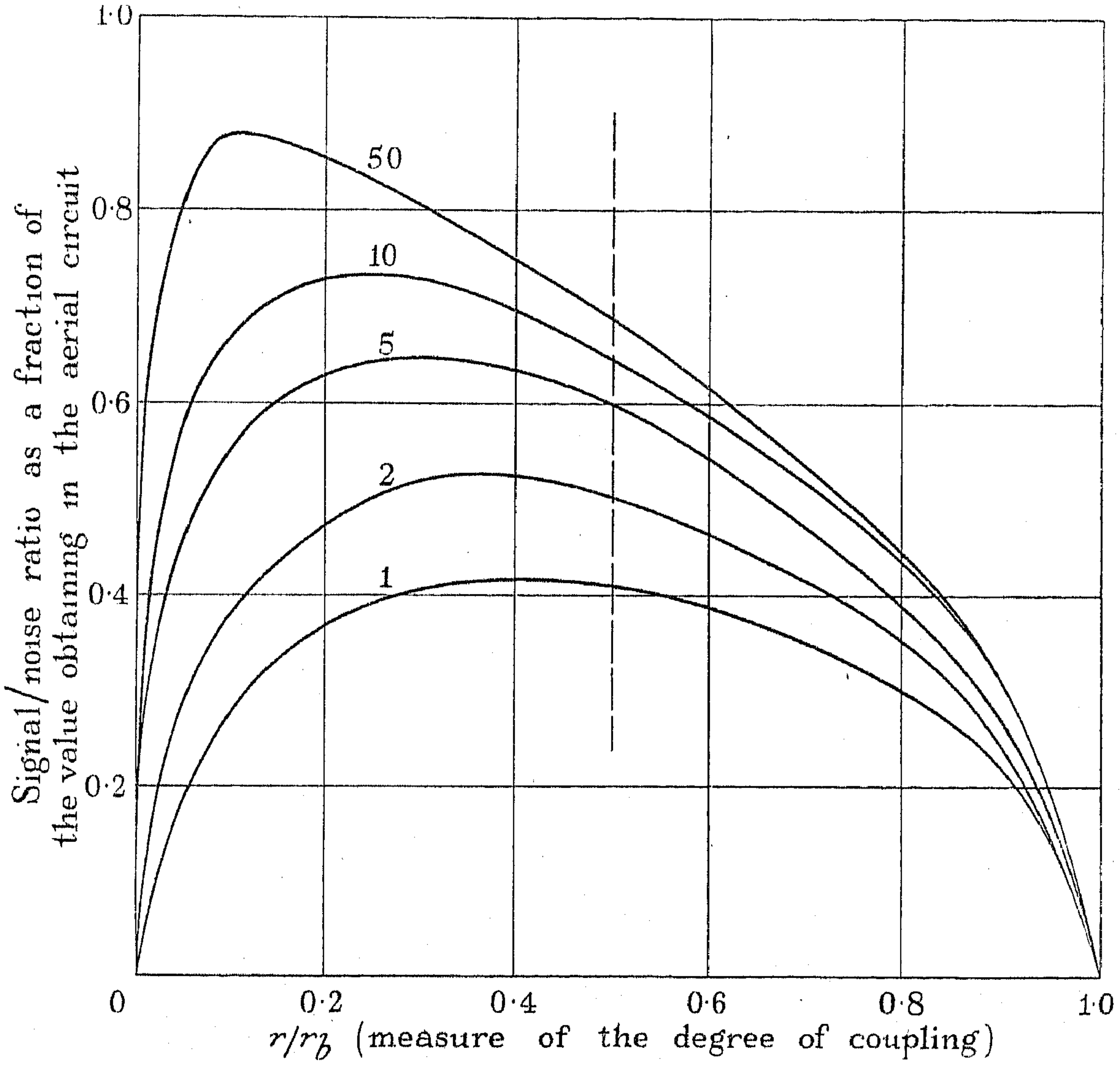

Fig. 10.—Dependence of signal/noise ratio on the degree of coupling between aerial and resonant circuit and on the fluctuations introduced subsequent to the first circuit. The dotted line shows the condition of optimum output. The figures on the curves give the relevant value of r_b/R.

But the reactive component of the impedance from A to A′ is zero, since the circuit is tuned; therefore

$$Z_{AA'} = r$$

Whence, from equation (3),

$$Z^2_{Aa} = \frac{r_a}{\dfrac{1}{r} - \dfrac{1}{r_b}}$$

And, with the same notation as before,

$$\frac{|v|^2}{v_s^2} = \frac{4k\tau\delta f\,.\,r_a}{e^2}\left(1 + \frac{r^2 + r_bR}{rr_b - r^2}\right)$$

The term outside the bracket is the (Noise/Signal)^2 ratio in the branch in which the signal is introduced. The expression within the brackets is a minimum when

$$r = R\left[\sqrt{\left(\frac{r_b}{R} + 1\right)} - 1\right]$$

The best signal/noise ratio is therefore obtained when the coupling between aerial and circuit is adjusted so that r has the value given above. Typical values of r_b and R are 50 kilohms and 5 kilohms respectively. With such values the best signal/noise ratio is obtained when the aerial loads the circuit to such an extent that r is about 11·5 kilohms. This value is probably less than that usually adopted, but the adjustment is not usually critical. Thus, with the figures given, the signal/noise ratio varies only about 5 % for values of r between 7·5 kilohms and 20 kilohms, and is within 30 % of the value existing in the aerial circuit. The dependence of the signal/noise ratio on the degree of coupling between aerial and resonant circuit under various circumstances is shown in Fig. 10. The abscissae of this Figure are values of r/r_b and measure the extent to which the aerial loads the resonant circuit. The ordinates give the signal/noise ratio obtained as a fraction of the limiting value obtaining in the aerial circuit itself. Curves are given for several ratios of circuit-loss resistance to equivalent fluctuation input resistance (r_b/R). Maximum output is always given when $r/r_b = 0 \cdot 5$. This condition is shown by the dotted line in the Figure.

---

* See Bibliography, (10).

It may be noted that when r_b/R is low, i.e. with circuits of low dynamic resistance and a first valve giving appreciable shot effect, maximum output corresponds closely to optimum signal/noise ratio. On the other hand, a good circuit combined with a quiet amplifier gives the best signal/noise ratio with a coupling closer than that corresponding to maximum output; thus when r_b/R is 50 an improvement of about + 25 % in signal/noise ratio can be obtained by adopting the optimum degree of coupling rather than that corresponding to maximum output.

This circuit has been considered by Llewellyn,* who suggested that maximum-output conditions should always be used. His analysis, however, made no allowance for the fluctuations generated in the anode circuit of the first or subsequent valves.

The practical method of testing a receiver for noise is to note the decrease in noise output as the input circuit is distuned. A large decrease indicates that the bulk of the fluctuation output is due to thermal agitation in the first circuit, and is a measure of r_b/R. Thus if θ_1 and θ_2 are the output deflections due to fluctuation voltages when the input circuit is tuned and distuned (or, preferably, short-circuited) respectively, then

$$\frac{r_b}{R} = \frac{\theta_1 - \theta_2}{\theta_2}$$

The aerial is supposed disconnected in the above tests.

The curves of Fig. 10 then yield the value of r/r_b relevant to optimum signal/noise ratio. If the aerial is connected and the circuit tuned the fluctuation output gives a deflection θ_3 such that

$$\frac{\theta_3 - \theta_2}{\theta_1 - \theta_2} = \frac{r}{r_b}$$

In this way the degree of coupling can readily be set by trial to the value corresponding with optimum signal/noise ratio. Be it noted that it may be necessary to use a dummy aerial in these tests to avoid interference from external sources, such as atmospherics. The optimum is not critical, and therefore the dummy need not be an exact equivalent of the aerial to be used.

(10) BAND-PASS FILTER AS AN INPUT CIRCUIT

If the band-pass filter shown in Fig. 6 is used as an input circuit for a radio receiver the aerial is coupled to the left-hand branch and the receiver to the right-hand branch. If satisfactory filter operation is to be obtained neither branch must be appreciably damped by such connection. The aerial must therefore be lightly coupled to the filter. This requirement is completely inconsistent with the condition for optimum signal/noise ratio, which demands that the aerial be responsible for the bulk of the input-circuit damping. Thus, if a good signal/noise ratio is required the filter characteristic must be sacrificed and the simpler and more efficient single circuit will give equal results as regards frequency response.

The exact analysis of the circuit is complex, but it is clear from the above discussion that band-pass filters should not be used if fluctuation noise is an important consideration.

(11) FLUCTUATION VOLTAGE IN CABLES

If the characteristic impedance of a cable is $(r_a + jx_a)$, where x_a is usually small, the fluctuation voltage in the small finite range δf appearing across the end of the cable is

$$|v|^2 = 4r_a k\tau\delta f$$

If the length of the cable be l and the attenuation per unit length $\epsilon^{-\alpha}$, then with uniform temperature the signal/noise ratio at the receiving end due to a signal E at the sending end is

$$\frac{E\epsilon^{-\alpha l}}{\sqrt{(4r_a k\tau \,.\, \delta f)}}$$

Reference to equations (2) and (3) shows that if the temperature is not uniform, but the attenuation is appreciable, the same expression holds provided τ is the temperature in the vicinity of the receiving end. The physical explanation is that it is unnecessary to consider temperature conditions elsewhere in the cable since the fluctuations there produced are severely attenuated before arriving at the receiver.

If the cable is of low characteristic impedance it is usual to step up the impedance by means of a resonant circuit or transformer, in order that valve noise shall not be predominant. In such cases the equivalent circuit is very closely approximate to that considered in Section (9), and the conditions for optimum signal/noise ratio deduced in that section are applicable. An identical experimental procedure can be adopted to determine the optimum degree of coupling.

(12) CONCLUSIONS

Thermal agitation fluctuations in any linear network can be regarded as due to equivalent fluctuation generators of mean square output voltage $4r_a k\tau_a df$, $4r_b k\tau_b df$, etc., acting in series with the resistances r_a, r_b, etc. The fluctuation output between any two points in the network is then given by equation (2). If the network is at a uniform temperature then Nyquist's equation (1*a*) is valid as a special case of equation (2). The resistance relevant to this formula is the equivalent power-loss resistance.

The best signal/noise ratio is obtained when the loading between the observation points is due mainly to the arm in which the signal is injected.

When a resonant circuit or transformer is used to couple an aerial or cable to the first stage of an amplifier, there exist optimum conditions as regards signal/noise ratio which are dependent on the losses in the circuit or transformer and the fluctuations subsequently introduced in the amplifier. The optimum condition has been discussed in Section (9).

---

* See Bibliography, (11).

The signal/noise ratio in a long cable is best when the ratio of attenuation per unit length to the square root of the characteristic impedance is greatest. The temperature of the cable in the vicinity of the receiving end is the only important temperature.

Band-pass filters or other filters should not be used to couple aerials or cables to amplifiers, as the signal/noise ratio is thereby reduced.

ACKNOWLEDGMENT

The research described in this paper was begun in the Engineering Laboratories of Oxford University and completed in the Electrotechnics Department of Manchester University. The author is indebted to Mr. E. B. Moullin for his interest in the work, and to Prof. R. Beattie for later facilities.

APPENDIX 1

Fig. 11 represents any network of linear impedances of which r_x is a typical resistance element. A generator G is supposed connected in series with r_x. A and A′ are any two points in the network and are furnished with a switch S by means of which they can be short-circuited.

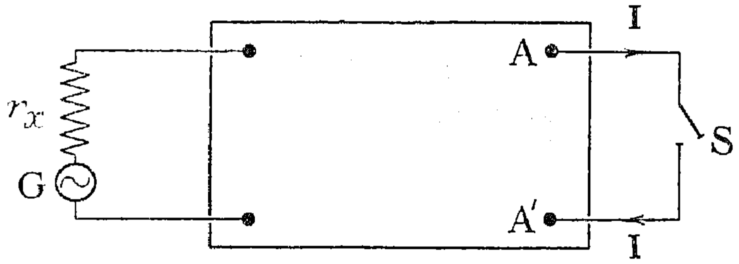

Fig. 11.

First suppose that the generator delivers a sinusoidal output **E** of the form $e = e_{max.} \sin \omega t$, and that the switch is closed. Then the current **I** flowing from A to A′ as shown is

$$\mathbf{I} = \frac{\mathbf{E}}{\mathbf{Ax}}$$

where $\mathbf{Z_{Ax}}$ is the vector transfer impedance from the generator to the short-circuit across AA′ relevant to the frequency $\omega/(2\pi)$. The mean-square value of i is

$$I^2 = \frac{e^2_{max.}}{2} \cdot \frac{1}{Z^2_{Ax}}$$

where Z_{Ax} is the modulus of the transfer impedance.

It follows that if the sinusoidal generator be replaced by an equivalent thermal agitation source yielding an output given by

$$|\, v \,|^2 = 4 r_x k \tau_x df$$

where df is supposed situated about the frequency $\omega/(2\pi)$, then the mean-square value of the fluctuation current, flowing through the switch due to thermal agitation in r_x, is

$$|\, i_x \,|^2 = 4kdf \cdot \frac{r_x \tau_x}{Z^2_{Ax}}$$

Similar fluctuation currents due to every other resistance element in the network flow in the short-circuit AA′. The mean-square value of the sum of any number of mutually independent fluctuation voltages or currents is the sum of their mean-square values: hence the total fluctuation current through the switch is

$$|\, i \,|^2 = 4kdf \sum \frac{r_x \tau_x}{Z^2_{Ax}}$$

Suppose now that the fluctuation sources are removed and the switch opened, and that owing to some impressed sinusoidal e.m.f. in the network there exists across the switch a p.d. **E**. If now the switch be closed, according to Thévenin's theorem* there will flow through the switch a current

$$\mathbf{I} = \frac{\mathbf{E}}{\mathbf{Z_{AA'}}}$$

where $\mathbf{Z_{AA'}}$ is the network impedance from A to A′.

Conversely, if the fluctuation current of mean-square value $|\, i \,|^2$ obtained under the previous conditions is interrupted by opening the switch, there will appear across the switch a mean-square fluctuation voltage given by

$$|\, v \,|^2 = Z^2_{AA'} 4kdf \sum \frac{r_x \tau_x}{Z^2_{Ax}}$$

which is the fluctuation voltage appearing between A and A′. This relation is equivalent to equation (2).

APPENDIX 2

Considering the same network as in Appendix 1, let an e.m.f. **E** of the form $e = e_{max.} \sin \omega t$ be applied across the points A and A′, it being supposed that fluctuation voltages are absent. Then the current in the resistance r_x is

$$\mathbf{I_x} = \frac{\mathbf{E}}{\mathbf{Z_{Ax}}}$$

where $\mathbf{Z_{Ax}}$ is now the transfer impedance from the generator to the arm r_x, but is the same as the $\mathbf{Z_{Ax}}$ already defined, since in linear networks the transfer impedance is the same in both directions.

The power loss in r_x is

$$p_x = r_x |\, i_x \,|^2 = \frac{1}{2} r_x \frac{e^2_{max.}}{Z^2_{Ax}}$$

The total power loss in the network is the sum of all such terms as p_x, and is given by

$$p = \frac{1}{2} e^2_{max.} \sum \frac{r_x}{Z^2_{Ax}}$$

But if $\mathbf{Z_{AA'}}$ has the form $(r + jx)$ the current entering the network is $\mathbf{I} = \mathbf{E}/\mathbf{Z_{AA'}}$, and the power loss can be expressed as

$$p = r \,|\, \mathbf{I} \,|^2 = \frac{1}{2} e^2_{max.} \frac{r}{Z^2_{AA'}}$$

---

* See, for example, T. E. SHEA: "Transmission Networks and Wave Filters," p. 55 (New York, 1929).

Whence, by comparison of the two expressions for p,

$$r = Z_{AA'}^2 \sum \frac{r_x}{Z_{Ax}^2}$$

BIBLIOGRAPHY

(1) J. B. JOHNSON: *Physical Review*, 1928, vol. 32, p. 97.

(2) H. NYQUIST: *ibid.*, 1928, vol. 32, p. 110.

(3) E. B. MOULLIN and H. D. M. ELLIS: *Journal I.E.E.*, 1934, vol. 74, p. 323.

(4) E. B. MOULLIN and H. D. M. ELLIS: *Proceedings of the Cambridge Philosophical Society*, 1932, vol. 28, p. 386.

(5) F. C. WILLIAMS: *Journal I.E.E.*, 1936, vol. 78, p. 326.

(6) F. C. WILLIAMS: *ibid.*, 1936, vol. 79, p. 349.

(7) F. C. WILLIAMS: *ibid.*, 1937, vol. 80, p. 218.

(8) W. JACKSON: *Proceedings of the Royal Society*, A, 1935, vol. 153, p. 158.

(9) F. B. LLEWELLYN: *Proceedings of the Institute of Radio Engineers*, 1930, vol. 18, p. 243.

(10) G. L. PEARSON: *Physics*, 1934, vol. 5, p. 233.

(11) F. B. LLEWELLYN: *Proceedings of the Institute of Radio Engineers*, 1931, vol. 19, p. 416.

THEORY AND PERFORMANCE OF THE ICONOSCOPE*

By V. K. ZWORYKIN, Ph.D., G. A. MORTON, Ph.D., and L. E. FLORY

(*Paper first received* 20*th May, and in revised form* 18*th September*, 1937.)

SUMMARY

Field tests have shown the present standard iconoscope to be a very satisfactory television pick-up device. However, from a theoretical point of view the efficiency of the iconoscope as a storage system is rather low. The principal factors responsible for the low efficiency are lack of collecting field for photo-electrons, and losses caused by the redistribution of secondary electrons produced by the beam.

Limits to the sensitivity of the standard iconoscope are set by the ratio of picture signal to amplifier and coupling-resistor "noise." Experimental and theoretical determinations indicate that an excellent picture can be transmitted with from 2½ to 6 millilumens per cm² on the mosaic.

Two methods are considered by which the sensitivity may be increased. The first is by the use of secondary-emission signal-multipliers and a low-capacitance mosaic, while the second makes use of secondary-emission image intensification. The sensitivity limits for the two cases are calculated.

INTRODUCTION

Experimental tests on the present standard iconoscope camera, illustrated in Fig. 1, have shown the iconoscope to be a very satisfactory television pick-up device. These tests include not only laboratory measurements but also extensive field tests by the National Broadcasting Co. at Rockefeller Centre, New York City. The conclusion arrived at from these tests is that the iconoscope is sufficiently sensitive to be used for outdoor pictures under a wide range of weather conditions, and in the studio without the need of unbearable illumination. However, it would be advantageous for both uses to have somewhat greater sensitivity. The following discussion, as well as dealing with the theory of operation of the standard iconoscope, describes two methods which have resulted in a marked increase in sensitivity. The tubes described are, however, still in the laboratory stage and not as yet ready for use in a commercial television system.

The principles and construction of the standard iconoscope, together with its associated equipment, have been described in detail elsewhere,† and a very brief description for the sake of continuity should suffice. The iconoscope consists of a photosensitive mosaic and an electron gun, assembled in a glass bulb which is highly evacuated. The electron gun is made up of an indirectly heated oxide-coated cathode, a control grid, a cylindrical first anode, and a second anode, also cylindrical but slightly larger in diameter. The gun assembly is shown diagrammatically in Fig. 2. This gun functions as an electron optical system for producing a narrow bundle of electrons which is made to scan the mosaic by means of magnetic deflecting coils.

The mosaic consists of a thin sheet of mica coated with a conducting metal film on one side, and covered on the other with a vast number of tiny, photosensitized silver globules. This mosaic is mounted in the blank in such a position that the electron beam strikes the photosensitized side at an angle of 30° from the normal, and the optical image to be transmitted is projected normal to the surface on the same side. The arrangement of these elements in the tube is shown in Fig. 3, while Fig. 4 shows an iconoscope with optically flat window.

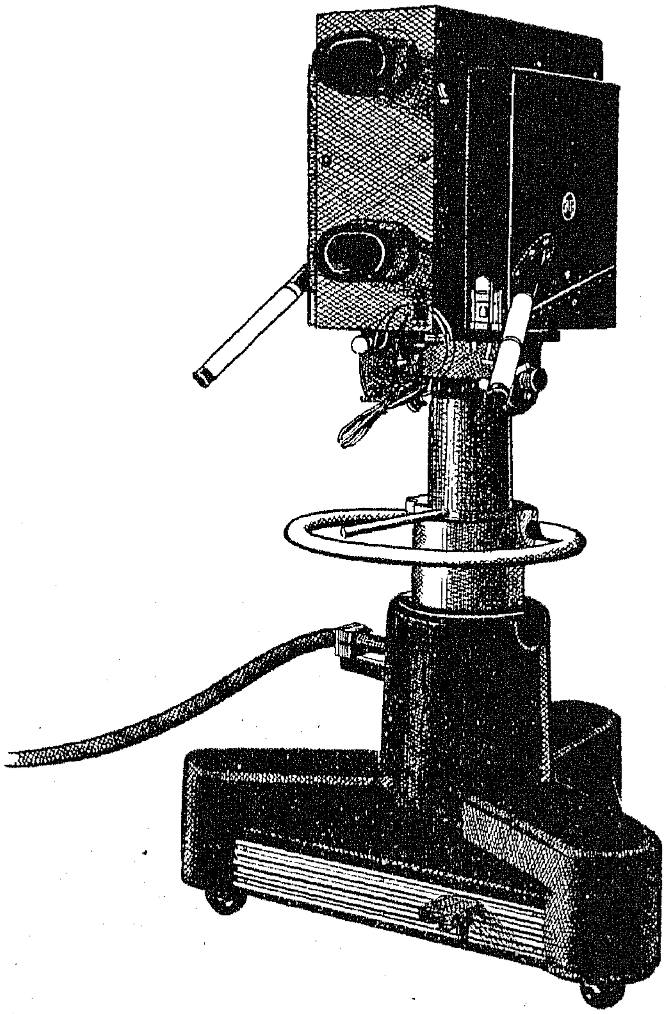

Fig. 1

Briefly, the iconoscope mosaic may be thought of as a 2-dimensional array of tiny photocells, each shunted by a condenser which couples them to a common signal lead. When the mosaic is illuminated these condensers are charged positively with respect to their equilibrium potential owing to the emission of photo-electrons from the photosensitive elements. For any particular element, this charging process continues for a time equal to

---

* Reprinted from *Journal I.E.E.*, 1938, vol. 82, p. 105.

† See Reference (1).

the picture-repetition interval, i.e. until the beam in the process of scanning returns to the element. When the beam strikes it, it is driven to equilibrium, releasing its charge and inducing a current impulse in the signal lead. The train of impulses thus generated constitutes the picture-signal output of the iconoscope. This description serves to illustrate the general principles of the iconoscope, but is not sufficiently accurate to form the basis of an analysis of its operation.

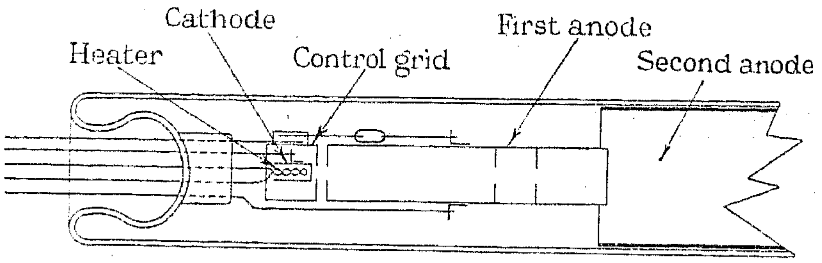

Fig. 2.—Electron gun.

MECHANISM OF OPERATION OF THE ICONOSCOPE

In considering the operation of the iconoscope, because of the fact that the silver globules are so small that a great number of them are under the beam at any instant the mosaic may be treated as a continuous surface which has infinite transverse resistance, and which has both a high secondary-emission ratio (in the neighbourhood of 5 to 7) and a good photosensitivity. This surface has a capacitance of about 100 $\mu\mu$F per cm^2 in the case of a standard tube. Considered in this way, it can be readily seen that the picture element is a purely fictitious concept when applied to the mosaic. Thus, instead of discussing the behaviour of discrete photo-electric elements, we shall deal with the mosaic as though it were a 2-dimensional continuum.

The average potential of the mosaic under bombardment, while no light is falling upon it, is between 0 and 1 volt negative with respect to the elements which collect the secondary emission from the mosaic, i.e. the second anode. However, the potential is not uniform over the entire surface. The area directly under the scanning beam will be at a potential of + 3 volts with respect to the second anode, this being the potential at which the secondary-emission ratio from caesiated silver becomes unity. Away from the point under immediate bombardment in the region which has just been traversed by the scanning beam the potential will be found to decrease, until at a distance equal to 25 %–30 % of the vertical scanning distance the potential reaches about $- 1\frac{1}{2}$ volts with respect to the second anode. The rest of the mosaic is at this potential. This decrease in potential is caused by electrons which leave the point under bombardment and return to the mosaic as a more or less uniform rain of low-velocity electrons. Fig. 5 shows a map of the instantaneous potential distribution over the mosaic.

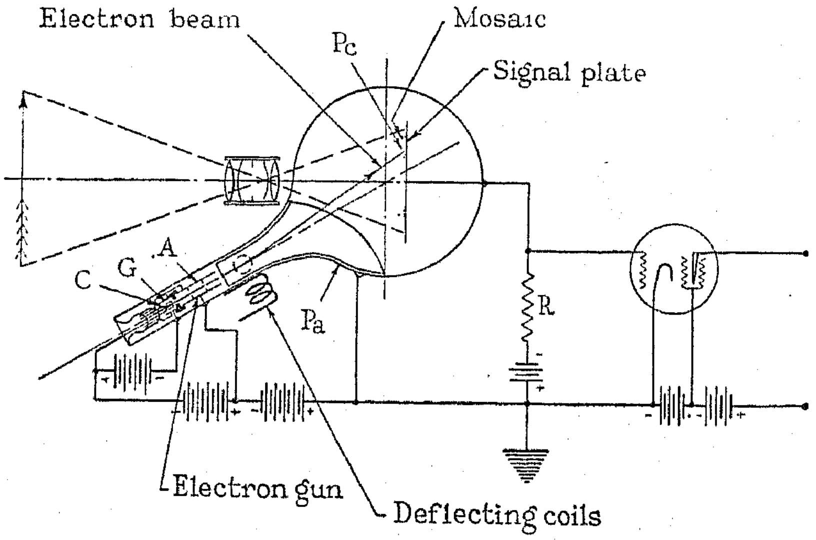

Fig. 3

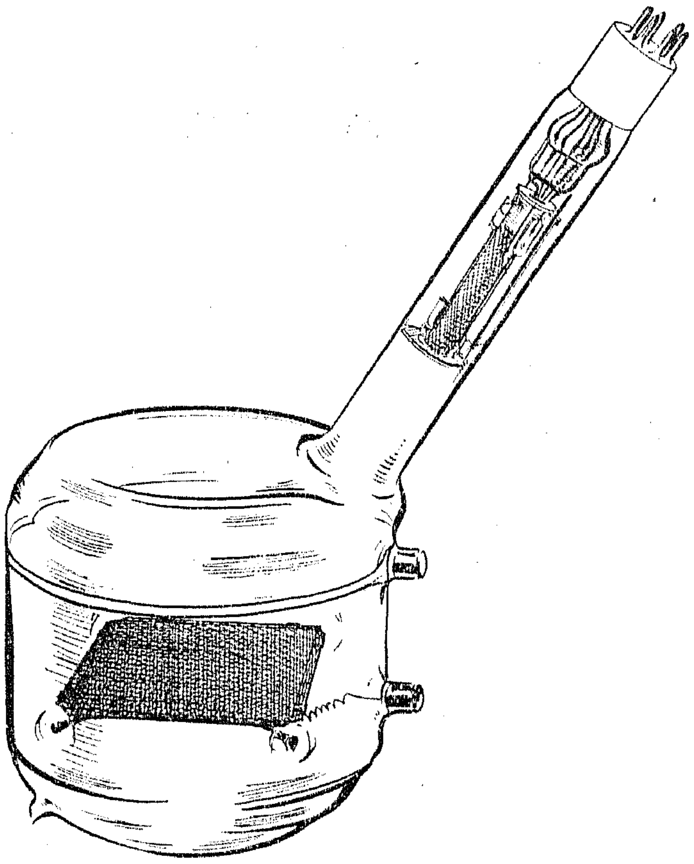

Fig. 4

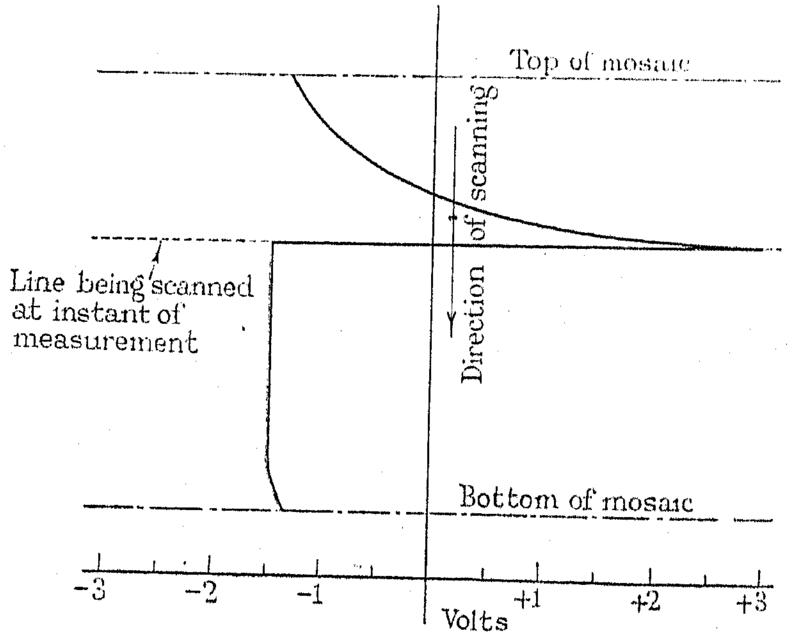

Fig. 5.—Instantaneous potential of the mosaic.

The scanning beam sweeping over the mosaic acts like a resistive commutator. The resistance in this case is determined by the current/voltage relation of the secondary electrons from the bombarded point. While this resistance is actually non-ohmic, we shall not introduce appreciable error if we assume it ohmic over the small voltage-range dealt with in the case of the iconoscope. Experimental measurements show this beam impedance, Z, to be given by the relation $Z = Z_0/i_b$, where i_b is the beam current and Z_0 is the coefficient of beam impedance. Z has a value between 1 and 2 ohm/ampere.

For purposes of computation, the beam current will be taken as $0 \cdot 5$ microampere, the spot as a square of $0 \cdot 025$ cm. side, and the linear spot velocity as $1 \cdot 6 \times 10^5$ cm. per sec.

Any small element of area, ds, of the mosaic when it is swept over by the scanning beam must change its potential from $-1\frac{1}{2}$ volts to its equilibrium value of approximately $+3$ volts. The capacitance of this area will be $C = C_0 ds$, where C_0 is the capacitance per unit area. The impedance through which this capacitance is discharged will be $Z = Z_0/(\rho ds)$, ρ being the current density of the beam. The equation of the discharge will therefore be

$$V = \left[V_2(xy) - V_1(xy)\right]\left[1 - e^{-t\rho/(C_0Z_0)}\right] \quad . \quad (1)$$

In this equation, V = change in potential of ds, $V_2(xy)$ = equilibrium potential at point xy under beam, $V_1(xy)$ = potential before bombardment, and t = time.

In order that the elements may reach equilibrium, the condition

$$V \simeq V_2 - V_1$$

must be fulfilled. For this to be true, the relation

$$\frac{Z_0C_0}{\rho} < T$$

(where T = length of time for which the beam is on the element ds, or
$T = h/V$, where h is the spot diameter and V is the beam velocity)

must be satisfied. From the operating conditions, we find that $T = h/V = 1 \cdot 5 \times 10^{-7}$ sec. and $Z_0C_0/\rho = 1 \cdot 2 \times 10^{-7}$ sec. Thus the requirements for establishing equilibrium are fulfilled.

In the above expression both V_1 and V_2 are given as functions of the co-ordinates of the mosaic, x and y. This is because both the equilibrium under the beam and the equilibrium away from the beam are not constant over the surface.

The net current leaving the elemental area under these conditions will be

$$di_e = -\left(C_0\frac{dV}{dt}\right)ds \quad . \quad . \quad . \quad . \quad (2)$$

Since the beam current reaching the element is $-\rho ds$, the total current from the element is

$$di_t = -\left(\rho + C_0\frac{dV}{dt}\right)ds$$

This entire current will not reach the second anode because, on the average, as much current must reach the mosaic as leaves it. Let $\chi(xyV)$ be the fraction of this current which reaches the second anode; then the current to the second anode can be written as

$$di_s = \chi(xyV)\left(\rho + C_0\frac{dV}{dt}\right)ds \quad . \quad . \quad . \quad (3)$$

The instantaneous current, i_s, reaching the second anode, is given by the integral of the above expression over the area of the scanning beam. Since the current i_s carries the picture signal, the solution of equation (3) would be very desirable. This integration, however, cannot be performed since the function $\chi(xyV)$ is not known.

It is possible to make certain approximations which will enable the calculation to be made of an average value for the redistribution function. Since the mosaic is an insulator, the average value of its function must be given by

$$\bar{\chi} = \frac{i_b}{i_T} = \frac{i_b}{i_b + i_e} \quad . \quad . \quad . \quad . \quad . \quad (4)$$

In this equation, i_b is known and i_e can be found as follows:—

$$i_e = \int C_0\frac{dV}{dt}ds$$

But we have

$$V = \left[V_2 - V_1\right]\left[1 - e^{-t\rho/(C_0Z_0)}\right]$$

and

$$\frac{dV}{dt} = (V_2 - V_1)\left(\frac{\rho}{C_0Z_0}\right)e^{-t\rho/(C_0Z_0)}$$

$$ds = hVdt$$

Therefore we can write

$$i_e = \frac{hV\rho}{Z_0}(V_2 - V_1)\int_0^T e^{-t\rho/(C_0Z_0)}dt$$

$$\simeq hVC_0(V_2 - V_1)$$

and

$$\bar{\chi} = \frac{1}{1 + \dfrac{hVC_0(V_2 - V_1)}{i_b}} \quad . \quad . \quad . \quad (5)$$

Evaluating this function, using the constants of the iconoscope, we find that $\bar{\chi} \simeq 0 \cdot 25$. This means that, out of the total charge released by an element when struck by the beam, only about 25 % will reach the second anode, the remainder being returned to the mosaic. In other words, only about 25 % of the stored charge is available for producing the picture signal.

As was mentioned above, $V_1(xy)$, $V_2(xy)$, and $\chi(xyV)$ are not constant over the mosaic, even when it is in darkness. As a consequence, there is a variation in the current reaching the second anode as the mosaic is scanned. This gives rise to a spurious signal which, if not compensated, produces irregular shading over the picture. The importance of this spurious signal is sufficient to warrant further discussion. It is evident from the nature of the factors upon which it depends that it may be regarded as divided into two parts. The first is the stored signal, which depends upon $V_1(xy)$, while the second is an instantaneous effect, depending upon the variation of $V_2(xy)$ and $\chi(xyV)$ over the mosaic.

The instantaneous component can be demonstrated very strikingly if a metal plate is substituted for the mosaic in an iconoscope. When this plate is scanned in the ordinary way, it being maintained at a potential close to that of the second anode, a spurious signal is produced very similar to that from the mosaic. While the mechanism of generation of this signal is not exactly the same as that in the case of the mosaic, it is quite similar. If the potential of the plate is made negative or positive with respect to the second anode, the secondary emission will be suppressed, or saturated, and the signal will disappear. In practice, the spurious signal from the iconoscope is compensated for by means of an electrical correcting network. Considerable work has been done, and further work is in progress, on methods of overcoming the effect of the spurious signal or entirely eliminating it.

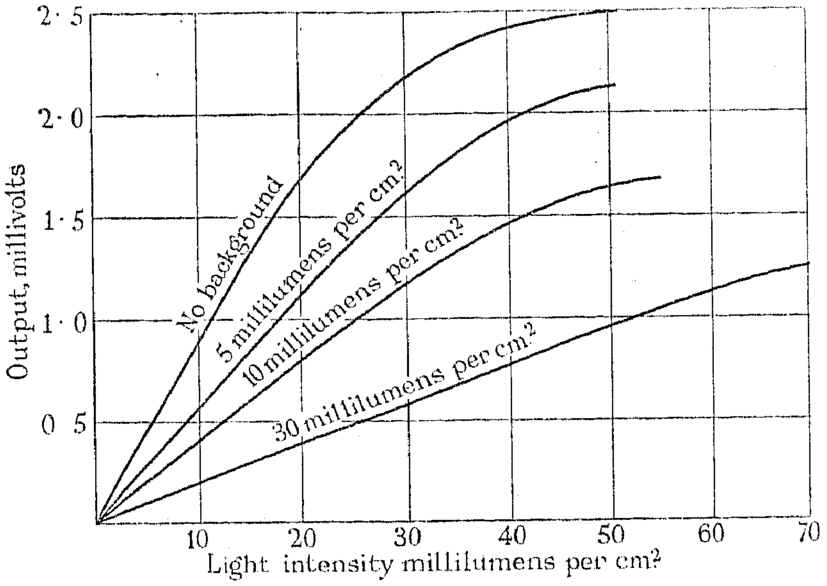

Fig. 6.—Variation of output with light intensity, for different values of background illumination.

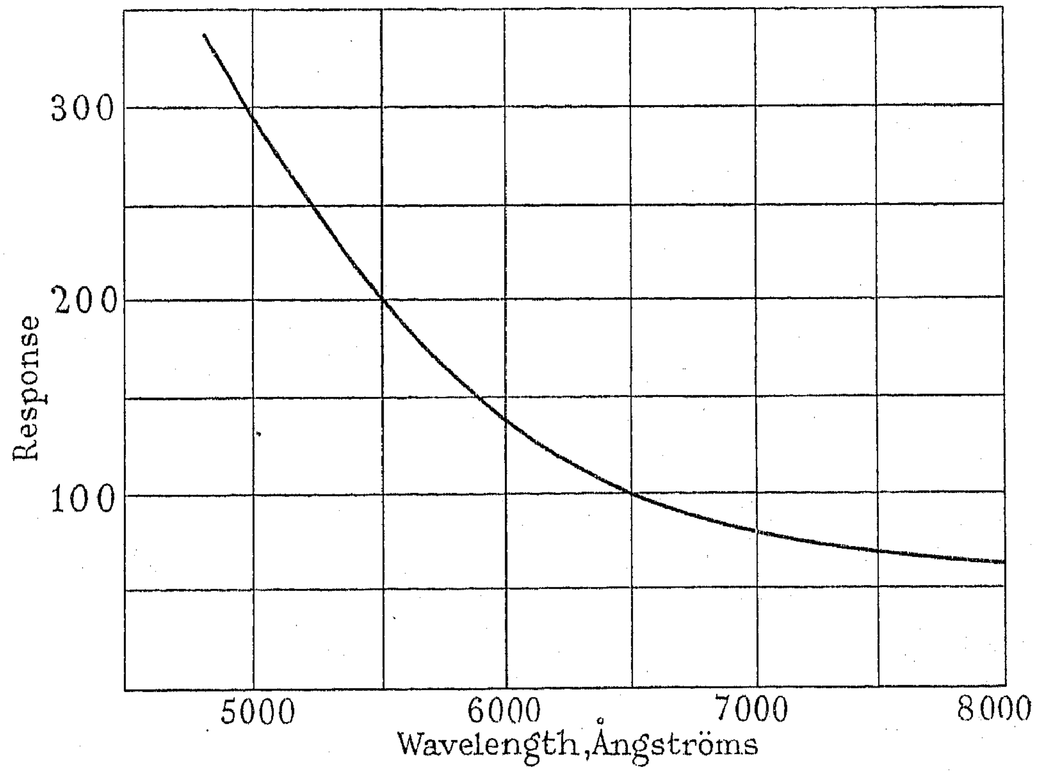

Fig. 7.—Colour response of standard iconoscope.

When an optical image is projected on to the mosaic, the illuminated area emits photo-electrons in proportion to the light falling on it. As a consequence, this area reaches a less negative final potential than an unilluminated area. In this connection it should be pointed out that, although the mosaic receives a continuous redistribution current, this current is very little altered by small changes in potential over small areas. In other words, the impedance shunting any element is very high. As a result of the difference in $V_1(xy)$ for an illuminated and an unilluminated region, there is a change in i_s. This fluctuation constitutes the picture signal.

Besides the inefficiency consequent on the redistribution losses, the photo-emission is also inefficient owing to the small fields drawing the photo-electrons away from the mosaic. The effective photo-emission of the mosaic in the standard iconoscope is only about 20 % to 30 % of its saturated value. This means that the overall efficiency of the iconoscope is only 5 % to 10 %. In spite of this inefficiency, the great advantage resulting from the use of the storage principle makes the iconoscope a very effective pick-up device.

Before we leave the discussion of the mechanism of operation of the iconoscope, mention should be made of the phenomenon of line sensitivity which results from the variation in potential over the surface of the mosaic. Referring to Fig. 5, it will be seen that the line on the mosaic just ahead of the scanning beam is subject to a strong positive field, and consequently has high photoelectric efficiency. The line is, in consequence, extremely sensitive. This can be demonstrated very strikingly in the following way. The image from a continuously-run motion-picture film (e.g. a picture projected by a moving-picture machine from which the intermittent shutter has been removed) is projected on to the mosaic of the iconoscope. The film is run at such a rate that the frame speed is equal to the picture frequency, and in such a direction that the picture moves in the opposite direction to that of scanning. Under these conditions the iconoscope is found to transmit a clear image of two frames of the moving-picture film, although to the eye there appears to be only a blur of light on the mosaic.

From the above description of the mechanism of operation of the iconoscope it is apparent that the efficiency decreases as the light intensity increases. Fig. 6 shows a family of measured curves illustrating this effect. The output is measured in millivolts across a 10 000-ohm coupling resistance, and the light input in lumens per cm² on the mosaic. The curve showing the greatest response represents the signal output from a small illuminated area when the remainder of the mosaic remains unilluminated. The effect of a background illumination over the entire mosaic is shown by the remaining curves of the family.

The colour response of an iconoscope depends upon the activation schedule and the operating conditions involved. Fig. 7 shows the colour response measured on the present type of standard iconoscope.

CALCULATION OF THE SENSITIVITY OF THE ICONOSCOPE

So far, we have considered only the magnitude of the signal output. If it were possible to amplify the signal output indefinitely without introducing spurious effects, the problem of attaining high sensitivity would merely be one of increasing the amplifier gain. However, the picture amplifier amplifies not only the signal output from the iconoscope but also the voltage generated by the thermal agitation in the coupling resistor (or other coupling device). If the voltage generated by the picture signal becomes of the same order as these fluctuations, the picture becomes lost in " noise." This sets a definite limit to the sensitivity that can be obtained.

In making any calculations concerning the sensitivity of the iconoscope we are faced with the problem of assigning quantitative values to the psychological effect of picture/noise ratio. Tests have been made to determine the effect on the observer of various ratios of peak picture-signal in an average picture, to root-mean-square noise. It has been found that if the r.m.s. noise is equal to 30 % of the picture signal, the picture is still recognizable, but the resolution is decreased and the picture is tiring to watch. In addition, if the ratio remains constant but the picture amplitude is decreased, the noise becomes less objectionable; however, there is no increase in the effective resolution. If the picture/noise ratio is 10 : 1, a very good picture can be obtained but the noise is still very noticeable. Such a picture is completely usable and has fair entertainment value. When the noise is reduced to 3 % of the picture, it becomes practically unnoticeable and the picture may be regarded as excellent.

Let us base our calculation of sensitivity on an allowable noise/picture ratio of 10 %. While under these conditions the amount of noise would be greater than would be tolerated if conditions made it possible to avoid such a high noise/picture ratio, nevertheless such a picture would have reasonably good entertainment value and could be broadcast, particularly where programme continuity made transmission necessary. To make the calculation the following data are necessary: Area of mosaic (A), 128 cm²; photosensitivity (p), 7 μA per lumen; overall efficiency (k), 0·05; coefficient of thermal e.m.f. (K_1), $1\cdot6 \times 10^{-20}$; coupling resistance (R), 10 000 ohms; frequency band (f), 2×10^6 cycles per sec.

If the region of maximum illumination receives a light flux F lumens per cm², the signal from the iconoscope from this point will be

$$I = Fpk\frac{A}{n}\frac{T_0}{T} \quad . \quad . \quad . \quad . \quad . \quad (6)$$

$$= FpkA$$

where n = number of elements, T_0 = picture (frame) time, and T = time for which the beam is on one picture element. But, since $T_n = T_0$, and substituting the values given above, the instantaneous current pulse is

$$i_s = 4\cdot5 \times 10^{-5} F \text{ amp.}$$

Since this is fed through a 10 000-ohm resistor, the picture voltage is

$$V_s = 0\cdot45\,F \text{ volts}$$

The coupling resistor alone does not generate the entire noise found in the picture amplifier. Noise voltages generated in the first amplifying valve and first plate resistor are each present in appreciable amount, particularly in an amplifier covering as broad a frequency band as is required. In order to take into account these factors, it will be assumed that the noise in the amplifier is equivalent to a resistance of 30 000 ohms across the input. The noise voltage will therefore be

$$V_N^2 = K_1 f R$$

$$= 9\cdot6 \times 10^{-10}$$

or an r.m.s. noise voltage of

$$\overline{V}_N = 3\cdot1 \times 10^{-5}$$

The picture/noise ratio under these conditions is therefore

$$N = 1\cdot45 \times 10^4 F$$

Further, if the minimum usable ratio is assumed to be 10, the smallest amount of light falling on the mosaic sufficient to give an adequate picture will be 7×10^{-4} lumen per cm². This corresponds to illumination on the high lights, and is of course somewhat higher than the average illumination of the picture. On the same basis, the illumination required to produce an excellent picture, i.e. where the noise is only 3 % of the picture signal, would be as follows: $N = 1\cdot45 \times 10^4 F = 33$; $F = 2\cdot3 \times 10^{-3}$ lumen per cm². Actual measurements on an average iconoscope show that an excellent picture can be transmitted from an object having a surface brightness of 20 to 50 candles per sq. ft., using an $f/2\cdot7$ lens. The illumination on the mosaic under these conditions will be:—

$$F = \frac{\pi B}{4(\text{Focal length of lens})^2} = 2\tfrac{1}{2} \text{ to } 6 \text{ millilumens per cm}^2$$

When allowance is made for reflection losses in the optical system and for the psychological element, the agreement will be seen to be fairly good.

METHODS OF INCREASING THE SENSITIVITY OF THE ICONOSCOPE

The problem of increasing the sensitivity of the iconoscope may be approached in three different ways: First, by keeping the signal sensitivity the same and reducing the noise generated; second, by increasing the quantity of charge per unit light flux acquired by the mosaic; third, by increasing the overall efficiency of the iconoscope. The third method has been studied extensively, and laboratory iconoscopes have been made with efficiencies as high as 50 %. This work is still in the early experimental stage, however, and will not be discussed here.

Let us consider the first method of increasing the sensitivity. Noise reduction is possible because of the fact that the effective circuit carrying the signal from the iconoscope is completed through the secondary emission from the mosaic. In other words, when the coupling resistor and amplifier are connected to an electrode which collects the secondary emission, a signal can be obtained which is equal to that from the signal plate. If these secondary electrons are led into a secondary-emission multiplier instead of being collected, it is possible to obtain the signal from the multiplier and thus completely eliminate the noise that would be introduced by the conventional coupling-resistor and amplifier.

Before taking up the question of the type of multiplier suitable for this purpose, or the methods used to get the electrons from the mosaic into the multiplier, let us consider the sensitivity and noise relations resulting from this scheme. The picture output will be equal to the signal at the mosaic times the gain of the multiplier; the latter will be written as B^n, B being the gain per stage and n the number of stages. Hence

$$I_s = FpkAB^n$$

On the other hand, the noise will be essentially the shot noise in the secondary emission from the mosaic. More exactly, the noise* is

$$I_N^2 = \frac{B^{2n+1}}{B-1} K_2 f \cdot 2i_b$$

Therefore, the picture/noise ratio will be

$$N = \frac{I_s}{I_n} = \frac{kA}{\sqrt{(K_2 f)}} \sqrt{\left(\frac{B-1}{2B}\right)} \frac{F}{\sqrt{i_b}} \quad . \quad . \quad (7)$$

Evaluating this, we find

$$N \simeq 40 \frac{F}{\sqrt{i_b}}$$

In actual practice the beam current in a standard iconoscope is about 0·5 microampere. If N is assumed to be 10, the illumination required will be

$$F \simeq 2 \times 10^{-4} \text{ lumen per cm}^2$$

This is to be compared with the result where a normal amplifier was used, and where the illumination was 7×10^{-4} lumen per cm^2; that is, this represents an increase in sensitivity of about 3 times.

The interesting point about this multiplier iconoscope is, however, that its sensitivity depends upon the beam current; therefore, if we can reduce the beam current without decreasing the efficiency, the iconoscope becomes more effective. It is not possible, in a multiplier iconoscope using a standard mosaic, to reduce the beam current without loss in efficiency owing to the increase of discharge time of the elements. When this condition occurs, the efficiency falls off and, furthermore, moving objects blur. In order to decrease the time-constant so that the beam current can be decreased, it is necessary to reduce the element capacitance. The simplest method of accomplishing this is by using a thicker insulating layer for the mosaic. Assuming that the time-constant is fixed, the beam current should be inversely proportional to the capacitance; in other words, approximately proportional to the mosaic thickness. It is interesting to carry the calculation down to the limiting case and to see what is the maximum sensitivity obtainable by this method. Obviously, the beam current cannot be reduced beyond the point where it becomes equal to the photocurrent. Under these conditions, we can calculate the sensitivity as follows:—

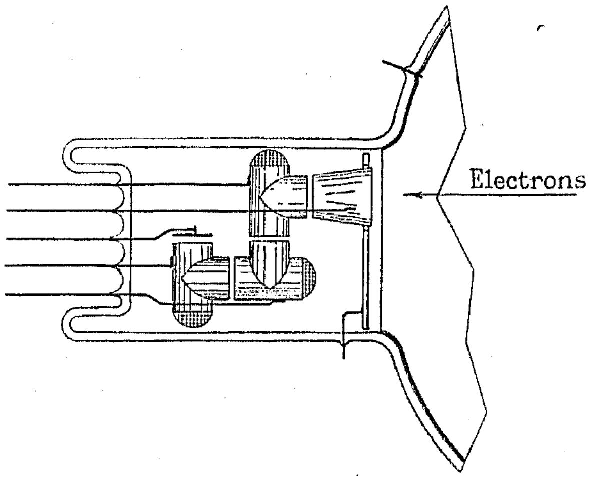

Fig. 8.—"T" type multiplier.

$$i_{phot.} = k'Fpah$$

where a and h are the length and height of the region considered, and k' is the fraction of photocurrent leaving the mosaic. The instantaneous beam equivalent must therefore be

$$i_0 = k'Fpah\frac{T_0}{Ta} = FpAk'$$

$$I_s = FpkA$$

Hence the picture/noise ratio will be

$$N = \frac{I_s}{I_n} = \frac{pkA}{\sqrt{(k_2 f)}} \sqrt{\left(\frac{B-1}{B}\right)} \frac{F}{\sqrt{2FpAk'}} \quad . \quad (8)$$

$$= \sqrt{\left[\frac{pk^2A(B-1)}{2k'K_2 fB}\right]} \sqrt{F}$$

Assuming, as before, that N must be at least 10, the minimum light that can be used will be $F = 5 \times 10^{-6}$

---

* See Reference (2).

lumen per cm². This would be the smallest amount of light that would suffice to transmit a satisfactory picture when noise suppression of this type was used. The value for the sensitivity just given must be regarded purely as a theoretical estimate. In practice, no tube has yet been made based on this principle with a sensitivity greater than 10 to 20 times that of the standard iconoscope.

Having arrived at certain theoretical conclusions as to the ultimate sensitivity that can be attained, let us now consider the practical details of construction. The multiplier suitable for this purpose is preferably one which does not involve the use of a magnetic field: it must be capable of multiplying a comparatively broad beam of electrons rather than a sharply defined spot, and must have a high gain per stage. It has been found that the " T " type* multiplier, whose construction is shown in Fig. 8, serves very adequately. There are, however, a number of possible types of multipliers that might be used.

In order to get the electrons away from the mosaic, a disc—run at from 25 to 100 volts positive with respect to the second anode—is placed at the entrance of the protuberance containing the multiplier. This disc is perforated with an aperture behind which is mounted a small truncated cone at a high positive potential, carrying the electrons through the aperture and into the multiplier. The disc, because of its area, determines to a great extent the field close to the mosaic, while the cone governs the field distribution close to the disc.

Several tubes were made to determine the most suitable location for the multipliers, with the results shown in the Table in col. 2 on this page.

Because of optical reasons, it is a difficult problem to locate the multiplier directly in front of the mosaic. It was found, however, that two multipliers located at 30° on either side of the normal to the mosaic, collected all of the electrons leaving the mosaic. This type of iconoscope is shown in Fig. 9. While work is still being done on this development, very satisfactory pictures under conditions of low illumination have been obtained from this type of tube. The principal problems yet to be dealt with are those of activating the multipliers and the mosaic simultaneously, and of obtaining a uniform distribution of the picture.

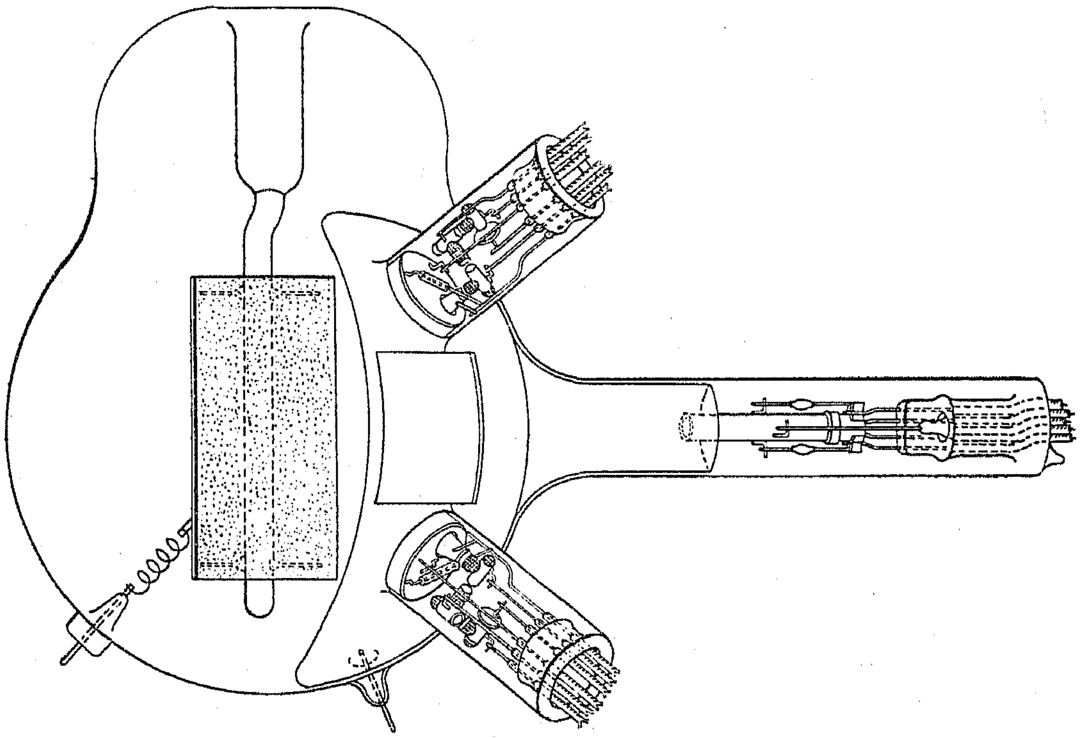

Fig. 9.—Signal-multiplier iconoscope.

The second method of increasing the sensitivity of the iconoscope is by the use of secondary-emission image intensification. This can be accomplished by allowing the electron image produced in some form of image tube to fall on a mosaic constructed in such a way that the elements extend through the mosaic. The elements on the side of the mosaic on which the electron image is projected are made secondary-emissive, so that for every electron striking the mosaic 6–8 electrons are emitted. Thus, the stored signal will be several times that which would be due to the original photo-electric current. The scanning beam sweeps across the back of the mosaic, removing the stored picture in the same way that the picture is removed from the ordinary one-sided mosaic. The gain in sensitivity will be proportional to the intensification at the mosaic. Furthermore, it is possible to produce semi-transparent photocathodes of the type used in the image tube with more than twice the photosensitivity of the ordinary mosaic. Considering both

Position	Percentage of electrons collected
Behind mosaic	10
Side of mosaic	50
At angle of 30° to normal	80
Front	100

---

* See Reference (2).

these factors, it is possible to increase the sensitivity by from 10 to 15 times.

Before examining the details of this type of tube, let us consider the limiting sensitivity that can be attained in this way. First, the gain obtainable is not of course limited to that which can be obtained from one stage of secondary-emission multiplication. It is perfectly possible, and has been accomplished in experimental tubes, to allow the electron image from an image tube to fall upon a secondary-emitting surface, and with a second electron optical system to refocus this enhanced image. Let us assume that this process can be repeated as many times as is desired, and the multiplied image be projected on a two-sided mosaic. In this way, the charge image stored on the mosaic may be made as large as is desired. However, as was the case with the low-capacitance tube, there are definite limits to the sensitivity that can be attained. The limit in this case is due to the statistical fluctuation in the photocurrent emitted from the photosensitive cathode upon which the image is initially projected.

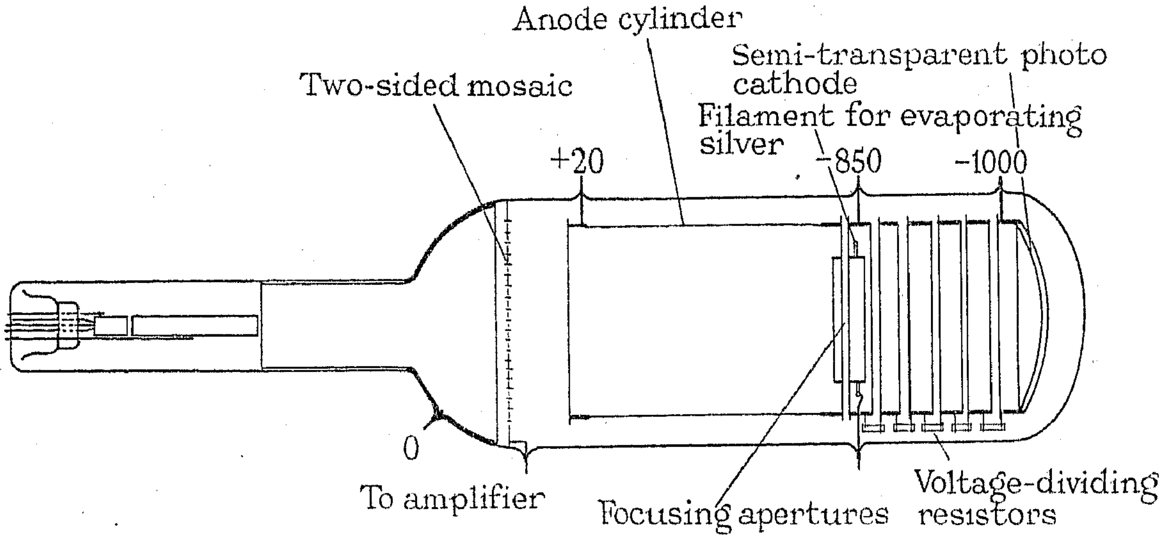
Anode cylinder
Semi-transparent photo cathode
Two-sided mosaic
Filament for evaporating silver
+20
-850
-1000
0
To amplifier
Focusing apertures
Voltage-dividing resistors

Fig. 10.—Image-multiplier iconoscope.

In order to estimate the ultimate sensitivity, let us assume that the gain of each stage of the secondary-emission multiplier is sufficiently great for the picture/noise ratio at the cathode to be not appreciably greater than it is at the mosaic. This is equivalent to assuming that the fraction $(B - 1)/B$, used above in multiplier calculations, is equal to unity, which is amply justified when gains of 7 or 8 per stage can be obtained. It can be shown that, if q is the photo-electric charge emitted by one picture element during one frame time, the mean-square fluctuation will be

$$\bar{q}_N^2 = eq$$

If, as before, we assume that the root-mean-square fluctuation should be 10 % of the total charge, we have

$$N = \frac{q}{\bar{q}_N} = \frac{q}{\sqrt{(eq)}} = \frac{i_p T_0}{\sqrt{(e i_p T_0)}}$$

But

$$i_p = Fap = \frac{FAp}{n}$$

where i_p is the photo-emission from one element, and a the area of an element. Thus, we have

$$N = \sqrt{\left(\frac{FApT_0}{en}\right)}$$

It can be demonstrated, by means of a Fourier transformation, that $T_0/n = 1/(2f)$; hence we may write

$$N = \sqrt{\left(\frac{FAp}{2ef}\right)}$$

Actually, the picture/noise ratio should have been written

$$N = \sqrt{\left(\frac{FAp}{2ef(1 + k'')}\right)}$$

where the factor k'' takes into consideration the fluctuations in the entire group of multiplied photo-electrons which strike the mosaic and induce "noise" directly on the signal plate. The value of k'' depends on a great many variables. Its value cannot be less than unity, and for the purpose of calculation will be assumed to be in the neighbourhood of 10.

On this basis, the limiting amount of light which will produce a picture signal equivalent to 10 times the r.m.s. noise will be

$$F = \frac{2ef(1 + k'')N^2}{Ap}$$

$$= 7 \times 10^{-7} \text{ lumen per cm}^2 \quad . \quad . \quad (9)$$

For the case just considered it would require an image multiplication of 500–1 000 to reach the limiting sensitivity. It is interesting to note that this limit is of about the same order of magnitude as for the case of the low-capacitance iconoscope. In general, it is possible to show that the limiting light sufficient to give a picture/noise ratio of N for an ideal storage television system (where the conversion efficiency is 100 %) will be

$$F = \frac{2efN^2}{Ap} \quad . \quad . \quad . \quad . \quad . \quad (10)$$

While experimental tubes have been made with more than one stage of image multiplication, this technique has not been developed to a sufficient extent to be applicable to a commercial iconoscope in use in the television field test.

Very successful single-stage image-multiplier iconoscopes have been built. Fig. 10 shows diagrammatically such a tube. It consists, essentially, of an electron image tube* which projects on to a secondary-emissive mosaic an electron reproduction of an optical image formed on the photocathode. The mosaic in this instance differs from that in the standard iconoscope in that the mosaic elements extend through the insulating matrix in such a way that the electron image can be formed on one side while the mosaic is scanned on the other. If the mosaic is scanned while the photocathode is in darkness, the potential of each element will be nearly the same as that of the second anode, owing to the action of the beam and the redistribution of electrons.

When light is projected on to the photocathode, electrons will be emitted. These electrons are accelerated by the electron optical system and refocused on the mosaic. Each element thus bombarded will emit secondary electrons which will be drawn to the anode cylinder, since the latter is at a positive potential with respect to the mosaic. If the secondary-emission ratio of an element is, for example, B, the net current to it will be $(B - 1)$ times the primary current incident upon it. It should be pointed out, however, that the average amplification of the mosaic will not be $(B - 1)$, owing to the fact that the elements do not cover the entire surface under the electron image. If c be the fraction of the surface covered by the elements, then the effective gain will be $c(B - 1)$.

The electron optical part of this iconoscope is identical with the electron image tube, for which purpose the latter was developed. It consists of a semi-transparent photocathode; a cathode cylinder composed of five rings, each at a successively higher positive potential; and an anode cylinder which is maintained at approximately 1 000 volts positive. The lens of this system may be regarded as being located between the cathode and the anode cylinder, though actually it is a thick lens occupying a considerable portion of the total length of the system. The magnification of such a system can be shown† to be $m = v/(2u)$, where u and v respectively are the object and image distances from the lens. For the type of tube illustrated, where unity magnification of the image is used, the length of the cathode cylinder is half that of the anode cylinder.

The cathode is curved, with a radius equal to the lens diameter. This curvature not only corrects for image distortion and for curvature of the image field but also reduces the astigmatism to such an extent that it no longer limits the resolution in any part of the field.

The semi-transparent photo-electric surface used is caesium on oxidized silver. It is formed by evaporating a thin layer of silver on to the cathode disc from a filament located directly behind the aperture forming the electron lens. This silver is then oxidized by means of an electric discharge in oxygen at a low pressure, until the layer becomes almost completely transparent. Caesium is admitted, and the tube is baked exactly as is done in activation of a photo-electric cell. As a final step, additional silver is evaporated on to the surface and the tube is again baked. This final silver sensitization not only increases the photosensitivity and conductivity of the film, but also adds to its stability. This type of surface will have a photo-sensitivity of 20 to 25 microamp. per lumen, and a colour response very similar to that of a caesium photocell.

The most difficult item in the image-multiplier iconoscope to construct is the mosaic. One method by which a suitable mosaic can be built is as follows: A fine-mesh, electrodeposited nickel screen forms the base. It is coated with a thin layer of special vitreous enamel in such a way that its entire surface is completely insulated. The interstices in the screen are then filled with silver oxide made into a paste with an appropriate binder. The screen is finally heated to a temperature just under the melting point of the enamel in order to drive off the binder and to reduce the silver oxide to metallic silver. The arrangement of the elements and the actual construction of this type of tube will be clear from Fig. 10.

Actual tests on this type of iconoscope show that its sensitivity is about 10 times greater than that of a standard iconoscope. This added sensitivity is due, in part, to the secondary-emission multiplication and, in part, to the greater photosensitivity of the light-sensitive surface. For the present, this type of tube must be regarded as a purely experimental device because of the difficulties of producing commercially screens free from blemishes, due to irregular electrical leakage between the mosaic elements and the base screen. There is every reason to believe, however, that this type of tube can be made commercially available in the near future.

CONCLUSION

In conclusion, it may be said that the iconoscope has, in actual field test, proved itself to be a very practical pick-up device in spite of its low theoretical efficiency. The tube has been accepted as the sole pick-up equipment in several extensive television broadcast projects, both in the United States and abroad, and has been rapidly gaining general recognition. It would, nevertheless, be very desirable to increase the sensitivity of the iconoscope, and this paper describes several methods by which this may be accomplished. Before these principles can be incorporated in tubes to be used for broadcast purposes, a great deal of research and development work must be done. Eventually, however, it will be possible to produce a tube which will operate at even lower light levels than at present.

The work described has been possible only through the co-operation of the members of the research staffs of both the Victor and the Radiotron Divisions of the RCA Manufacturing Co. Particular mention should be made of the work of the late Mr. G. N. Ogloblinsky and that of Messrs. H. Iams and A. W. Vance, who have contributed so materially to the developments described in this paper.

REFERENCES

(1) V. K. Zworykin: "The Iconoscope—the Modern Version of the Electric Eye," *Proceedings of the Institute of Radio Engineers*, 1934, vol. 22, p. 16;

---

* See Reference (3).

† *Ibid.*, (4).

V. K. ZWORYKIN: "Television," *Journal of the Franklin Institute*, 1934, vol. 217, p. 1; V. K. ZWORYKIN: "Iconoscopes and Kinescopes in Television," *RCA Review*, 1936, vol. 1, p. 60; V. K. ZWORYKIN: "Television with Cathode-Ray Tubes," *Journal I.E.E.*, 1933, vol. 73, p. 438.

(2) V. K. ZWORYKIN, G. A. MORTON, and L. MALTER: "The Secondary Emission Multiplier—A New Electronic Device," *Proceedings of the Institute of Radio Engineers*, 1936, vol. 24, p. 351.

(3) G. A. MORTON and E. G. RAMBERG: "Electron Optics of an Image Tube," *Physics*, 1936, vol. 7, p. 451.

(4) V. K. ZWORYKIN and G. A. MORTON: "Applied Electron Optics," *Journal of the Optical Society of America*, 1936, vol. 26, p. 181.

MEETINGS OF THE WIRELESS SECTION

138TH MEETING OF THE WIRELESS SECTION, 3RD NOVEMBER, 1937

Dr. E. Mallett, the retiring Chairman of the Section, took the chair at 6 p.m.

The minutes of the meeting held on the 5th May, 1937, were taken as read and were confirmed and signed.

The Council's award of Premiums (see *Journal I.E.E.*, vol. 80, page 678) for papers presented to the Section during the session 1936–37 was reported. Dr. Mallett then vacated the chair, which was taken by the new Chairman, **Mr. T. Wadsworth, M.Sc.**

A vote of thanks to Dr. Mallett for his services as Chairman during the session 1936–37, proposed by Dr. R. L. Smith-Rose, Ph.D., and seconded by Mr. H. Bishop, B.Sc.(Eng.), was carried with acclamation.

Mr. Wadsworth then delivered his Inaugural Address (see page 1).

A vote of thanks to the Chairman for his Address, proposed by Sir George Lee, O.B.E., M.C., President, was carried with acclamation.

11TH INFORMAL MEETING OF THE WIRELESS SECTION, 23RD NOVEMBER, 1937

Mr. T. Wadsworth, M.Sc., Chairman of the Section, took the chair at 6.30 p.m.

The minutes of the Informal Meeting held on the 23rd March, 1937, were taken as read and were confirmed and signed.

A discussion, opened by Mr. H. L. Kirke, took place on "Electrical Gramophone Reproduction."

At the conclusion of the discussion a vote of thanks was accorded to Mr. Kirke for his introductory remarks.